

DEPOSITIONAL ENVIRONMENT, DIAGENESIS AND DOLO-
MITIZATION OF THE HENRYHOUSE FORMATION,
IN THE WESTERN ANADARKO BASIN AND
NORTHERN SHELF, OKLAHOMA

By

GEOFFREY BONSER BEARDALL, JR.

Bachelor of Science

Mary Washington College

Fredericksberg, Virginia

1979

Submitted to the Faculty of the Graduate College
of the Oklahoma State University
in partial fulfillment of the requirements
for the Degree of
MASTER OF SCIENCE
December, 1983

Thesis
1983
B368d
cop. 2



DEPOSITIONAL ENVIRONMENT, DIAGENESIS AND DOLO-
MITIZATION OF THE HENRYHOUSE FORMATION,
IN THE WESTERN ANADARKO BASIN AND
NORTHERN SHELF, OKLAHOMA

Thesis Approved:

Zuhair al-Shaich

Thesis Adviser

~~*[Signature]*~~

Gary F. Stewart

Norman D. Rucka

Dean of the Graduate College

1170155

ACKNOWLEDGMENTS

I wish to express my appreciation to my major adviser, Dr. Zuhair Al-Shaieb, for suggesting this topic and providing numerous ideas and enthusiastic, stimulating leadership throughout this study. I gratefully acknowledge the help and suggestions of Drs. Gary Stewart and Mateu Esteban. Dr. John Shelton and Rick Fritz also provided valuable insights and information. ERICO provided funding for this thesis.

Thanks are due to many friends in the Geology Department who helped me complete the program; particularly my roommate, David McConnell, for his merciless encouragement and relentlessly bland cooking.

A special thanks to Dr. William Back of the U. S. Geological Survey for his initial advice and help.

Thanks also go to Grayce Wynd for typing and helping format this thesis, and Hienz Hall for skillfully photographing the cores.

Finally, I wish to thank my parents for their patience and guidance, without which I could not have completed this study.

TABLE OF CONTENTS

Chapter	Page
I. INTRODUCTION	1
Location	1
Statement of Purpose	1
Structural Setting and Geologic History	1
Methods of Investigation	3
II. PREVIOUS WORK	6
Stratigraphy	6
Environment of Deposition	8
Petrography	8
Porosity	9
Dolomite	9
III. DEPOSITIONAL FACIES AND DEPOSITIONAL ENVIRONMENT	11
Introduction	11
Depositional Facies	11
Facies I	13
Facies II	13
Facies III	13
Depositional Environment	14
Core Summaries and Interpretations	21
Apexco Green-Natomas No. 1, 31-10N-26W	
Cored Depth: 19599-19770 ft	22
Tenneco Jordan No. 2-34, 34-T22N-R14W	
Cored Depth: 8464-8570 ft	22
Tenneco Jordan No. A-1, 3-T21N-R14W	
Cored Depth: 8471-8614 ft	26
Kirkpatrick, Natol, and NCRA Wichert No. 1	
Cored Depth: 7770-7810 ft	33
Kirkpatrick and Natol Nichel No. 1, 34-22N-12W	
Cored Depth: 7880-7907 ft	33
Cleary Rose No. 1-12, 12-T22N-R12W	
Cored Depth: 7553-7590 ft	37
Amax Hickman No. 1-24, 24-T17N-R18 W	
Cored Depth: 13500-13550 ft	42
Lone Star Hanan No. 1, 6-T19N-R24W	
Cored Depth: 14322-14389 ft	42
N. F. C. Dietz No. 6-30, 30-T23N-R13 W	
Cored Depth: 7743-7779 ft	47

Chapter	Page
Glover-Hefner-Kenedy No. 1, 1-T14N-R16W Cored Depth: 14250-14349 ft	47
IV. PETROGRAPHY OF THE DOLOMITE	54
Introduction	54
Petrographic Characterization	54
Facies I	54
Facies II	58
Facies III	58
Porosity	64
Porosity Types	64
Porosity Controls	68
Diagenetic Events and Processes	73
Pre-compaction	74
Post-compaction	87
V. DOLOMITIZATION	94
Introduction	94
Petrographic Evidence	95
Indications of Hypersalinity	95
Indications of Fresh Water Mixing	96
Geochemical Evidence	101
Carbon Isotopes	101
Oxygen Isotopes	104
Dolomitization Model	104
Phase I - Hypersaline Dolomitization	104
Phase II - Mixed Water Dolomitization	106
VI. CONCLUSIONS	109
REFERENCES CITED	111
APPENDIX - CORE DESCRIPTIONS	116

LIST OF TABLES

Table	Page
I. Type and Number of Data Samples	4
II. Dolomite Textures and Fabrics	55
III. Accessory Minerals and Paragenetic Sequence. Sutured Contacts and Stylolization Were Used as Compaction Indicators	75
IV. Stable Isotopic Compositions of Henryhouse Carbonate .	102
V. Summarization of Evidence for Hypersaline and Mixed Water Dolomitization	105

LIST OF FIGURES

Figure	Page
1. Area of Study and Local Structural Setting	2
2. Hunton Stratigraphy	7
3. Relative Abundance of Principal Facies Criteria	12
4. Typical Vertical Sequence of Sedimentary Structures, Fauna, and Mineralogy Relationships Observed in Core and Thin Sections. Facies Interpretations Indicate Marine Regression/Shoreline Progradation	15
5. Stratigraphic Cross-section Based on Electrical Logs and Core, Illustrating Facies Relationships. The Uncon- formity at the top is the Woodford Shale	16
6. Stratigraphic Cross-section Based on Electrical Logs and Core, Illustrating Facies Relationships. The Unconformity at the top is the Woodford Shale	17
7. Stratigraphic Cross-section Based on Electrical Logs and Core, Illustrating Facies Relationships. The Uncon- formity at the top is the Woodford Shale	18
8. Schematic Cross-section Showing Distribution of Henryhouse Depositional Facies. Vertical Scale is Greatly Exag- gerated	20
9. (A) Facies I - Laminated Dolomite and Crystal Algal Fabrics in a Dolomudstone (AG-19615); (B) Facies I - Laminated Birds-eye Fenestral Fabric in a Dolomudstone (AG-19633)	23
10. (A) Facies I - Possible Storm Layer in Dolomudstone (AG- 19679); (B) Facies I - Pelloid-rich, Irregular Lami- nations in a Lime Mudstone (AG-19733)	24
11. Facies I - Photomicrograph of Laminations Preserved in Dolomite	25
12. Facies I - Photomicrograph of Cryptal Algal Fenestral Fabric	25

Figure	Page
13. Facies IIa - Photomicrograph of Moldic Porosity in a Dolowackestone	27
14. Facies I - Silty Dolomudstone With Irregular Laminations	27
15. Facies I - Silty, Massive, Vertically Fractured, Dolomudstone Containing a Chert Nodule	28
16. Facies IIa - Oil-stained, Burrow Mottled, Dolowackestone With Good Moldic and Vuggy Porosity	28
17. Facies IIa - Same as Figure 12	29
18. Facies I - Photomicrograph of Faint Laminations Preserved in Dolomite	29
19. (A) Facies IIa - Oil-stained, Burrow Mottled, Porous Dolomudstone/Wackestone; (B) Facies IIa - Same as 8489	30
20. (A) Facies IIa - Faintly Mottled Dolomudstone With High Amplitude Stylolite; (B) Facies IIb - Dolomitic Wackestone Containing Pelmatozoans, Trilobites, Bryzoans, and Brachiopods	31
21. Photomicrograph of Moldic Porosity in Hypidiotopic Facies IIa Dolomite	32
22. Photomicrograph of Undissolved Fossils in Facies III Dolomitic Mudstone	34
23. Facies IIa - Excellent Porosity in an Extensively Burrowed Dolowackestone	34
24. Facies IIa - Possible Laminations in a Dolomud-Wackestone	35
25. Photomicrograph Showing Irregular Distribution of Intercrystalline Porosity Related to Burrowing	35
26. Photomicrograph of Enlarged Moldic and Intercrystalline Porosity in a Dolowackestone	35
27. Facies IIb - Medium Light Grey, Burrow Mottled Dolowackestone With Excellent Porosity	38
28. Facies IIb - Burrow Mottled Dolowackestone	38
29. Photomicrograph of Moldic Porosity in a Facies IIb Hypidiotopic Dolowackestone	39

Figure	Page
30. Facies IIa - Burrow Mottled, Oil-stained, Dolowackestone	39
31. Facies IIa - Excellent Porosity in a Burrow Mottled Dolomudstone	40
32. Facies IIa - Dark Oil-Stained, Burrow Mottled Dolomudstone	40
33. Photomicrograph of Facies IIa Mold Filling Baroque Dolomite	41
34. (A) Facies II - Excellent Moldic Porosity in a Burrow Mottled Dolowackestone; (B) Same as Figure 35A	43
35. Facies II - Burrow Mottled Wackestone With Recemented Molds	44
36. Photomicrograph of Facies II Moldic Porosity Infilled by Late Calcite Cement	44
37. Facies IIb - Abundant Microfractures in a Subtly Burrowed Dolomudstone	45
38. Facies IIb - Unsorted Dolomudstone Containing Medium-grained Quartz, Rounded and Unrounded Intraclasts that are Lithologically Varied	45
39. Facies IIb - Burrow Mottled Dolomudstone Containing Chert Nodules	46
40. Facies III - Undissolved Fossils in what is Overall a Dolomitic Mudstone. Fossils Include Pelmatozoans, Brachiopods, and Ostracods	48
41. Facies II - Burrow Mottled Dolowackestone	48
42. Facies III - Dolomitic Mudstone, Slightly Burrow Mottled	49
43. Facies III - Dolomitic Mudstone, Undissolved Thin Fossils, Limpid Idiomatic Dolomite Rhombs	49
44. (A) Facies IIb - Generally Featureless, Silty, Dolomudstone; (B) Facies III - Dark Grey, Silty, Dolomitic Wackestone	51
45. Facies III - Dark Grey, Dolomitic Wackestone	52

Figure	Page
46. Photomicrograph of Dolomitic Mudstone	53
47. Photomicrograph of Preserved Trilobite Fragment in Dolomitic Mudstone With Idiomatic Rhombs	53
48. Particle Packing and Particle Contact	56
49. x40 Plane Polarized Light. Facies I Idiomatic Dolomite, 20-50 Microns	57
50. x100 Plane Polarized Light. Facies I Hypidiomatic Dolomite	57
51. x40 Plane Polarized Light. Facies I Xenomatic Dolomite	59
52. x100 Plane Polarized Light. Facies II Brown Xenomatic Dolomite	59
53. x100 Plane Polarized Light. Facies II Brown Hypidio- topic Dolomite, Especially Well-formed Near Porosity	60
54. x100 Plane Polarized Light. Facies II Brown Hypidio- topic/Xenomatic Dolomite	60
55. x100 Plane Polarized Light. Facies II Brown Hypidio- topic Dolomite	61
56. x100 Plane Polarized Light. Facies III Dolomitic Mudstone with Typical Idiomatic Halo Type Rhombs . . .	61
57. x40 Plane Polarized Light. Facies III Cloudy Centers, Clear or White Rims	62
58. x100. Plane Polarized Light	62
59. x100 Plane Polarized Light. Facies III Idiomatic Rhombs Impinging on an Unreplaced Crinoid Ossicle . .	63
60. x40 Plane Polarized Light. Typical Facies III Dolomitic Mudstone With Calcite Fossils Stained red and Idiomatic Halo Rhombs Floating in the Unreplaced Micrite Matrix	63
61. x40 Plane Polarized Light. Moldic Porosity Developed in Facies II Dolowackestone	65
62. As Above	65
63. x20 Plane Polarized Light. Moldic Porosity Developed in Facies II Dolowackestone	66

Figure	Page
64. As Above	66
65. x20 Plane Polarized Light. Moldic Porosity in Facies II Dolowackestone	67
66. Plane Polarized Light. Extensive Intercrystalline Porosity in an Oil-stained Facies II Dolowackestone .	69
67. Plane Polarized Light. Extensive Intercrystalline Porosity in an Oil-stained Facies II Dolowackestone .	69
68. x200 Plane Polarized Light. Intercrystalline Porosity Enlarged at the Expense of Matrix Dolomite	70
69. x400 Plane Polarized Light. Partially Dissolved Rhombs Bordering or Floating in Intercrystalline Pores	70
70. x200 Plane Polarized Light. Common Dissolved Rhombs Associated With Intercrystalline Pores	71
71. x400 Plane Polarized Light. Facies I Intercrystalline Porosity Partially Occluded by Late Calcite Cement .	71
72. Relationships Between Depositional Facies, Porosity Percent, Dolomite Percent, and Porosity of Zones With 90 Percent Dolomite	72
73. x100 Plane Polarized Light	76
74. x200 Plane Polarized Light, Large White or Limpid Rims can be Seen Developed Into Previous Pore Space	76
75. x400 Plane Polarized Light. Large, Limpid or White Rhombs Growing in or Into Pore Space	78
76. x40 Plane Polarized Light. Large, White Rhombs Infilling a Vug	78
77. x400 Plane Polarized Light. Pre-compressional Idio- topic Rhombs Now-distorted by Compaction Into Hypidiotopic Rhombs	79
78. x200 Plane Polarized Light. Dolomite cut by Stylolite	79
79. x100 Plane Polarized Light. Brown, Cloudy Dolomite and the Clean Rims Affected by Compaction Along a Stylolite	80
80. x40 Plane Polarized Light. Syndepositional Fenestral Pores in Facies I	80

Figure	Page
81. x200 Plane Polarized Light. Algae Surrounded by Equant Calcite Cement in a Fenestral Pore	81
82. SEM Photograph of Small Anhydrite Lath with EDAX Element Peaks	82
83. x400 Crossed Nicols. Anhydrite Lath Bent by Compaction Across a Dolomite Rhomb. Anhydrite was Formed Before Compaction	83
84. Core Photograph of Early Replacive Chert	83
85. Closeup of Replacive Chert Nodule Showing Rhombs Floating in the Early Silica	84
86. Photomicrograph of Replacive Chert Showing Early Well-formed Rhombs	84
87. x40 Plane Polarized Light. Typical Fibrous Ghost Structure Observed in Replacive Euhedral Quartz, Indicating Former Anhydrite	85
88. x100 Plane Polarized Light. Fibrous Texture and Organic Matter Observed in Quartz	85
89. x100 Plane Polarized Light. Fibrous Texture and Organic Matter Observed in Quartz	86
90. x200 Crossed Nichols. Bright Anhydrite Inclusion in Quartz	86
91. Core Photograph of Rounded Nodules of Replaced Anhydrite. Center Nodule is 4 cm Across	88
92. Core Photograph of Large (6 cm) Anhydrite Nodule that has been Rimmed by Replacive Euhedral Quartz, Partially Dissolved, and Oil-stained	88
93. x100 Plane Polarized Light. Intercrystalline Calcite Cement Stained red	89
94. x100 Crossed Nicols. Vug Filling Late Calcite Cement Stained red	89
95. x400 Crossed Nicols. Rare Intercrystalline Polyhalite (?)	90
96. x200 Crossed Nicols Polyhalite (?) Cement Replacing Dolomite	90
97. x400 Crossed Nicols. Rare Late Anhydrite Cement	91

Figure	Page
98. x20 Crossed Nicols. Vug Filling Baroque Dolomite . . .	91
99. x40 Plane Polarized Light. Mold Filling Baroque Dolomite	92
100. x40 Crossed Nicols. Fracture Filling Baroque Dolomite	92
101. x100 Plane Polarized Light. Late Sphalerite Surrounded by Baroque Dolomite	93
102. x100 Plane Polarized Light. Anhydrite Inclusions in Quartz Replaced by Pyrite	93
103. x40 Cathode Luminescence	98
104. x200 Cathode Luminescence	98
105. x100 Plane Polarized Light	99
106. Cathode Luminescence of Above Thin Section Reveals Typical Four-part Zonation With Final Bright rim . .	99

CHAPTER I

INTRODUCTION

Location

The subject of this investigation is the Henryhouse Formation (Hunton Group, Niagaran and Cayugan Series, Silurian System) in the Western Anadarko Basin and Northern Shelf area in Western Oklahoma (Figure 1).

Statement of Purpose

Development of evidence toward defining conditions that lead to reservoir quality rock in the Henryhouse is the intent of this thesis. This formation was chosen because it has been an important yet elusive producer of oil and gas. Depositional environment and dolomitization models are proposed based on depositional facies and diagenesis observed in samples from ten Henryhouse cores. Relationships between porosity and these models are discussed.

Structural Setting and Geologic History

The Anadarko Basin (aulocogen) is highly asymmetric, with a steep and highly faulted southern margin. This margin constitutes the Frontal Wichita's fault zone to the north of the Wichita Mountain Uplift. The slope into the basin is gentle from the adjacent shelf areas to the northeast, north, and west (Figure 1).

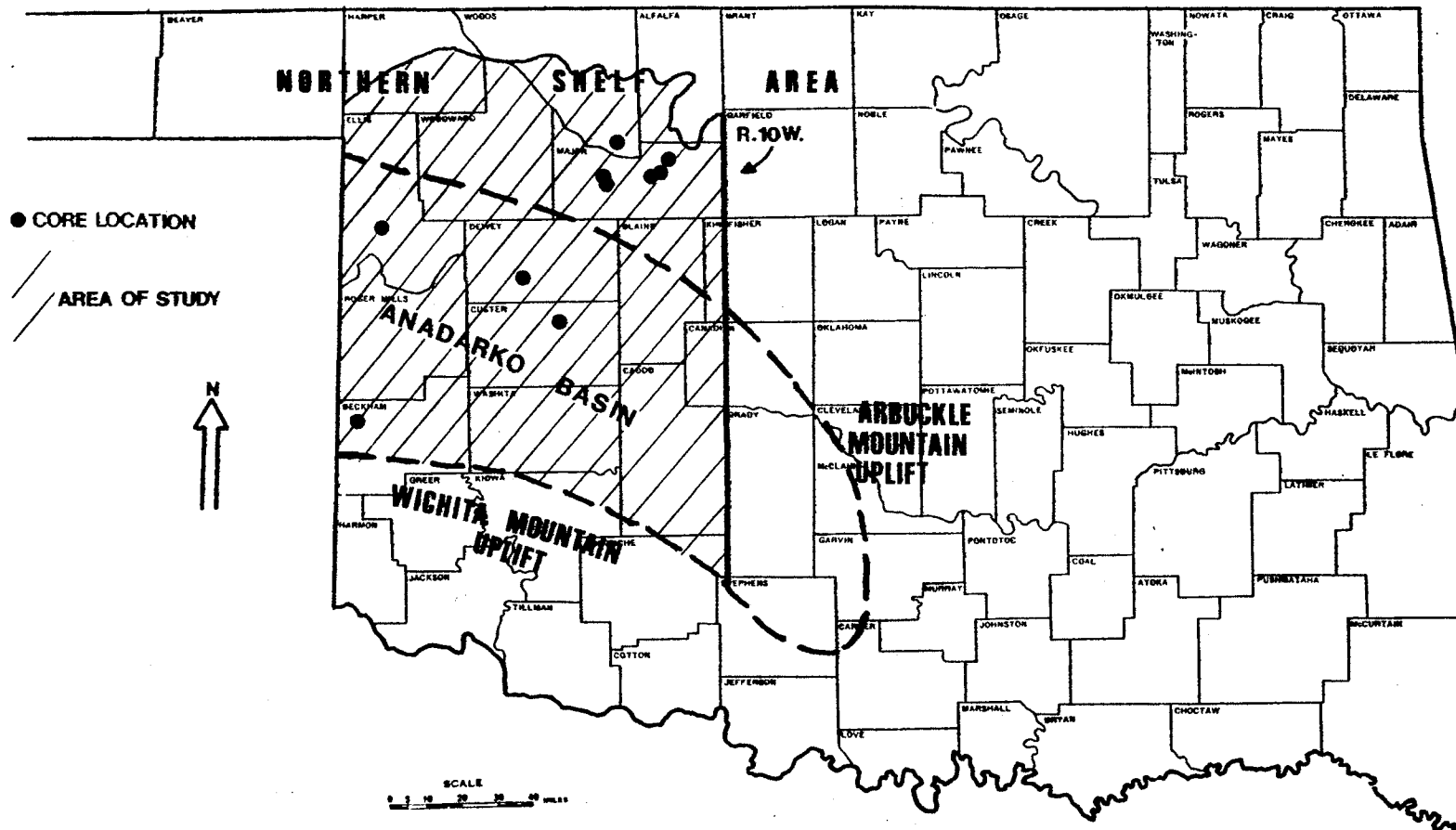


Figure 1. Area of Study and Local Structural Setting.

The Hunton Group is a series of carbonates that was deposited over most of the central and northern Oklahoma Platform during Upper Ordovician, Silurian, and Lower Devonian time. In contrast to Lower Paleozoic carbonates, the Hunton represents a relative hiatus resulting from an extremely slow rate of subsidence (Adler, 1979). It has been suggested that the Henryhouse was deposited during a tectonically stable period (Harvey, 1968) which is indicated by a relatively constant regional thickness (Shannon, 1962) and a very gradual thickening into the basin.

Following Hunton deposition, erosion truncated the sequence from the northernmost areas, leaving it absent over some of the platform. During this major hiatus, stream erosion superimposed a dendritic drainage pattern directed toward the southwest (Harvey, 1968; Isom, 1973; Amsden, 1975). This topographic surface was then filled in and buried during transgressive deposition of the Late Devonian, Early Mississippian Misner sandstone and Woodford shale. The broad Southern Oklahoma Geosyncline was subsequently transformed into the narrow, elongated, asymmetrical, NW-SE trending Anadarko Basin during Pennsylvanian time (Ham and others, 1964).

Methods of Investigation

Porosity is developed as a consequence of either depositional processes, diagenetic processes, or both. In an attempt to define suitable conditions for porosity development in the Henryhouse, evidence that facilitates construction of a depositional model and paragenetic sequence was compiled. The methods, summarized in Table I, include:

1. Description and interpretation of ten Henryhouse cores from west central Oklahoma, with special attention given to the environment

of deposition suggested by sedimentary structures and fauna. Each core was slabbed and selected pieces polished.

2. Thin section examination to support environmental interpretation using microfacies evidence (Flügel, 1982), determine diagenetic relationships, and observe general petrographic characteristics.

TABLE I
TYPE AND NUMBER OF DATA SAMPLES

CORE	TOTAL FT	THIN SECTIONS	X-RAY	EDAX	ISOTOPES
1. NFC Dietz	37	6	10	5	-
2. A. Hickman	50	7	16	3	-
3. C. P. Rose	37	5	12	-	-
4. A-1 Jordan	123	16	18	2	4
5. 2-34 Jordan	96	26	25	2	8
6. K. Wichert	40	5	8	-	-
7. K. Nichel	27	4	7	-	-
8. L. S. Hanan	49	10	10	3	1
9. GHK Hoffman	84	9	23	-	2
10. A. Green	<u>170</u>	<u>21</u>	<u>29</u>	<u>3</u>	<u>4</u>
	663	109	158	18	18

3. Construction of stratigraphic cross-sections using well logs and core data to help define the depositional environment.

4. X-ray diffraction and scanning electron microscopy (equipped with energy dispersive x-ray analyzer) for quantitative petrologic

description.

5. Oxygen and carbon isotope analyses to obtain information about the nature of the formation fluid responsible for diagenetic minerals, especially dolomite.

6. Cathodoluminescence to reveal microfabrics and composition changes developed during diagenesis.

CHAPTER II

PREVIOUS WORK

Stratigraphy

The Henryhouse Formation was originally distinguished in outcrop as a subdivision of the Hunton by Reeds (1911). Later studies by Reeds (1927) and Amsden (1957, 1960, 1975) endorse this subdivision (Figure 2). The contact with the subjacent Chimney Hill Formation (Late Ordovician, Early and early Late Silurian) is a well defined, lithostratigraphic boundary (Shannon, 1962; Amsden, 1975). The nature of the contact with the overlying Haragan Formation has been interpreted several ways. According to Amsden (1975), the boundary represents a significant unconformity separating Upper Silurian from Lower Devonian. This division is made based on differences in megafauna as the two strata are indistinguishable lithologically. As a consequence of the difficulty in lithologically defining the Henryhouse Formation, Amsden (1975) proposed that it may largely be correlated in the subsurface as the *Kirkidium* biofaces. This biofacies is defined by the presence of two large pentamerid brachiopods reported to be present throughout much of the subsurface of central and western Oklahoma and the Texas Panhandle (Amsden, 1975). Presence of a Haragan-Henryhouse unconformity has been discounted by Shannon (1962) (Figure 2). He concluded that "there were no significant periods of erosion during

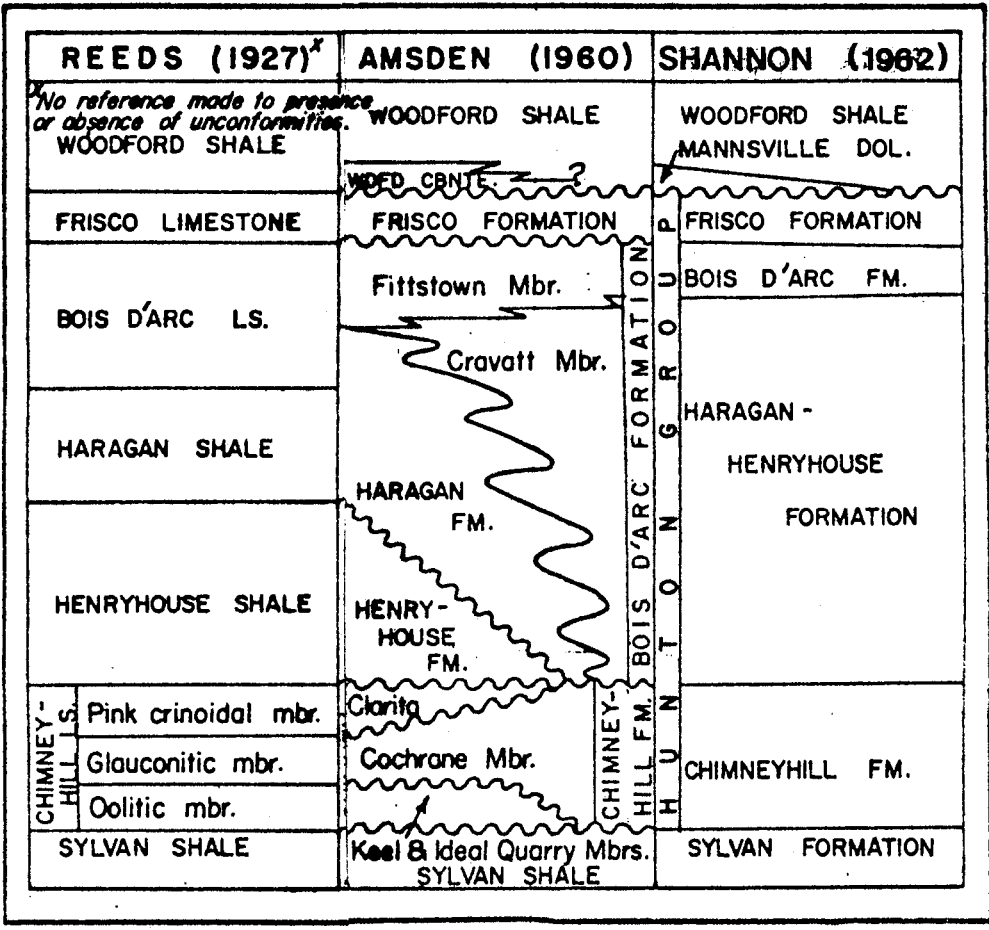


Figure 2. Hunton Stratigraphy

the time represented by the Haragan-Henryhouse" (p. 14), and "slight differences in the two faunal assemblages within the Haragan-Henryhouse interval are attributed to environmental shift instead of hiatus" (p. 25).

Environment of Deposition

The environment of deposition suggested by Amsden (1975) following investigation of surface exposures is "a low-energy environment well removed from active wave and (or) current action yet shallow enough to develop a richly varied marine fauna" (p. 28). Amsden (1975) also described Late Silurian strata in the subsurface. Various biofacies were described and related to different lithofacies with corresponding paleoenvironmental interpretations. Briefly summarized, these paleoenvironments include: 1) a low-energy environment from shallow to deep sublittoral representing the marlstone facies; 2) increased wave and current action in the Kirkidium lithofacies toward the northwest indicating a possible shoaling away from the deeper marlstone facies, and 3) a relatively high energy facies further northwest with less fossil diversity and a calcareous sand bottom (see Amsden, 1975, for further explanation).

Petrography

Petrographic investigations of the Hunton Group are rare. Regional subsurface investigation of the Hunton Group including comprehensive description of Henryhouse microfabrics and textures was accomplished by Amsden (1975). Isom (1973) used binocular inspection of core and cuttings to describe the Henryhouse in Woods, Major, and Woodward Counties.

A report centered on deep burial diagenesis of the Hunton interval by Borak (1978) included petrographic description of microfabrics and textures using cuttings from the Lone Star Baden well (30,050 feet deep) and cores and cuttings from throughout the Texas Panhandle.

Porosity

Porosity in Silurian Hunton has created excellent reservoirs in the western part of Oklahoma in Kingfisher, Blaine, Major, Alfalfa, Woods, Harper, Woodward, Ellis, and Custer Counties (Amsden and Rowland, 1971). Porosity in the Hunton has commonly been related to dolomite (Amsden, Borak, Isom, Harvey). Amsden (1975) provides a thorough description of porosity in the Henryhouse and equivalent Kirkidium biofacies. According to his description, porosity is "closely related to the distribution of crystalline dolomite" (p. 65) but porosity varies greatly and abruptly within the crystalline dolomite. It is also stated that some of the porosity in the dolomite is associated with development of a crystalline texture, but significant porosity is largely due to dissolution of fossils and partial removal of the micritic matrix. The significant porosity was similarly described by Borak (1978).

Dolomite

Amsden (1975) reported a regional concentration of dolomite in the Silurian of Oklahoma. He noted numerous stratigraphic and geographic variations in the degree of dolomitization, but maintains that a progressive trend of increasing dolomite is present from the limestone of the Arbuckle Mountains-Criner Hills to the magnesium rich strata northward and westward. Northwest of the highly dolomitized area, Silurian rocks

are reported to grade rather abruptly into low magnesium limestones (Amsden, 1975).

Textural variations in Silurian Hunton caused by progressive dolomitization were recognized by Amsden (1975), especially well documented in the Henryhouse formation. According to Amsden, low magnesium carbonate rocks will have common to abundant euhedral crystals in a finely divided calcium carbonate matrix. Intermediate magnesium carbonate rocks will have abundant dolomite crystals which impinge against and corrode fossil boundaries. High magnesium carbonate rocks (at least 28 percent $MgCO_3$) will have interlocking crystals of dolomite and fossils presented only as molds or by calcspar or dolospar. Amsden also noted that zones containing unreplaced fossils with floating euhedral rhombs abruptly pass into zones with crystalline dolomite and dissolved fossils. Similar stages of dolomitization were reported by Borak (1978).

Isom (1973) described two types of dolomitization: a penecontemporaneous replacement dolomitization, and a secondary, late stage type which he relates to the circulation of magnesium-rich waters moving along the Woodford unconformity and related fractures. Amsden (1973) proposed that Silurian dolomite represents a regional dolomitization not related to any tectonic features or to the Woodford unconformity (p. 46). He also interpreted the Silurian dolomite as a penecontemporaneous replacement in a marine environment seaward of the tidal zone. Some shallowing of the water is proposed from the limestone to the dolomite limestone to the dolomite lithofacies, although no shallow water sedimentary structures were observed. Some late sparry dolomite is reported filling cavities.

CHAPTER III

DEPOSITIONAL FACIES AND DEPOSITIONAL ENVIRONMENT

Introduction

During Silurian time, the developing Anadarko Basin subsided at an extremely slow rate (Adler, 1971; Feinstein, 1981). Under these stable tectonic conditions the Henryhouse Formation was deposited over much of Oklahoma with no major unconformities breaking deposition (Shannon, 1962). It does not seem unreasonable to assume that regionally similar depositional conditions produced these carbonates.

Before a depositional model can be considered for the Henryhouse, similar facies must be regionally identified. These facies can then be related to a similar mode of development.

Depositional Facies

Diagenetic influence (compaction, dolomitization, and dissolution) has somewhat obscured the original sedimentary structures and fossil content of the Henryhouse Formation. Despite this influence, sufficient evidence remains to recognize three distinct depositional facies. Core slab, thin section, and x-ray diffraction data are used to characterize each facies. Environmental interpretations attached to the following facies were arrived at by using the various criteria (Flügel, 1983) shown in Figure 3.

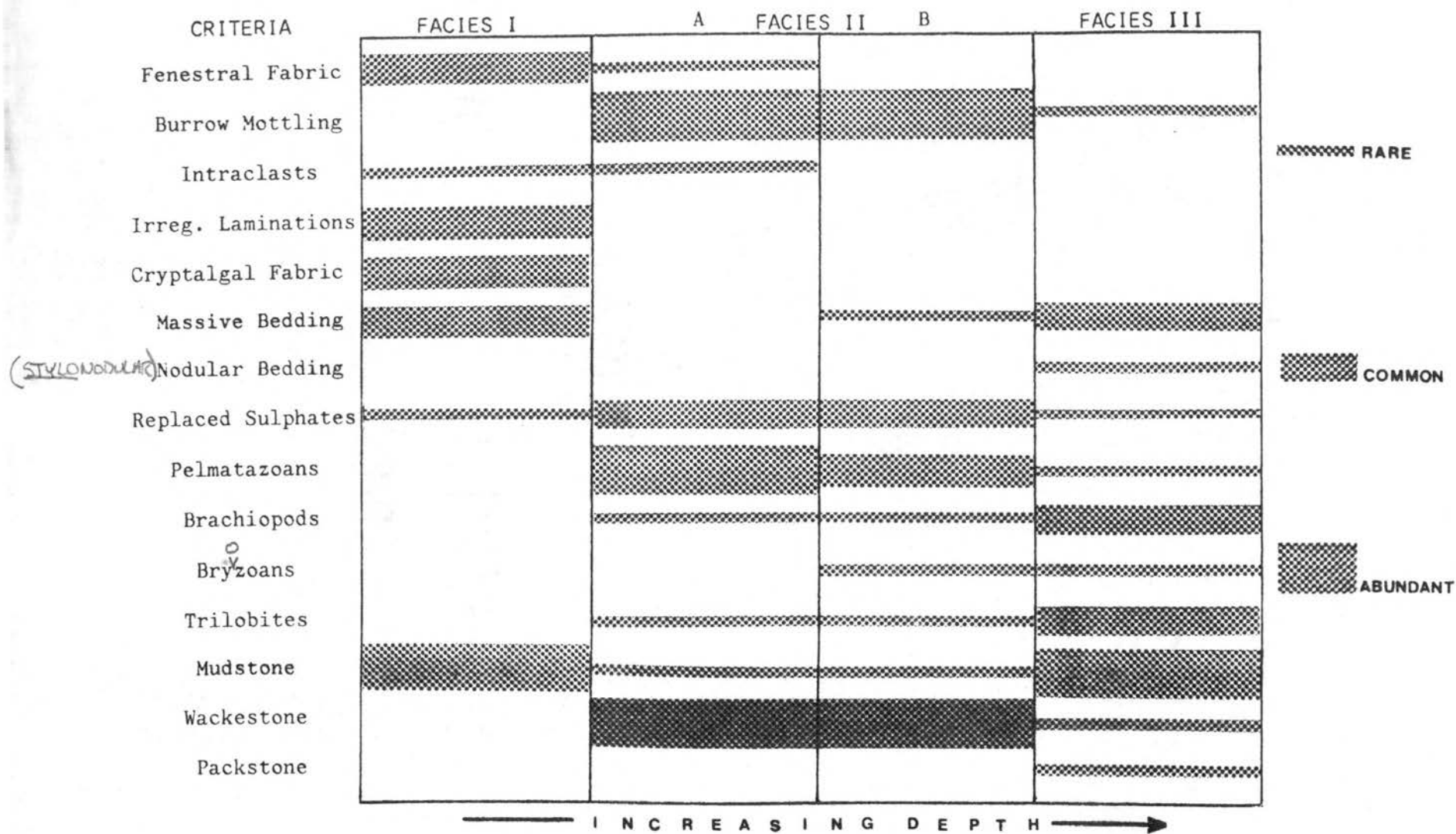


Figure 3. Relative Abundance of Principal Facies Criteria

Facies I

Cryptal algal fabrics, fenestral fabrics, irregular laminations, lack of fossils, and lack of burrow mottling are the salient features of this facies. Silica nodules, silt sized quartz, intraclasts, peloids, and low amplitude stylolites may all be present in what is typically a light colored dolomudstone with no porosity. A shallow, restricted shoreline environment is indicated particularly by the lack of fossils and non-burrowed irregular laminations.

Facies II

Burrow mottling makes this facies visually distinct. All samples of this facies are fully dolomitized with good to excellent porosity, and are predominantly wackestone. Fossil percent and type were usually estimated, due to dissolution of the original grains. Molds and occasionally remaining grains indicate that crinoids were the most common fossil. Intraclasts, silica and carbonate nodules, and silt sized quartz are likely to be present; stylolites are rare and generally high amplitude. The highly burrowed appearance and accumulation of rather sorted coinoid fragments suggests shallow, but more seaward conditions with increased water agitation in or adjacent to the zone of wave action.

Facies III

This facies is typically a medium dark, silty, dolomitic mudstone. Fossils include brachiopods, with less common trilobites, ostracods, bryzoans, and echinoderms. This facies is often featureless, but may exhibit burrow mottling, nodular bedding, or storm type deposits. The

more diverse fauna and delicate, unsorted, well preserved fossils indicate a lower energy, shallow open shelf environment below normal wave base.

Depositional Environment

Ten Henryhouse cores from the Anadarko Basin in western Oklahoma were examined. Six of these cores are concentrated on the Northern Shelf of the basin with four located to the south and west (Figure 1). Using specific facies criteria (Figure 3), it was possible to identify the carbonate in each core as one or more of three depositional facies. These three facies can be integrated into a depositional model with the variation between facies reflecting the range of conditions within this model.

The most reliable method to avoid erroneous environmental interpretations is to use vertical sequences of associated sedimentary features and their implied transitions (Ginsburg, 1975; Enos, 1983). The typical vertical sequence of facies recognized in the Henryhouse is shown in Figure 4. Although no cored intervals contain all three facies, six of the cores contain two. In each case, shallower water facies are above deeper water facies, indicating marine regression or shoreline progradation creating a net regressive effect. Stratigraphic correlations (Figures 5, 6, 7) of the cores taken from the Northern Shelf demonstrate a consistent shallowing upwards nature, lateral persistence, relatively uniform thickness along depositional strike, and very gradual thickening to the south toward the paleodepocenter.

The general depositional setting suggested by vertical and lateral relationships is a broad, shallow, low energy, epicontinental sea

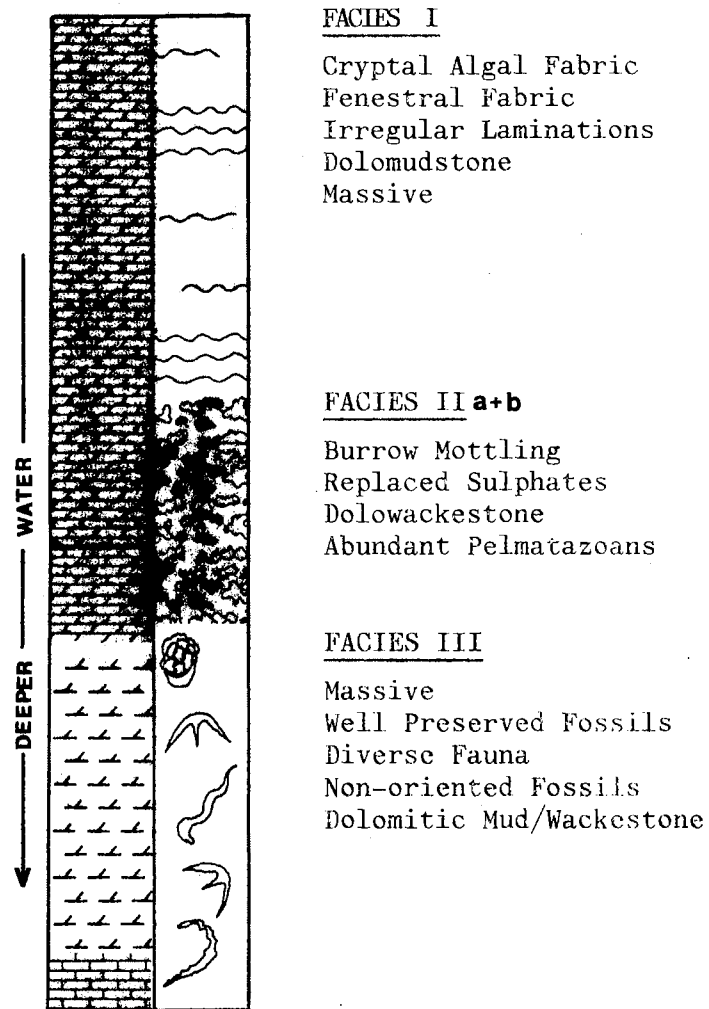


Figure 4. Typical Vertical Sequence of Sedimentary Structures, Fauna, and Mineralogy Relationships Observed in Core and Thin Sections. Facies Interpretations Indicate Marine Regression/Shoreline Progradation

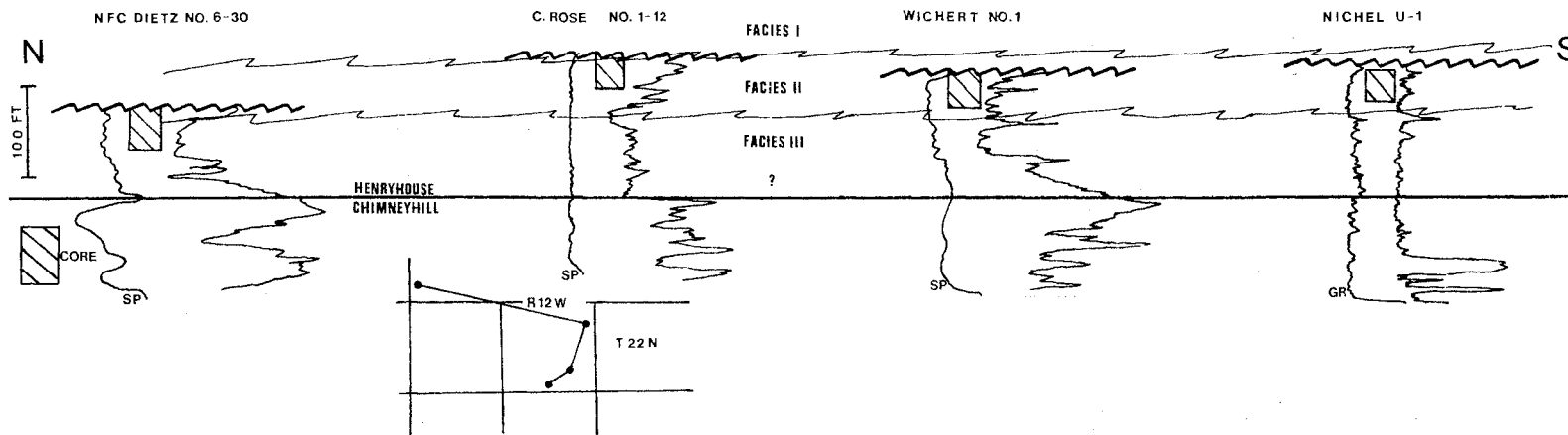


Figure 5. Stratigraphic Cross-section Based on Electrical Logs and Core, Illustrating Facies Relationships. (The formation above the unconformity at the top is the Woodford shale.)

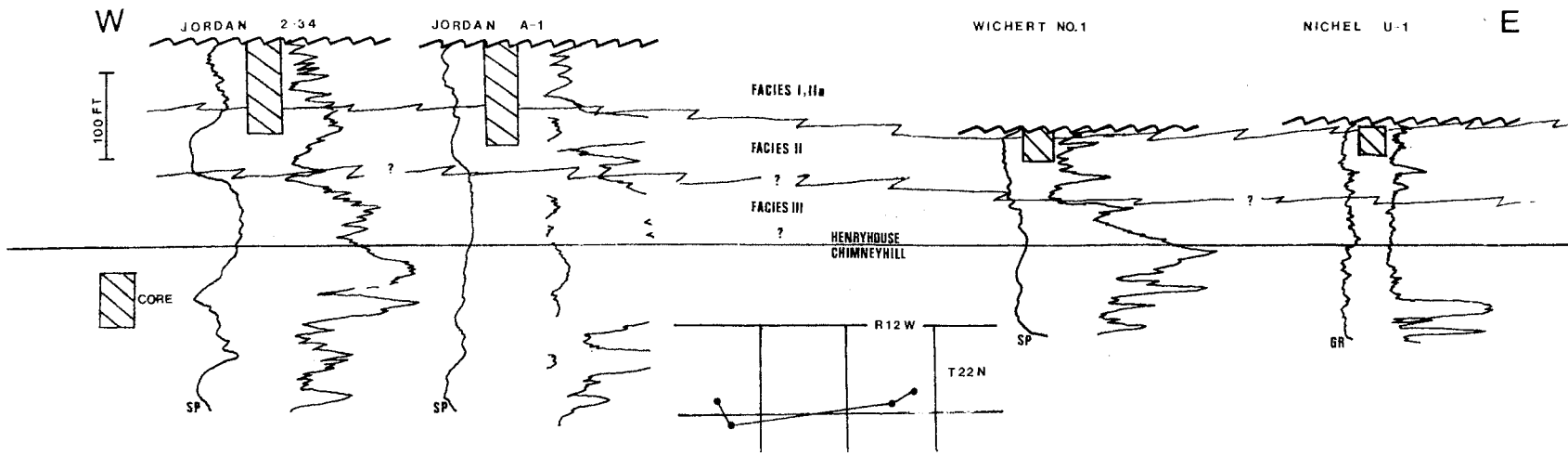


Figure 6. Stratigraphic Cross-section Based on Electrical Logs and Core, Illustrating Facies Relationships. (The formation above the unconformity at the top is the Woodford shale.)

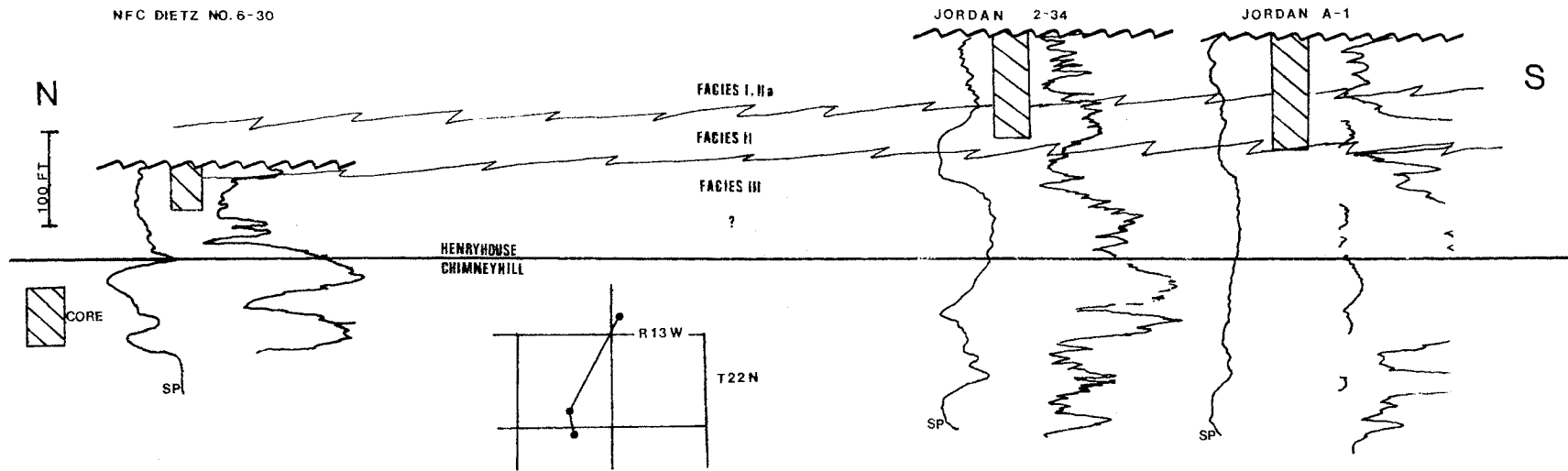


Figure 7. Stratigraphic Cross-section Based on Electrical Logs and Core, Illustrating Facies Relationships. (The formation above the unconformity at the top is the Woodford shale.)

producing broad facies bands oriented parallel to the paleoshoreline (Irwin, 1965). Figure 8 is a figurative cross-section illustrating the interpreted facies relationships within this general setting at any one time during deposition of the Henryhouse Formation. Associated sedimentary structures and their vertical sequence indicate three basic environments:

1. Upper intertidal to supratidal-tidal flat, deposited very near or above mean high tide; exposed a minimum of once or twice daily (Facies I).

2. Shallow, restricted subtidal to upper intertidal; deposited within or just below normal high tide and normal low tide; exposed a maximum of once or twice daily (Facies II a and b).

3. Open shelf subtidal, continually submerged (Facies III).

During transgression or regression, each facies environment would migrate, allowing deposition of continuous rock bodies of similar carbonate facies types over wide areas (Irwin, 1965). The very minimal depositional slope was apparently quite uniform, interrupted rarely by local topography. Even without significant physiographic barriers, the damping effect of broad reaches of shallow water resulted in restricted shoreline conditions (Facies I and IIa), elevating salinity (Enos, 1983).

Cores of the entire Henryhouse sequence are not available. The cores examined unanimously exhibit a shallowing upwards nature. However, it is likely that less developed transgressive events are present in some areas of the basin, in some sections of the vertical sequence. The thickness of a complete facies sequence is considerably less than the thickness of the entire Henryhouse Formation, indicating stacking of several sequences. Long periods of relative tectonic stability except

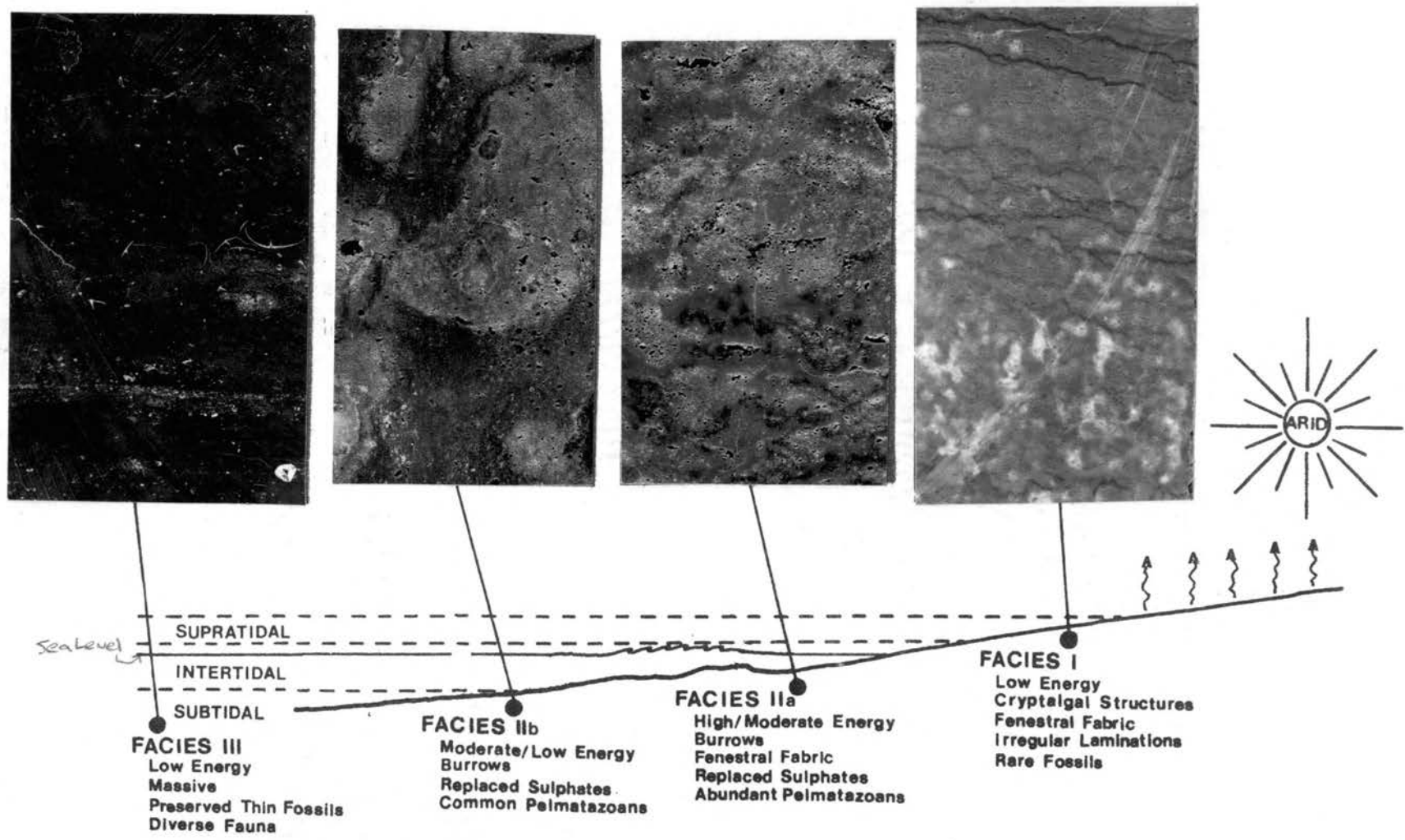


Figure 8. Schematic Cross-section Showing Distribution of Henryhouse Depositional Facies. Vertical Scale is Greatly Exaggerated. (Modified after Esteban and Klappa, 1983 p. 2.)

for minor subsidence explains predominant regressive sedimentation (Roehl, 1967).

Regional facies correlation was not attempted, but regressive vertical sequences containing similar depositional facies criteria were observed over a wide area, suggesting a similar depositional model is applicable (see core descriptions of Lone Star Hanan, G. H. K. Hoffman, and Apexco Green). The Apexco Green core is especially interesting because it is located near the thickest Hunton Group buildup, yet has a thick section of shallow water facies (Facies I). This indicates sedimentation was rapid enough to keep pace with the subsidence rate and maintain shallow water sedimentation throughout the basin.

Although supratidal and upper intertidal features were observed in cores from the shelf area, a ^{thick preserved} fully developed Facies I interval was found only in the Apexco Green core. It seems unlikely that depositional conditions were so variable as to permit only a localized supratidal environment to develop. The consistently shoaling upwards sequences examined on the shelf are truncated by the overlying Woodford shale. The Henryhouse carbonates removed by pre-Woodford erosion ^{included} were very probably the ~~missing well developed~~ Facies I.

Core Summaries and Interpretations

The Henryhouse cores were selected for examination and sampling. Core locations are plotted on Figure 1, and core descriptions can be found in the Appendix. Cores were examined for gross lithology, fossils, and sedimentary structures. Analysis of the cores, especially the sedimentary structures and vertical sequence, aided in determination of sequential facies and depositional environment. Each of the cores is briefly

summarized and interpreted in the following paragraphs. Cores with inferred Facies I features are presented first, Facies IIa and b second, and Facies III last.

Apexco Green-Natomas No. 1, 31-10N-26W

Cored Depth: 19599-19770 ft

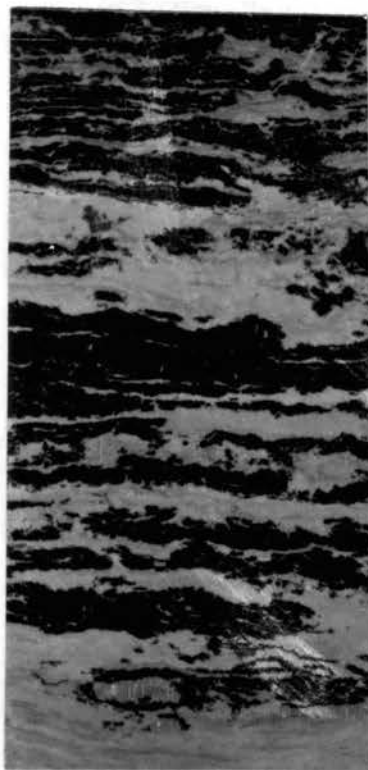
The cored interval consists largely of a single facies with a second possibly present at the base, indicating marine regression. The upper facies (19599-19770 ft) is a light-to medium dark grey dolomite, dolomitic and lime mudstone, and peloidal limewackestone. Fossils are rare or absent. Fenestral fabrics, algal laminations, irregular carbonate laminations, and massive fabrics are all common. Intraclasts are rare and fine, low amplitude stylolites are abundant, especially in the lime mudstone (Figures 9-12). The lack of fossils and type of fabrics is indicative of a restricted tidal flat depositional environment (Facies I).

The lower 10 ft (19,760-19,770 ft) is represented by a small number of samples, making recognition of facies criteria difficult. Two thin sections exhibit good porosity, resulting from what are interpreted as molds and enlarged molds, along with a burrowed appearance. The increase in fossils and presence of burrows seem to indicate transition into a zone of higher energy (Facies IIa)(Figure 13).

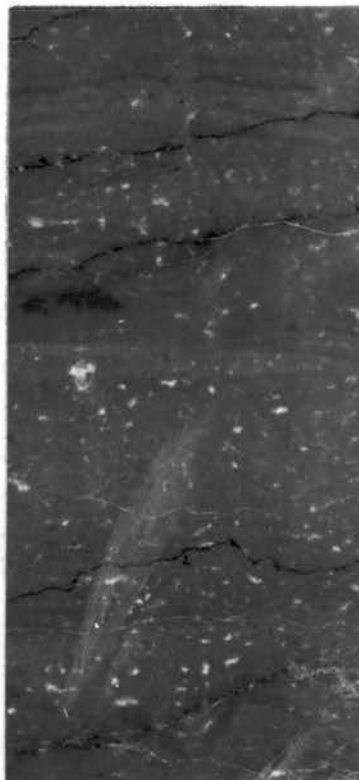
Tenneco Jordan No. 2-34, 34-T22N-R14W

Cored Depth: 8464-8570 ft

The interval cored may be divided into two discrete facies which imply marine regression. The upper facies (8464-8539 ft) is a light



(A)



(B)

Figure 9. (A) Facies I - Laminated Dolomite and Cryptal Algal Fabrics in a Dolomudstone (AG-19615);
(B) Facies I - Laminated Birds-eye Fenestral Fabric in a Dolomudstone (AG-19633)

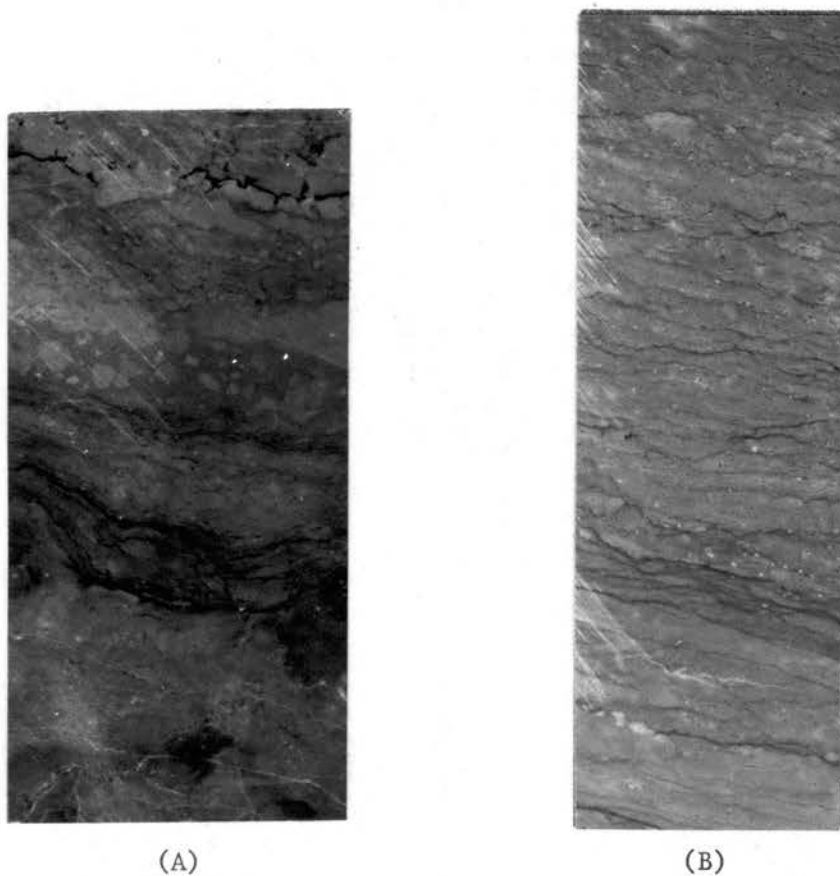


Figure 10. (A) Facies I - Possible Storm Layer in Dolomudstone (also note possible enterolithic structure at top (AG-19679); (B) Facies I - Pelloid-rich, Irregular Laminations in a Lime Mudstone (AG-19733)

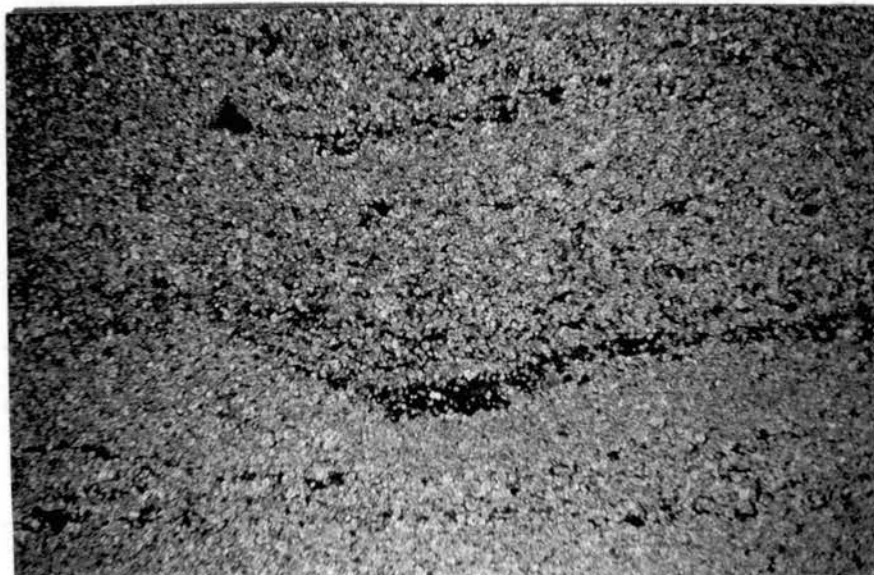


Figure 11. Facies I - Photomicrograph of Laminations Preserved in Dolomite (AG-19624 x 10 plane polarized light)

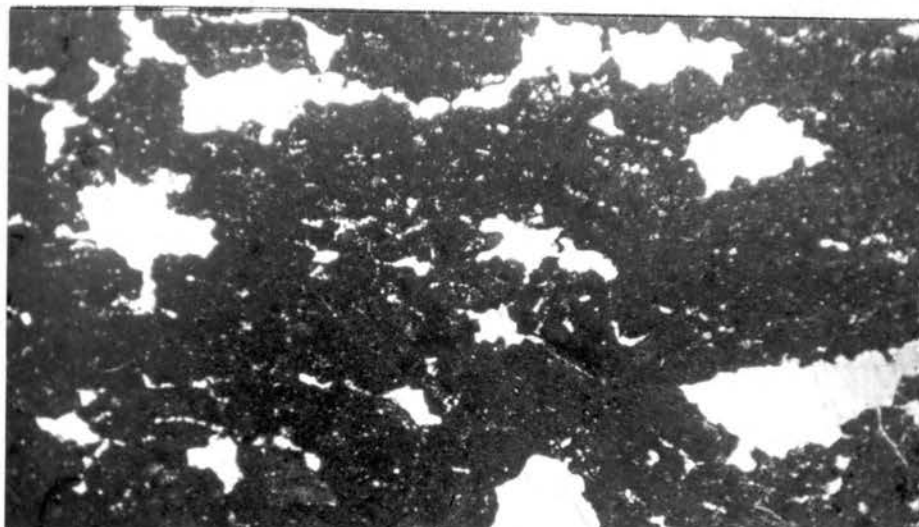


Figure 12. Facies I - Photomicrograph of Cryptal Algal Fenestral Fabric (AG-19733 x 40 plane polarized light)

grey, silty, dolomudstone. Fossils are rare or absent; occasional irregular laminations are visible but not obvious. Siliceous nodules^(replaced sulphates) are common; closed fractures and low amplitude stylolites are present (Figures 14, 15, and 18). The inferred environment of deposition is a restricted tidal flat (Facies I).

The lower facies (8540-8570 ft) has a sharp upper contact and is an oil-stained dolowackestone. The fossils are comprised chiefly of crinoid fragments, many of which have been dissolved, creating moldic porosity. Burrow mottling is very well developed. Nodules of^{saddle} dolomite, calcite, and less significant silica and pyrite are present (Figures 16 and 17). The inferred environment of deposition is intertidal (Facies II).

Tenneco Jordan No. A-1, 3-T21N-R14W

Cored Depth: 8471-8614 ft

The cored interval contains two distinct depositional facies that indicate marine regression. The upper facies (8489-8579 ft) is a medium grey, dolomudstone. The upper 32 ft is oil-stained brown. Most of the fossils have been dissolved; crinoids were the predominant fossil identified from molds; some brachiopods are present. Burrow mottling is strongly developed to the depth of 8547 ft, where sedimentary structures become subdued or absent. Nodules containing^{saddle} dolomite, quartz and chert are common; nodules containing anhydrite are present. Stylolites are rare but usually very high amplitude (Figures 19-21). The lower 31 ft of this interval is generally barren of facies criteria but seems to suggest a slightly lower energy environment than the upper part of this interval (Facies IIa).

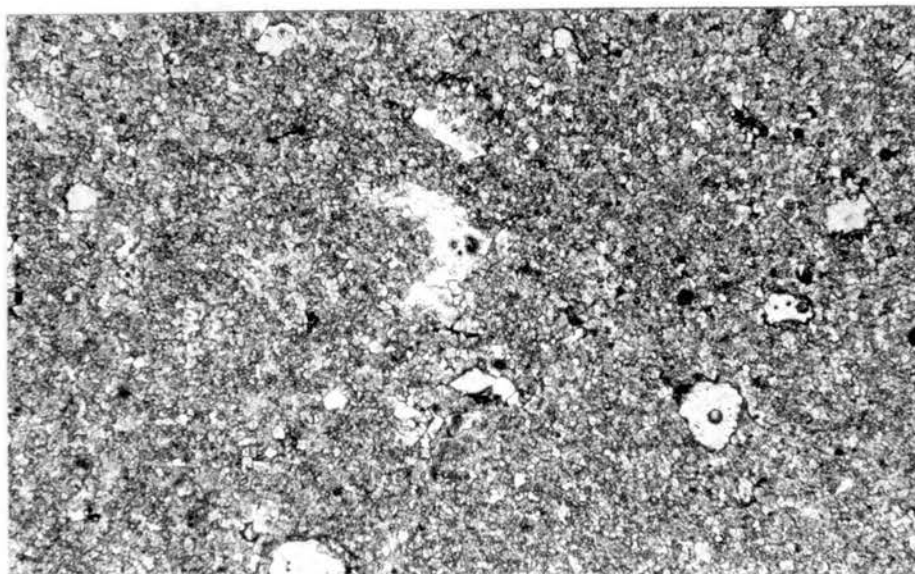


Figure 13. Facies IIa - Photomicrograph of Moldic Porosity in a Dolowackestone (AG-19770 x plane polarized light)

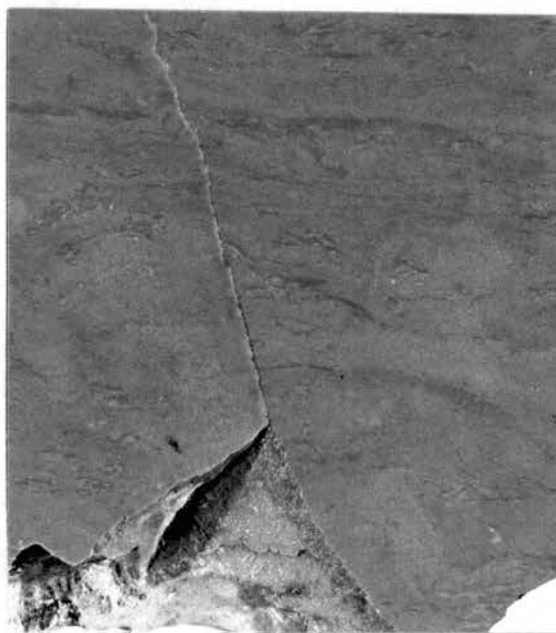


Figure 14. Facies I - Silty Dolomudstone With Irregular Laminations (JT 2-34-8511)

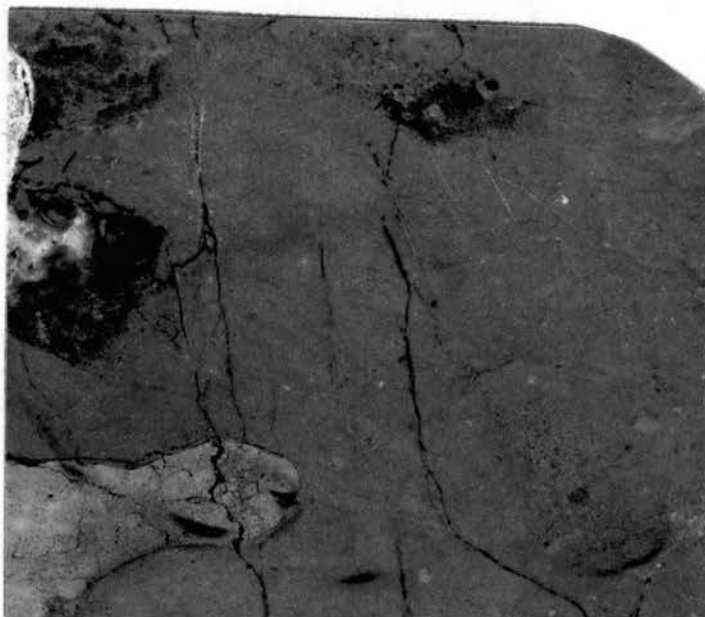


Figure 15. Facies I - Silty, Massive, Vertically Fractured, Dolomudstone Containing a Chert Nodule (JT 2-34-8467)

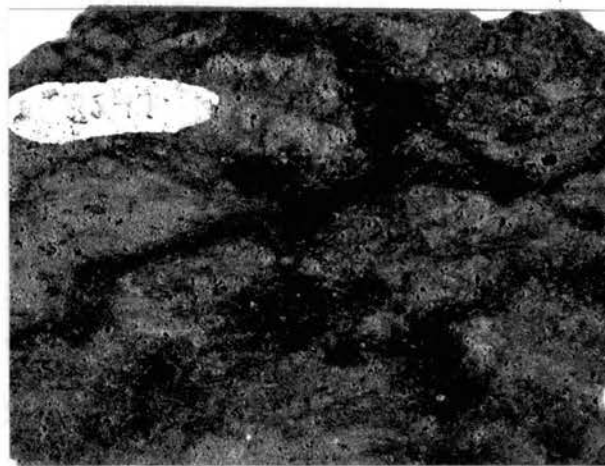


Figure 16. Facies IIa - Oil-stained, Burrow Mottled, Dolowackestone With Good Moldic and Vuggy Porosity (JT 2-34-8547)



Figure 17. Facies IIa - Same as Figure 16 (JT 2-34-8857)

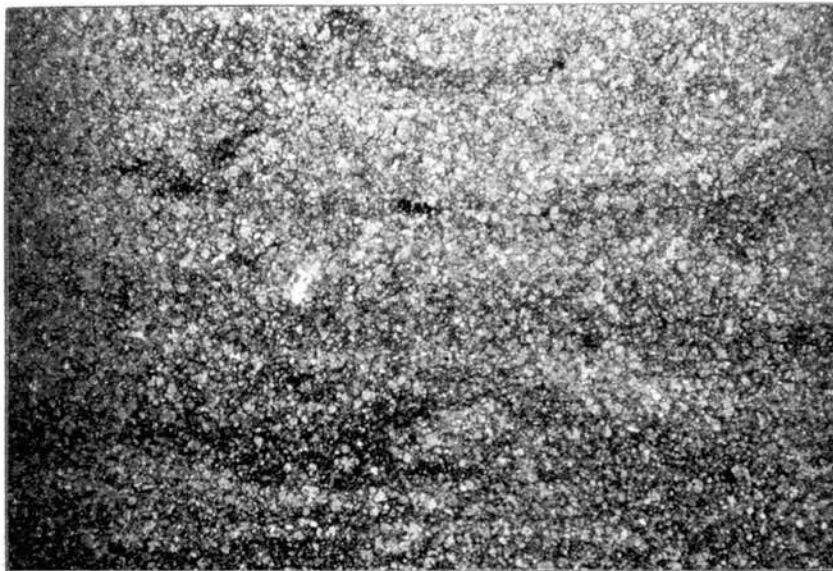


Figure 18. Facies I - Photomicrograph of Faint Laminations Preserved in Dolomite (JT 2-34-8500)



(A)



(B)

Figure 19. (A) Facies IIa - Oil-stained, Burrow Mottled, Porous Dolomudstone/Wackestone (JT A-1-8489); (B) Facies IIa - Same as 8489. (Note pseudomorphic quartz and calcite nodules (JT A-1-8530))

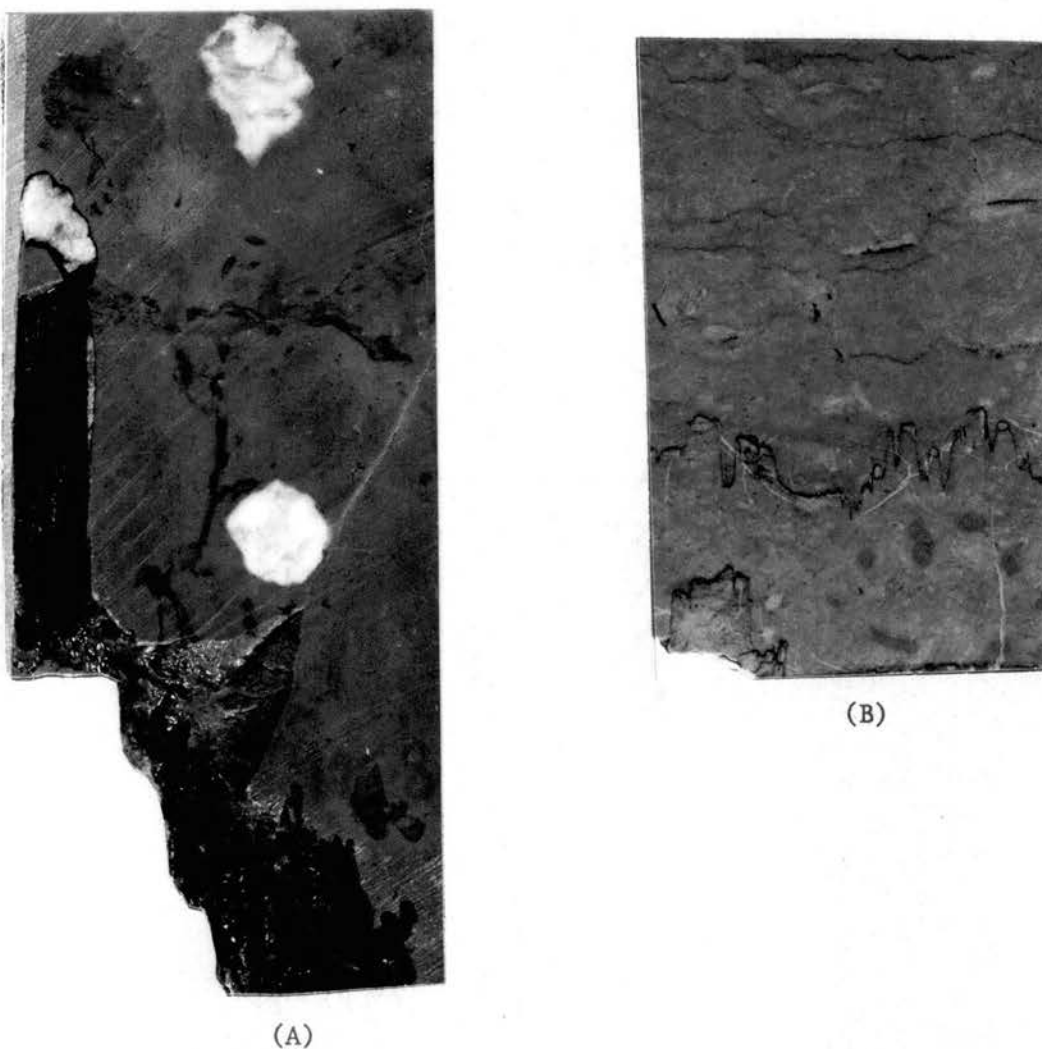


Figure 20. (A) Facies IIa - Faintly Mottled Dolomudstone With High Amplitude Stylolite. (Note rounded nodule of pseudomorphic quartz and calcite trapped along stylolite seam, indicating pre-stylolite formation) (JT A-1-8560); (B) Facies IIb - Dolomitic Wackestone Containing Pelmatozoans, Trilobites, Bryzoans, and Brachiopods (JT A-1-8602)

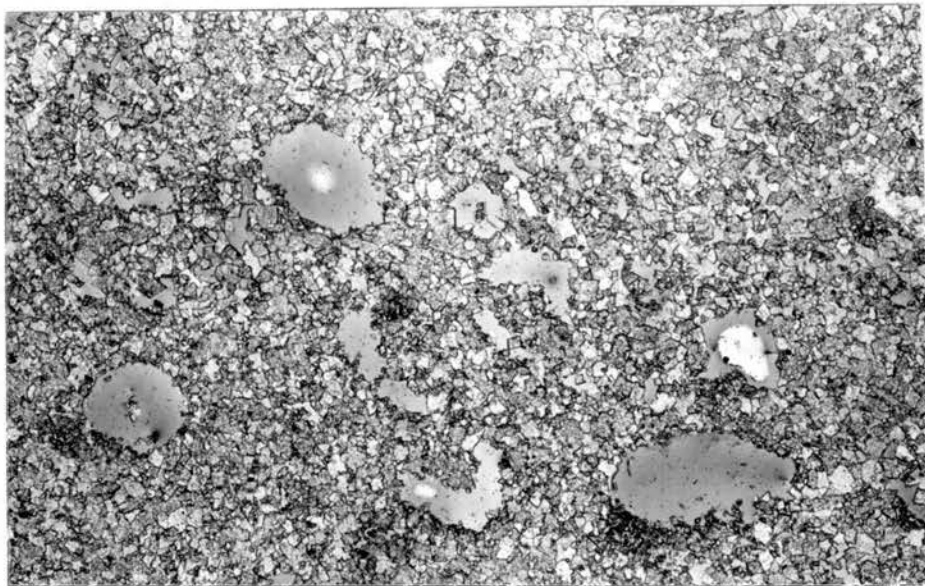


Figure 21. Photomicrograph of Moldic Porosity in Hypidiotopic Facies IIa Dolomite (JT A-1 8563 x 10 plane polarized light)

The subjacent interval is a medium dark to light grey, dolomitic mudstone, wackestone, and packstone. Mottling and nodular bedding are present. Fossils include pelmatozoans, brachiopods, trilobites, and bryzoans (Figure 22). Nodules containing quartz, calcite, and dolomite are present. Stylolites are low to medium amplitude and become abundant probably due to diminished dolomitization. The fabric and faunal changes indicate a higher energy, less restricted environment (Facies IIb, III).

Kirkpatrick, Natol, and NCRA Wichert No. 1,

26-T22N-R12W. Cored Depth: 7770-7810 ft

The cored interval is a medium light grey dolowackestone. The fossils are predominantly dissolved, creating excellent moldic porosity. The molds and few remaining fossils indicate crinoids were the dominant skeletal material. Burrow mottling is abundant and is associated with the most porous zones. Faint laminations are present throughout the core and coincide with less burrowing, fossil grains, and porosity. Low amplitude stylolites and nodules containing quartz and calcite are present (Figures 23-26). This interval suggests normal marine conditions with moderate to low wave energy (Facies IIa).

Kirkpatrick and Natol Nichel No. 1, 34-22N-12W,

Cored Depth: 7880-7907 ft

This core was taken within two miles of the Wichert No. 1 and is almost identical. The cored interval is medium light grey dolowackestone. The fossils have been largely dissolved and consist mainly of crinoidal fragments. A few bryzoans, trilobites, and brachiopods were identified by Amsden (1975). Burrow mottling is abundant and associated

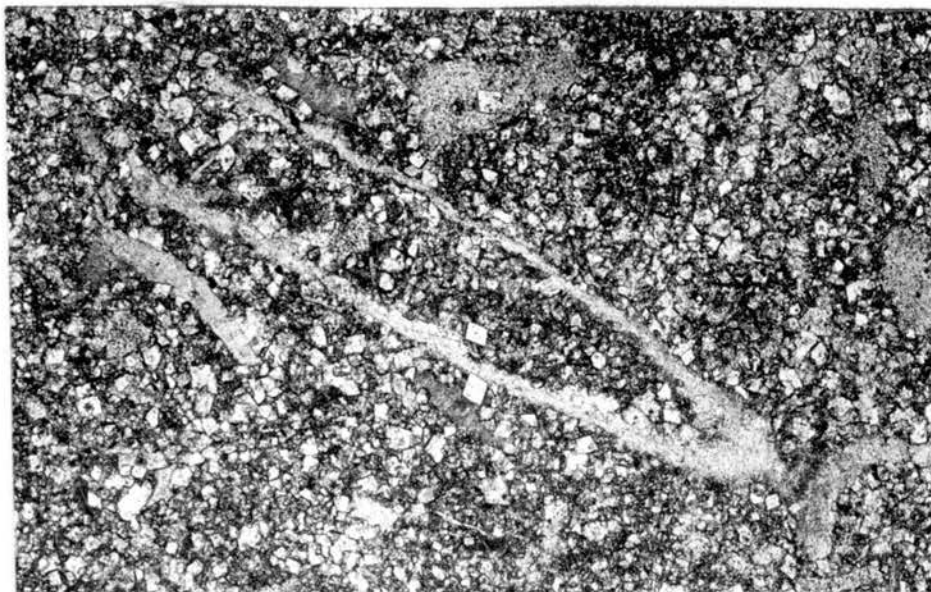


Figure 22. Photomicrograph of Undissolved Fossils in Facies III Dolomitic Mudstone. (Note limpid idiopic rhombs.) (JT A-1-8604 x 40 plane polarized light)



Figure 23. Facies IIa - Excellent Porosity in an Extensively Burrowed Dolowackestone (KW-7780)

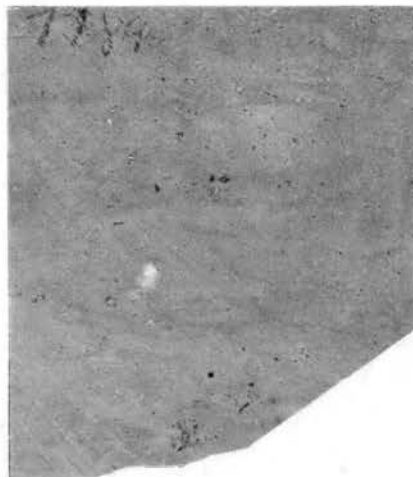


Figure 24. Facies IIa - Possible Laminations in a Dolomud-Wackestone (KW-7789)

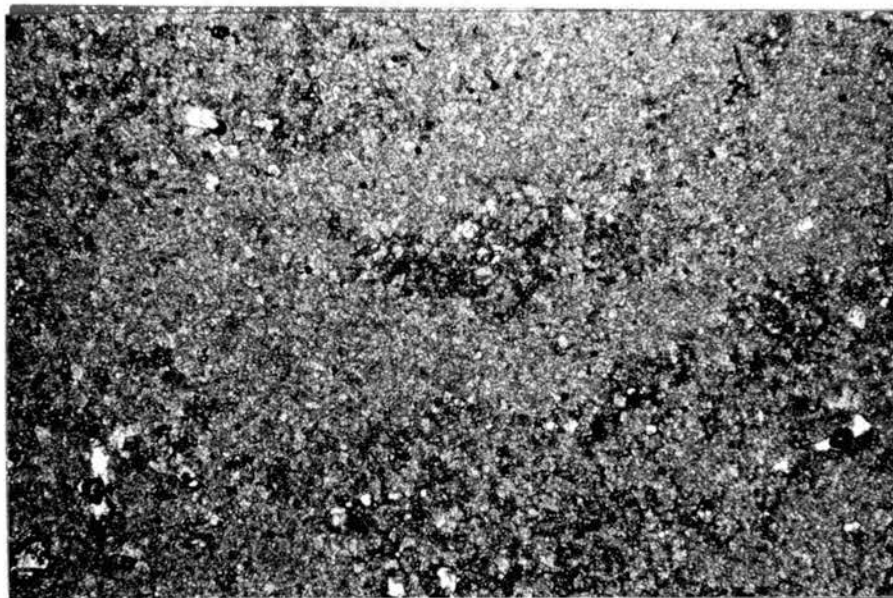


Figure 25. Photomicrograph Showing Irregular Distribution of Intercrystalline Porosity Related to Burrowing (KW-7783 x 20 plane polarized light)

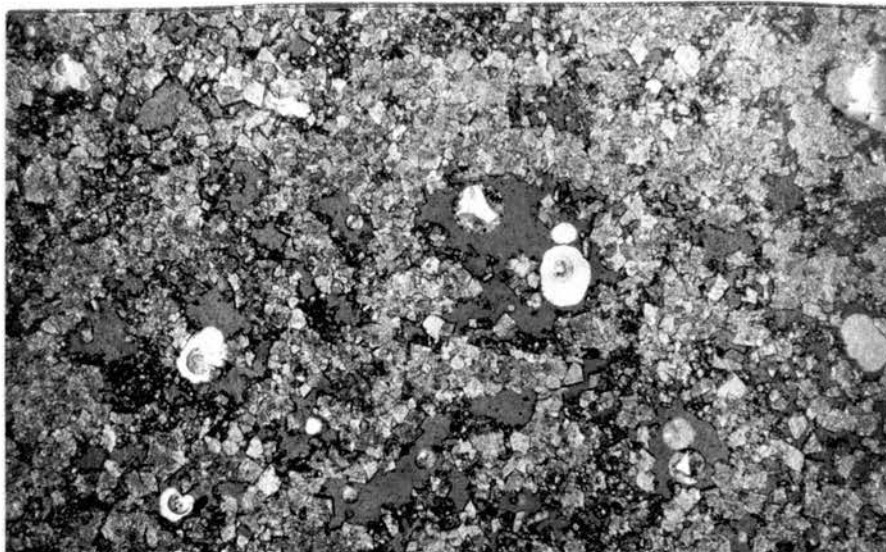


Figure 26. Photomicrograph of Enlarged Moldic and Intercrystalline Porosity in a Dolowackestone (KW-7771 x 20 plane polarized light)

with the greatest porosity. Horizontally elongated vugs are occasionally observed and suggest stromatactus fenestral pores. Quartz and later calcite comprise occasional nodules. Trylobites are low to medium amplitude and common (Figures 27-29). The burrowing and crinoidal debris indicate normal salinity and moderate wave action, while the bryzoan, brachiopod, and trilobite fragments suggest a slightly deeper environment than the Wichert No. 1 (Facies IIb).

Cleary Rose No. 1-12, 12-T22N-R12W

Cored Depth: 7553-7590 ft

The interval cored is a light to medium grey dolowackstone that is stained brown (live oil) in the upper part (7560-7582 ft) and blackish (dead oil) in the lower part. The fossils have largely been dissolved, creating moldic and enlarged mold/vug porosity. The shapes of the molds and the few remaining fossils indicate crinoids were the predominant fossil. The entire core is strongly burrow mottled; subtle, disturbed laminations are rare. The top six ft. is silty and appears to have been less fossiliferous than the remaining core. Silica, calcite, and baroque dolomite are common in nodules. Stylolites are low amplitude and rare (Figures 30-33). The intense burrow mottling and crinoid fossils indicate high energy and adequate circulation for normal marine salinity (Facies IIA). The small amount of fossils in the top six ft, along with faint laminations suggest a more restricted environment (Facies I).

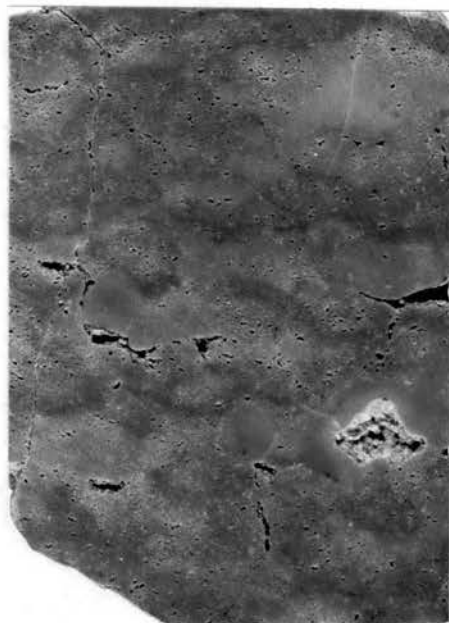


Figure 27. Facies IIb - Medium Light Grey, Burrow Mottled Dolowackestone With Excellent Porosity (KW 7890)

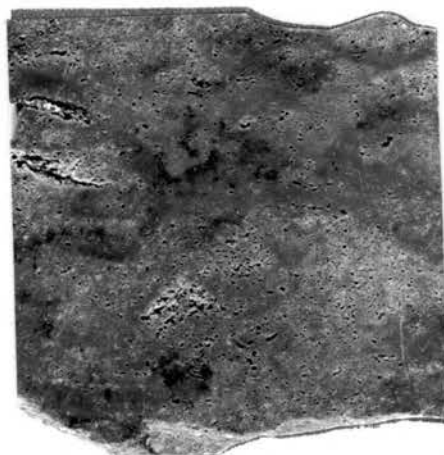


Figure 28. Facies IIb - Burrow Mottled Dolowackestone. (Note irregular porosity distribution.) (KN-7899)

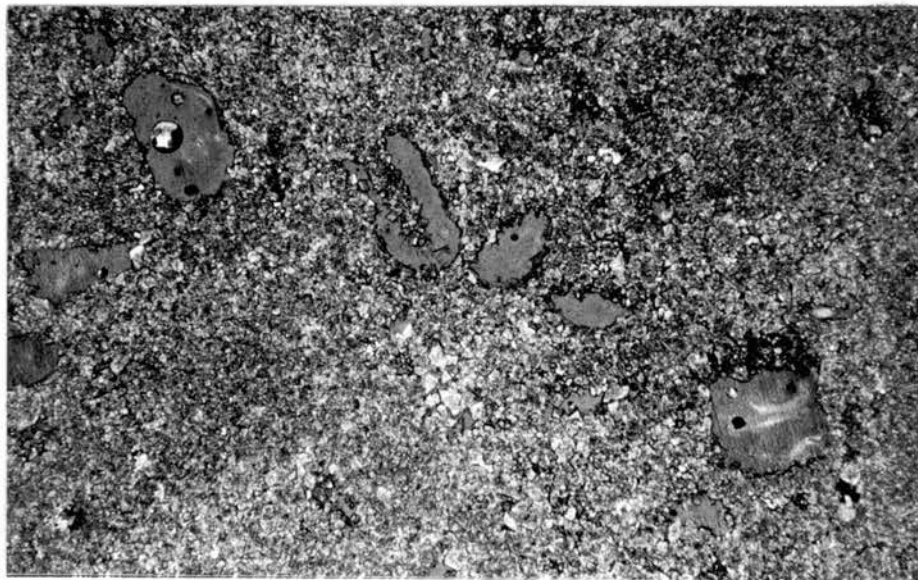


Figure 29. Photomicrograph of Moldic Porosity in a Facies IIb Hypidiotopic Dolowackestone (KW-7887 x 20)

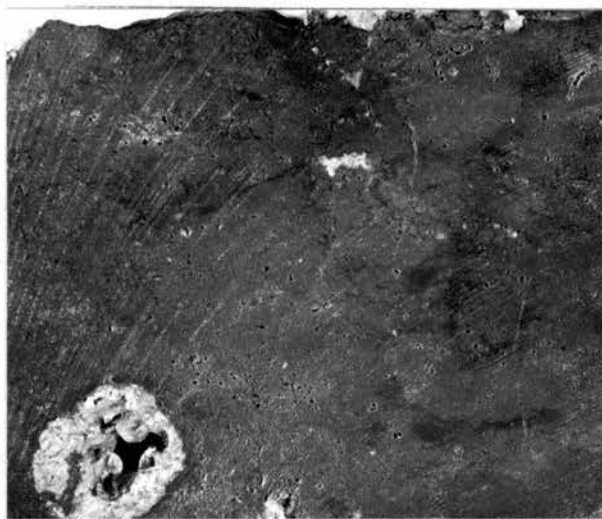


Figure 30. Facies IIa - Burrow Mottled, Oil-stained, Dolowackestone. (Note probable displacive nature of replacive quartz and baroque dolomite nodule.) (CPR-7562)

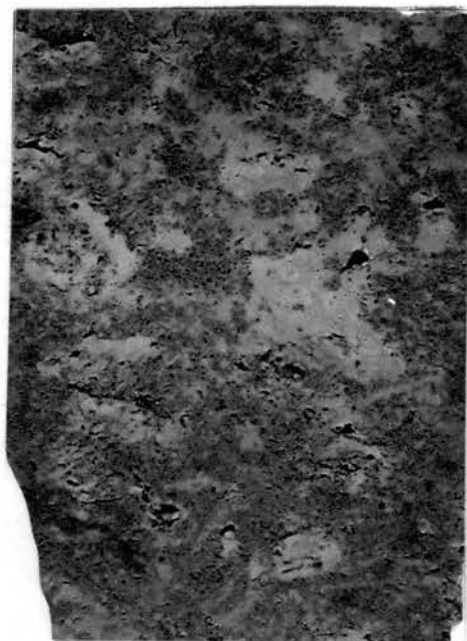


Figure 31. Facies IIa - Excellent Porosity in a Burrow Mottled Dolomudstone. (Possibly some disrupted algal laminations.) (CPR-7579)

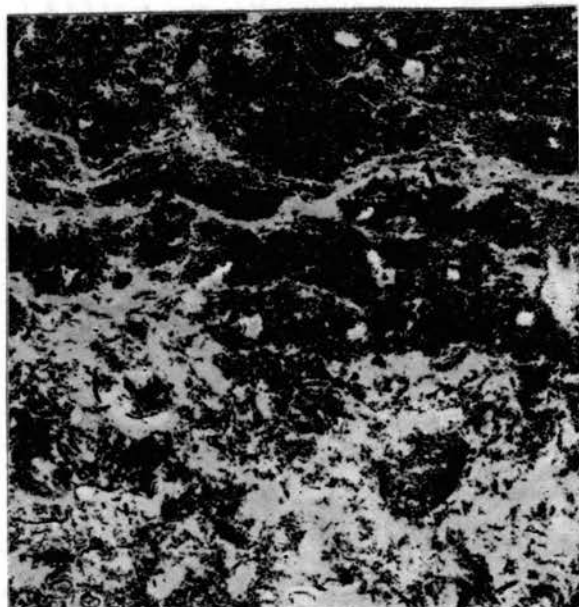


Figure 32. Facies IIa - Dark Oil-stained, Burrow Mottled Dolomudstone. (~~Possibly~~ burrowed algal mat.) (CPR-7583)

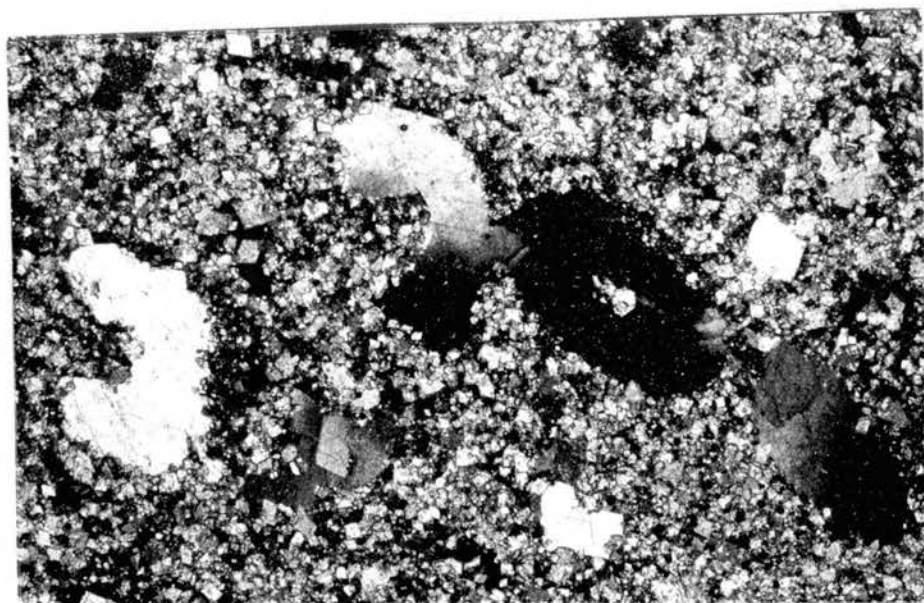


Figure 33. Photomicrograph of Facies IIa Mold Filling Baroque Dolomite (CPR-7589 x 40 crossed nichols)

Amax Hickman No. 1-24, 24-T17N-R18W,

Cored Depth: 13500-13550 ft

The entire cored interval is a strongly burrow mottled dolowackestone that exhibits excellent porosity and is oil-stained in thin section. The lower 15 ft has slightly less porosity due to an increase in vug-mold filling calcite. Vug-mold filling anhydrite and silica are present in small amounts. The shape of the molds indicates pelmatozoans; chiefly crinoids were the dominant fauna. The vuggy porosity is believed to be largely the result of enlarged molds (Figures 34-36). The environment of deposition was relatively high energy with probable wave action (Facies II).

Lone Star Hanan No. 1, 6-T19N-R24W,

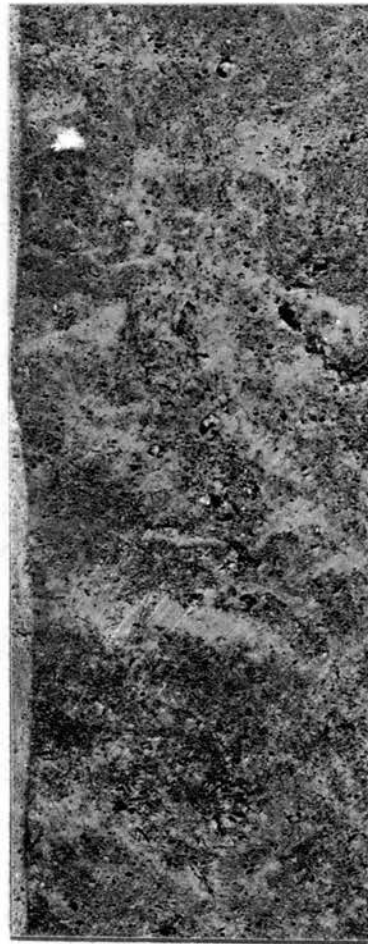
Cored Depth: 14322-14389 ft

The cored interval exhibits a distinct lithologic and faunal change that suggests marine regression with a resulting facies change. The upper facies (14342-14383 ft) is a medium grey, silty, dolomudstone. Brachiopods were the lone fossil type found and are rare. Burrow mottling is present. Pebble sized intraclasts, sand sized detrital quartz, microfractures, and medium amplitude stylolites are present (Figures 37-39). The environment of deposition is interpreted as one with moderate energy with possible tidal channel influence suggested by intraclasts and rounded quartz grains (Facies IIb).

The lower facies, beneath a gradational upper contact, is a dark grey, generally massive, dolomitic mudstone-wackestone. The fossils include numerous pelmatozoan, brachiopods, and trilobites, with



(A)



(B)

Figure 34. (A) Facies II - Excellent Moldic Porosity in a Burrow Mottled Dolowackestone (AH-13503); (B) Same as Figure 35A (AH-13520)

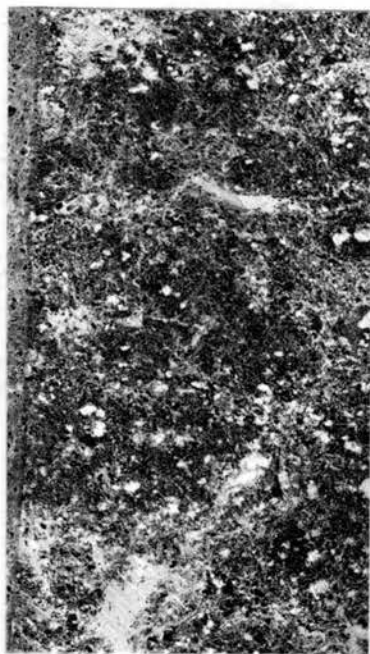


Figure 35. Facies II - Burrow Mottled Wackestone With Recemented Molds (AH-13544)

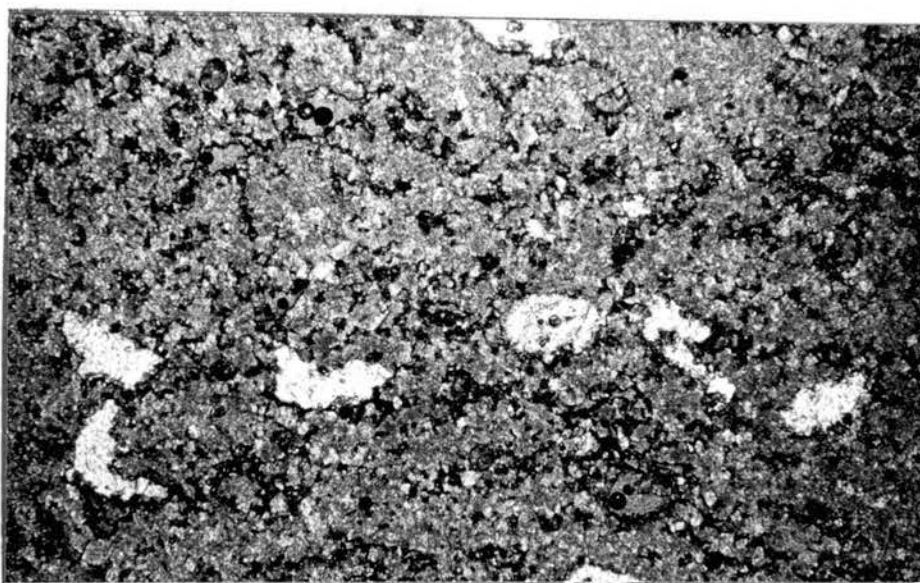


Figure 36. Photomicrograph of Facies II Moldic Porosity Infilled by Late Calcite Cement (AH-13530 x plane polarized light)

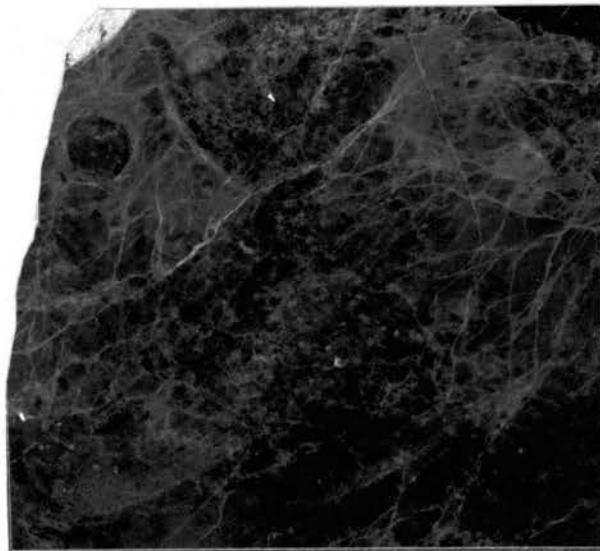


Figure 37. Facies IIb - Abundant Microfractures in a Subtly Burrowed Dolomudstone (LSH-14346)

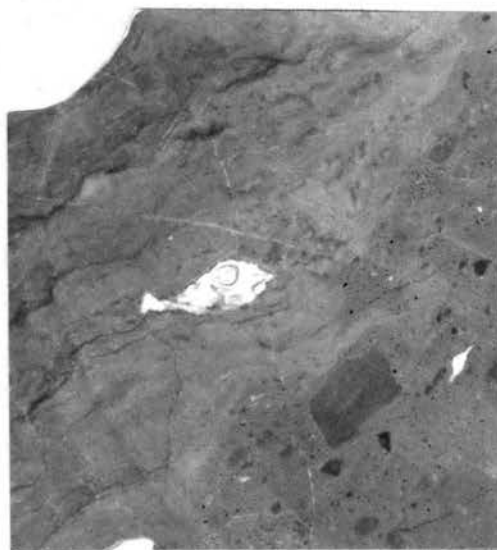


Figure 38. Facies IIb - Unsorted Dolomudstone Containing Medium-grained Quartz, Rounded and Unrounded Intracrysts that are Lithologically Varied. (Possibly tidal channel or storm influence.) (LSH-14362)

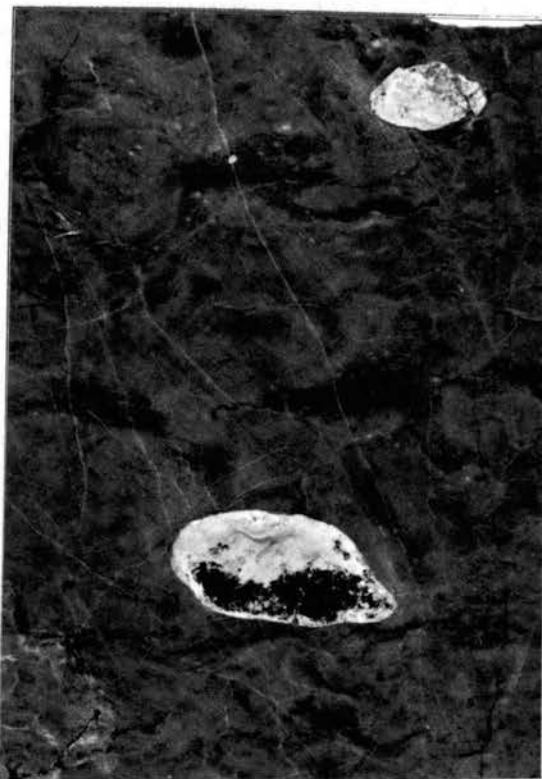


Figure 39. Facies IIb - Burrow Mottled Dolomudstone
Containing Chert Nodules (LSH-14365)

occasional bryzoan and ostracods. Chert, fractures, and fine anastomosing stylolites are present (Figure 40). The depositional environment seems to be deeper water with good circulation (Facies III).

N. F. C. Dietz No. 6-30, 30-T23N-R13W,

Cored Depth: 7743-7779 ft

The cored interval may be divided into two facies that suggest regression. The upper interval (7743-7760 ft) is a medium light grey porous, dolomudstone-wackestone. The top four ft is oil-stained brown. The fossils are almost restricted to crinoids with an occasional brachiopod fragment. Burrow mottling is abundant; stylolites are low amplitude and rare. Small (< 2 cm) nodules are present, comprised of quartz and calcite (Figure 41). Burrowing and dominant crinoids characterize this as Facies II.

The lower cored interval is a dolomitic mudstone. The fossils are more diverse, including crinoids, brachiopods, trilobites, bryzoans, and ostracods. Some mottling is probably present due to burrowing, while some may be the result of compaction. Quartz and calcite nodules and fine, low amplitude stylolites are rare (Figures 42 and 43). Changes in mineralogy, sedimentary structures, and fossil content suggest a deeper water environment (Facies III).

Glover-Hefner-Kennedy No. 1, 1-T14N-R16W,

Cored Depth: 14250-14349 ft

The upper 71 ft of the cored interval is a dark grey, silty, dolomudstone. Brachiopods are the only conspicuous fossil and are generally well preserved, with very few crinoids. This interval is

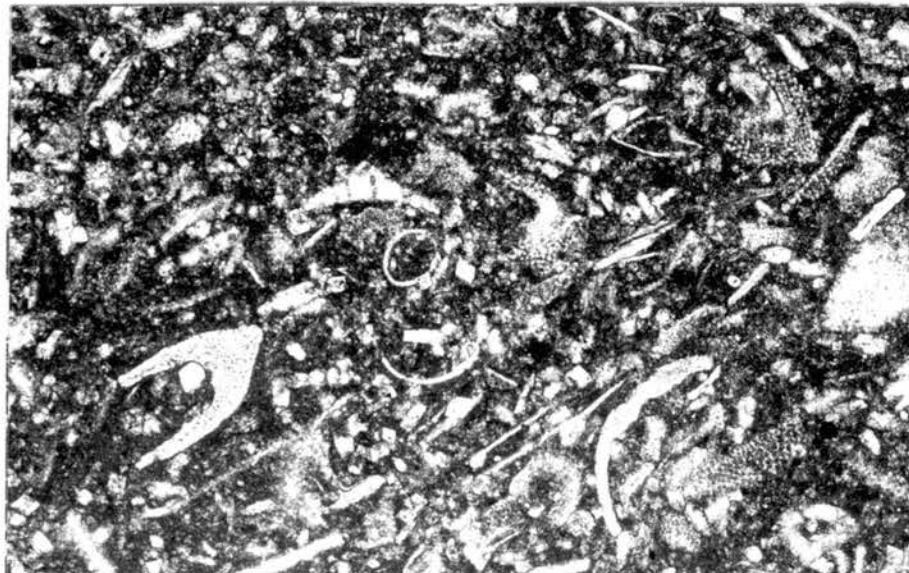


Figure 40. Facies III - Undissolved Fossils in what is Overall a Dolomitic Mudstone. Fossils Include Pelmatozoans, Brachiopods, and Ostracods (LSH-14388)

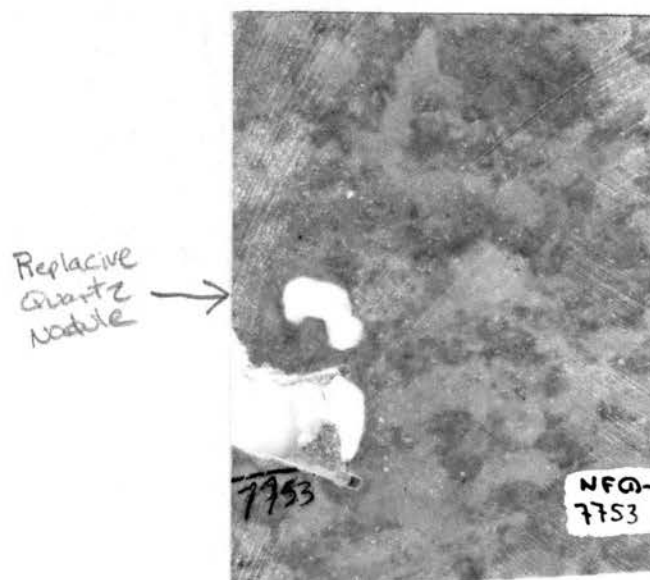


Figure 41 . Facies II - Burrow Mottled Dolowackestone. (Note the replacive quartz nodule.) (NFO-7753)



Figure 42. Facies III - Dolomitic Mudstone, Slightly Burrow Mottled (NFC-7777)

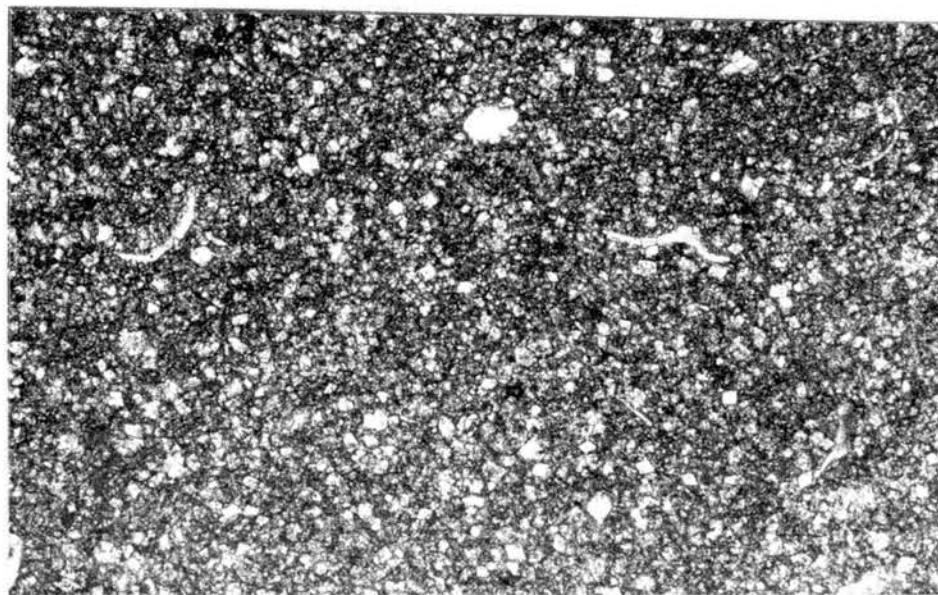


Figure 43. Facies III - Dolomitic Mudstone, Undissolved Thin Fossils, Limpid Idiopathic Dolomite Rhombs (x 40 plane polarized light)

relatively massive with low to medium amplitude stylolites rare, and occasional vertical fractures cemented with dolomite (Figure 44A). Lack of sedimentary structures and well preserved brachiopods suggest a low energy depositional environment, below the area of strong wave action (Facies IIb).

The bottom 28 ft (14321-14349 ft) is a dark grey, silty (especially near the base), dolomitic mudstone-wackestone. Well preserved, thin shelled, brachiopods and some crinoids are occasionally condensed, but non-oriented into planar beds. Chalcedonic silica and dolomite vug filling are rare (Figures 44B~~0~~⁴⁷). Decreasing dolomite and increasing well preserved brachiopods indicate a slightly deeper water environment (Facies III).

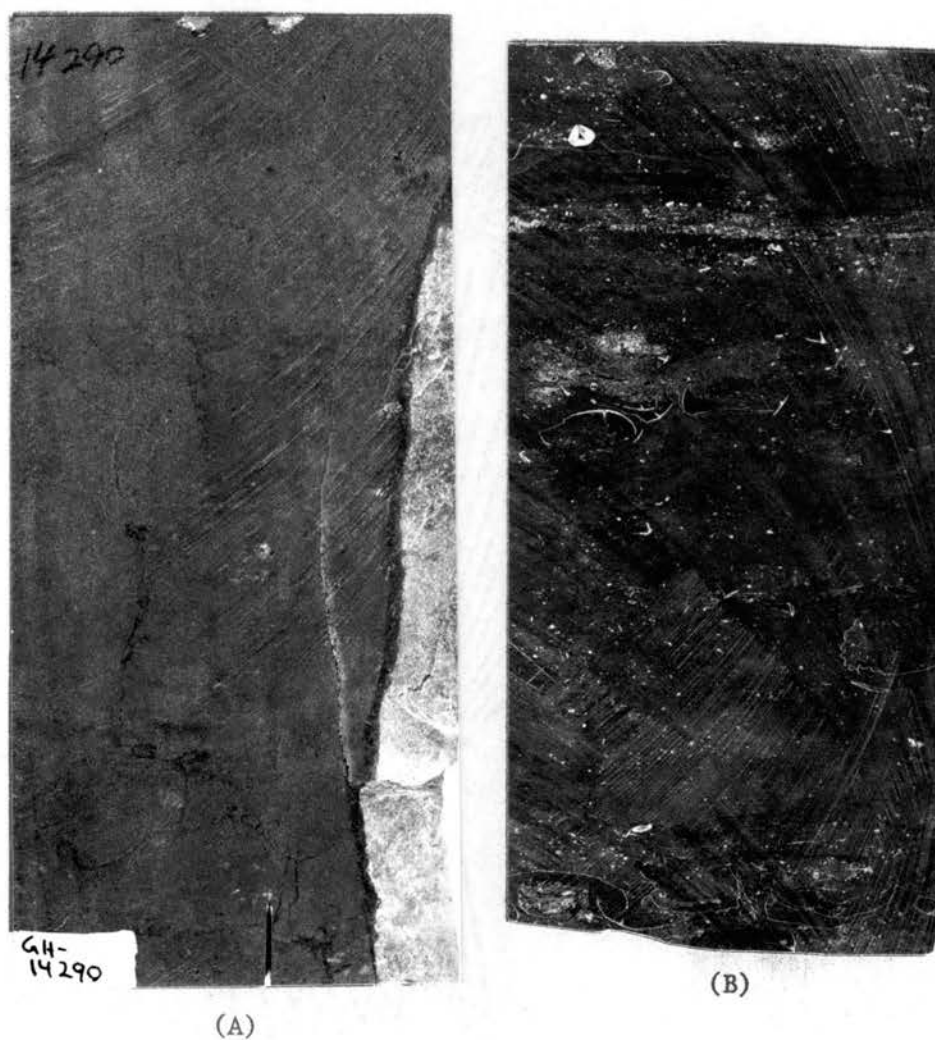


Figure 44. (A) Facies IIb - Generally Featureless, Silty, Dolomudstone (GKH-1490); (B) Facies III - Dark Grey, Silty, Dolomitic Wackestone. (Thin-shelled brachiopods are well preserved and non-oriented.) (GHK-14330)



Figure 45. Facies III - Dark Grey, Dolomitic Wackestone. (Thin-shelled benthonics suggest low energy deposition.) (GHK-14336)

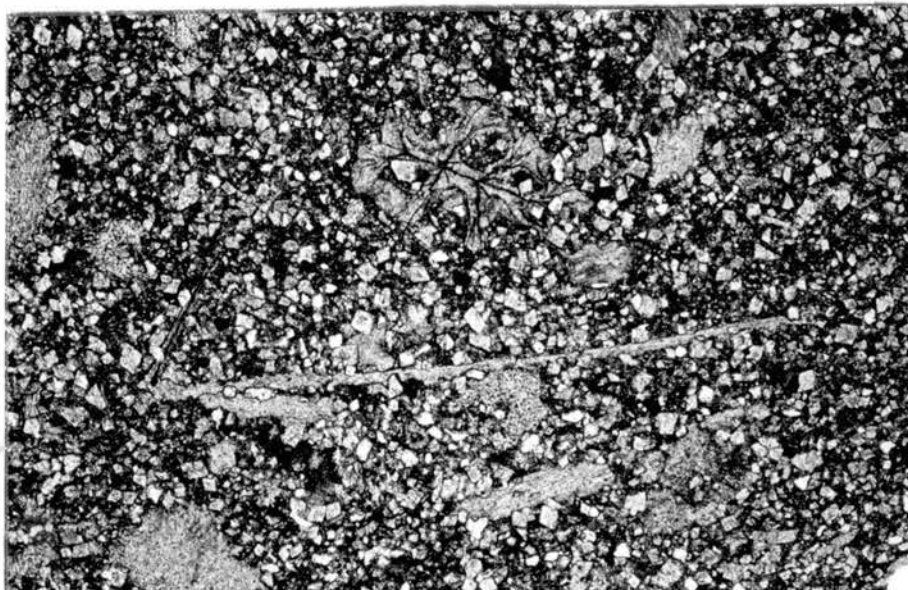


Figure 46. Photomicrograph of Dolomitic Mudstone. (Note delicate preserved fossils and idiotopic rhombs.) (GHK-14336)

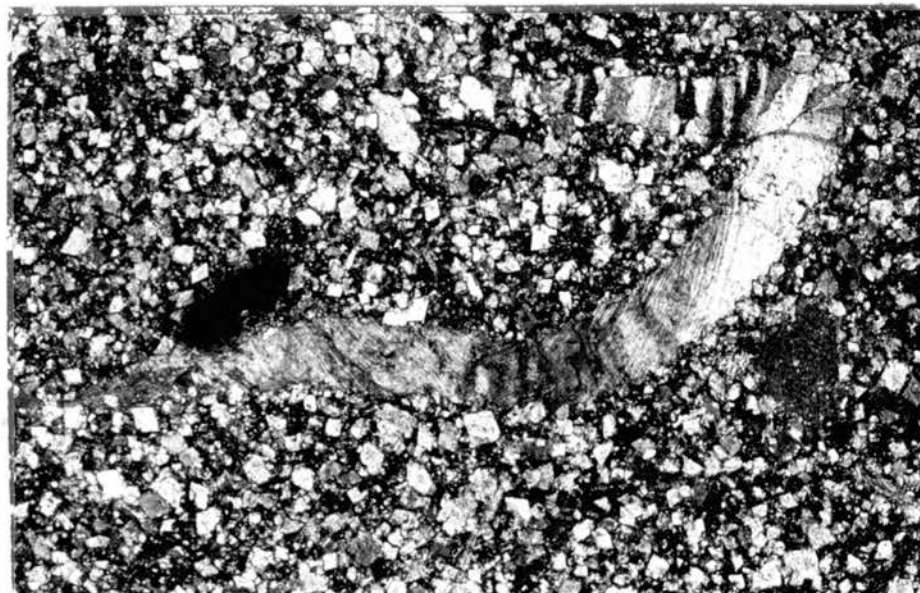


Figure 47. Photomicrograph of Preserved Trilobite Fragment in Dolomitic Mudstone with Idiotopic Rhombs (GHK-14324 - Facies III)

CHAPTER IV

PETROGRAPHY OF THE DOLOMITE

Introduction

Friedman (1965) introduced a textural classification for crystalline sedimentary rocks (Table II) which was specifically applied to dolomites by Friedman and Sanders (1967). The terms neomorphism and recrystallization are used as defined by Folk (1965) and Bathurst (1976). Pore filling cement "sparite" (Folk, 1959) and neomorphic sparite are distinguished following the criteria of Bathurst (1975). Descriptions of particle packing and contacts follow that of Taylor (1950) (Figure 48). The following microscopic characterization of each depositional facies was completed with the intent of revealing any links between depositional environment and diagenetic fabric and texture later developed.

Petrographic Characterization

Facies I

The dolomite in this restricted, shallow water facies is the least uniform. Specimens are generally entirely crystalline with rare fossils (Figures 49-51). Exceptions to this are sections of pelloidal and algal limestone in the Apexco Green core. Rhombs generally appear dirty brown with cloudy centers and clear rims. The size of the rhombs ranges

TABLE II

DOLOMITE TEXTURES AND FABRICS
 (from Friedman, 1965, and Friedman
 and Sanders, 1967.)

Crystal Texture

- | | |
|---|--|
| 1) Individual crystal | 2) Majority of crystals in rock as a whole. |
| (a) Euhedral
(b) Subhedral
(c) Anhedral | (a) Idiomatic
(b) Hypidiomatic
(c) Xenotopic |

Crystal Fabrics

- | | |
|-----------------|--|
| 1) Equigranular | 2) Inequigranular |
| | (a) Porphyrotopic- large dolomite crystals in a matrix of small crystals |
| | (b) Poikilotopic- large dolomite crystals in a matrix of small crystals of a different mineral |
-

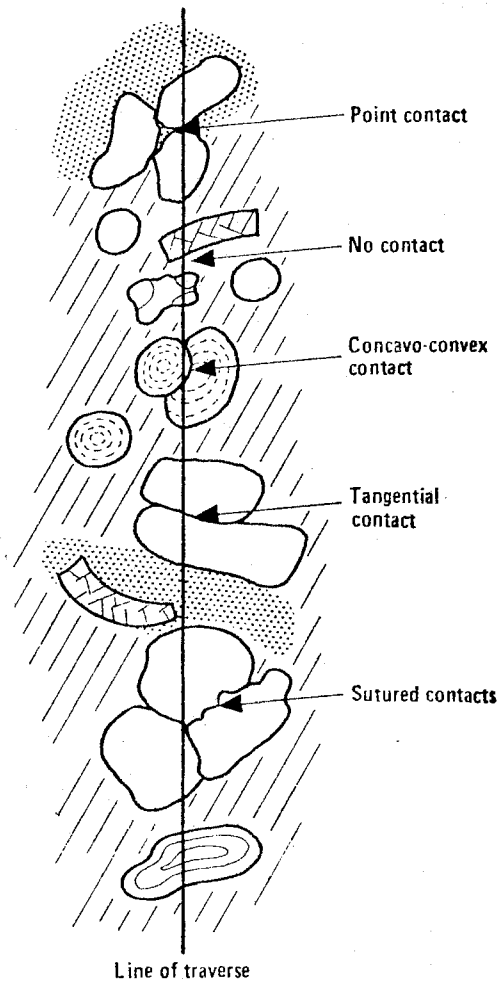


Figure 48. Particle Packing and Particle Contact (terminology after Taylor, 1950)

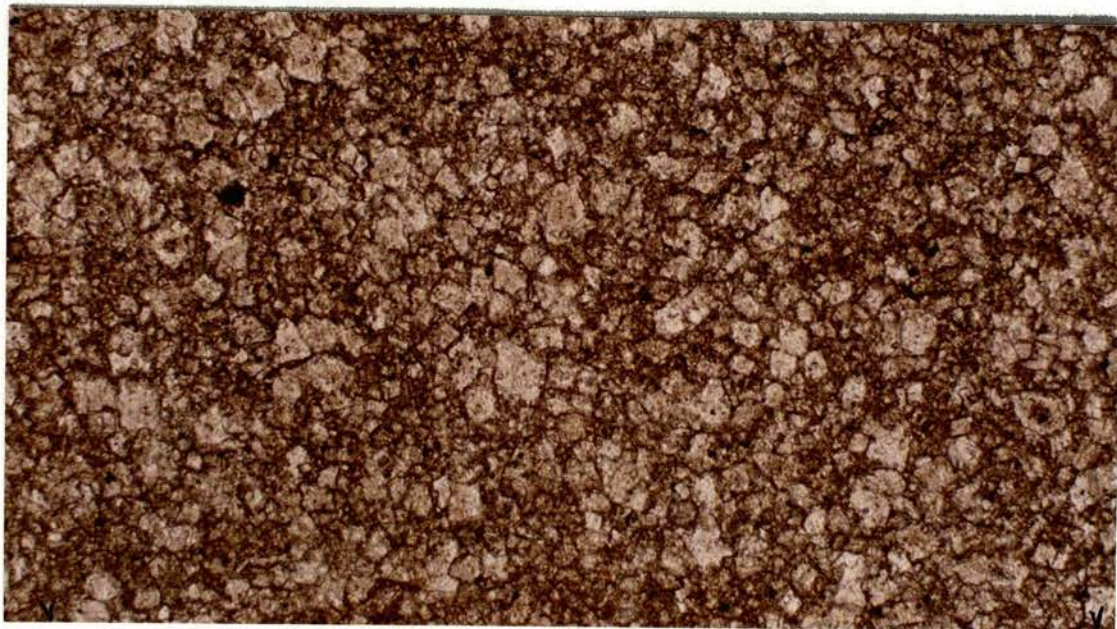


Figure 49. x40 Plane Polarized Light. Facies I Idiopathic Dolomite, 20-50 Microns. (Note cloudy centers and clear rims.)



Figure 50. x100 Plane Polarized Light. Facies I Hypidiomorphic Dolomite. (Complete to sutured contacts; average 60-80 microns.)

from 10-100 microns, usually between 50-70 microns. The dolomite texture ranges from rare idiotopic rhombs found in algal micrite to the more common xenotopic and hypidiotopic. Hypidiotopic is most common. Crystals are predominantly in complete contact and often sutured. Porosity is rare and insignificant.

Facies II

The highest dolomite percent was found in this facies. Rhombs most often have a dirty brown color with clean rims (Figures 51-54). The size of the rhombs ranges from 20-150 microns, and are usually between 60-80 microns. The dolomite texture ranges from idiotopic to xenotopic; usually it is hypidiotopic. Gradations in predominant texture may be seen within the same thin section. Rhombs bordering or growing in vugs are commonly more euhedral than the tight matrix dolomite, and often display larger clean overgrowths (Figure 55). Crystal contacts are predominantly tangential and point contact; sutured contacts are common. All specimens with significant porosity were from this facies. Porosity is moldic, intercrystalline, and vuggy.

Facies III

This facies invariably corresponds to the lowest dolomite percentages. Rhombs invariably have a cloudy center with white or clear rims (Figures 56-58). Fossils are less common than Facies II, but are usually preserved with the original texture (Figures 59-60). Rare recrystallized fossils were observed. The size of the rhombs ranges from 20-100 microns and is generally 50-70 microns. The dolomite texture is consistently idiotopic rhombs floating in a cryptocrystalline

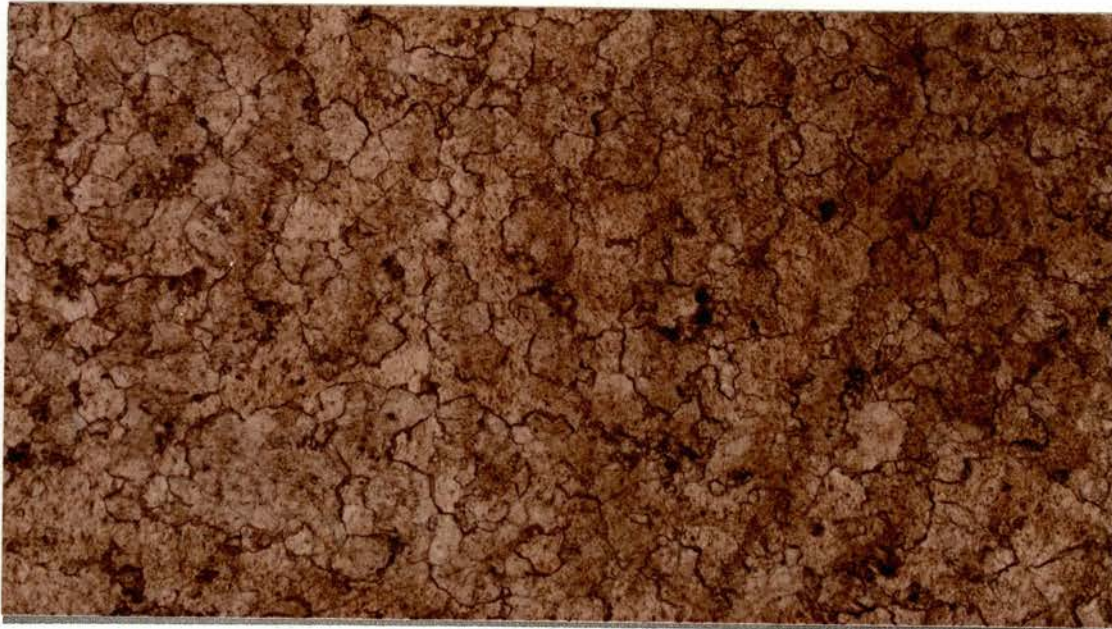


Figure 51. x40 Plane Polarized Light. Facies I Xenotopic Dolomite

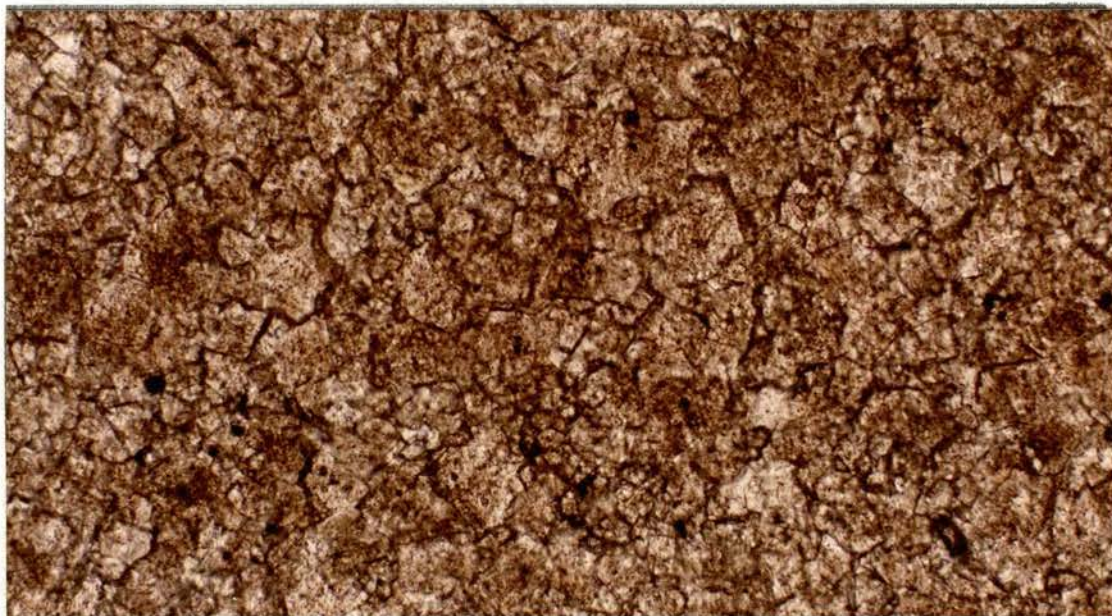


Figure 52. x100 Plane Polarized Light. Facies II Brown Xenotopic Dolomite (40-130 microns)

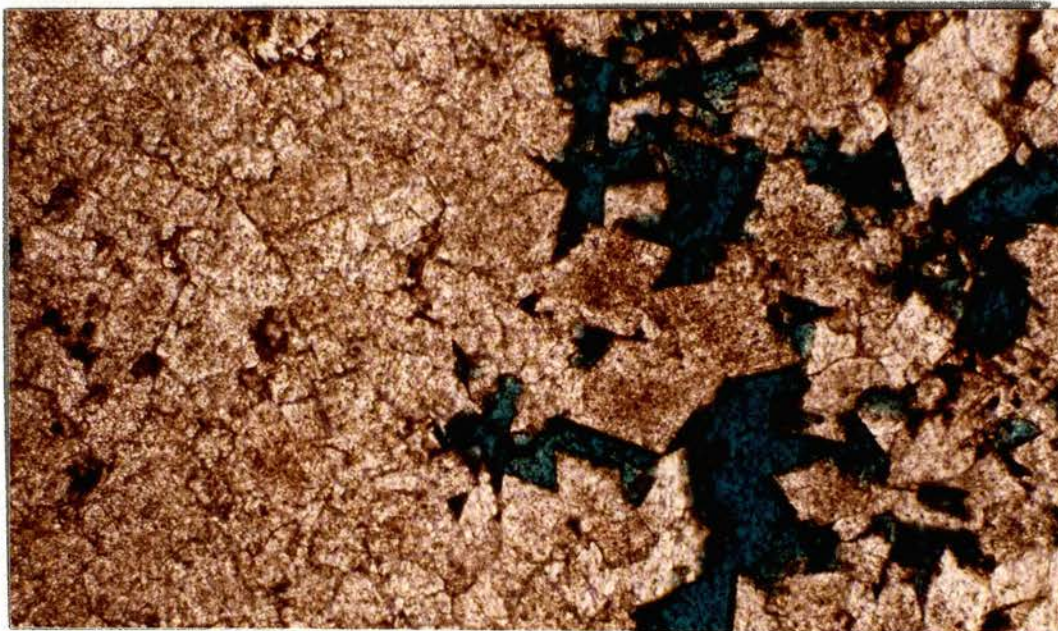


Figure 53. x100 Plane Polarized Light. Facies II Brown Hypidiotopic Dolomite, Especially Well-formed Near Porosity. (Note dead oil lining some pores.)

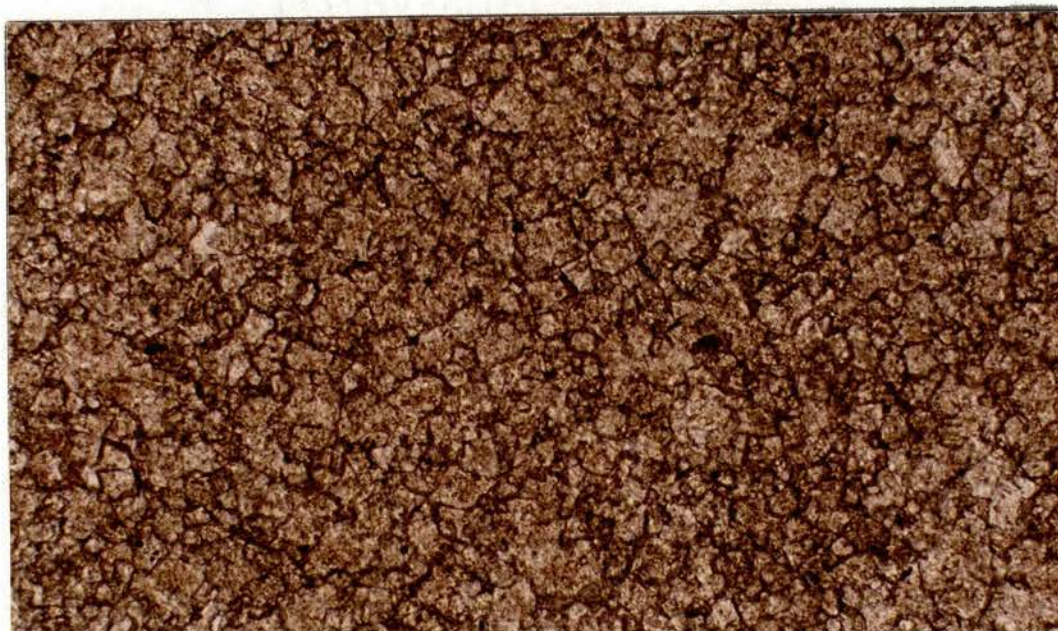


Figure 54. x40 Plane Polarized Light. Facies II Brown Hypidiotopic/Xenotopic Dolomite (20-90 microns)

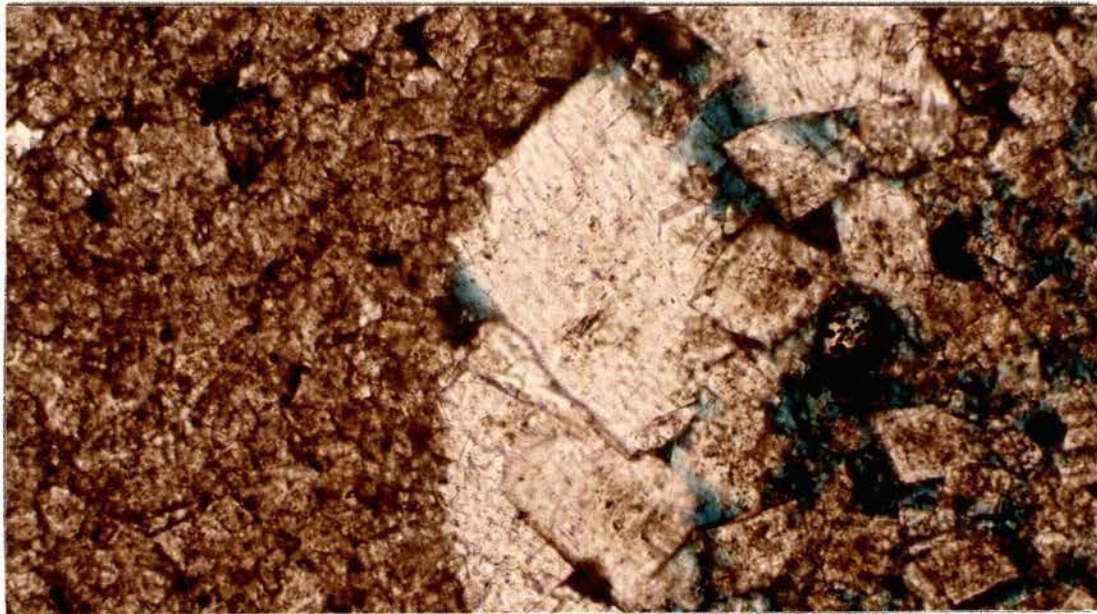


Figure 55. x100 Plane Polarized Light. Facies II Brown Hypidiotopic Dolomite. (Note latter large limpid or white rims and separate rhombs growing in pore space.)

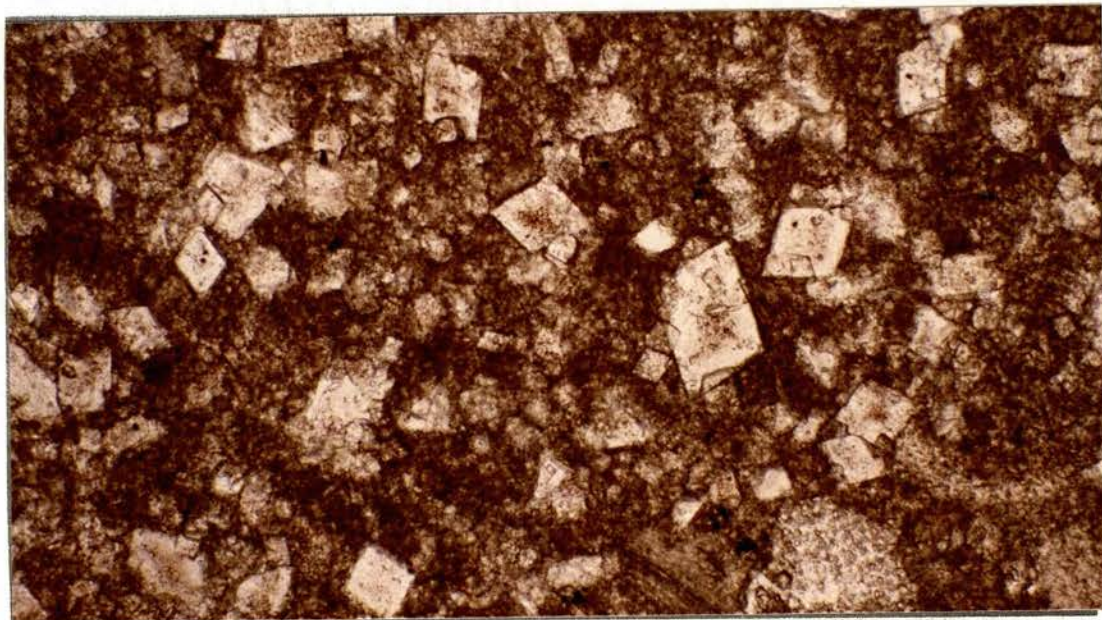


Figure 56. x100 Plane Polarized Light. Facies III Dolomitic Mudstone with Typical Idiopathic Halo Type Rhombs (30-120 microns)

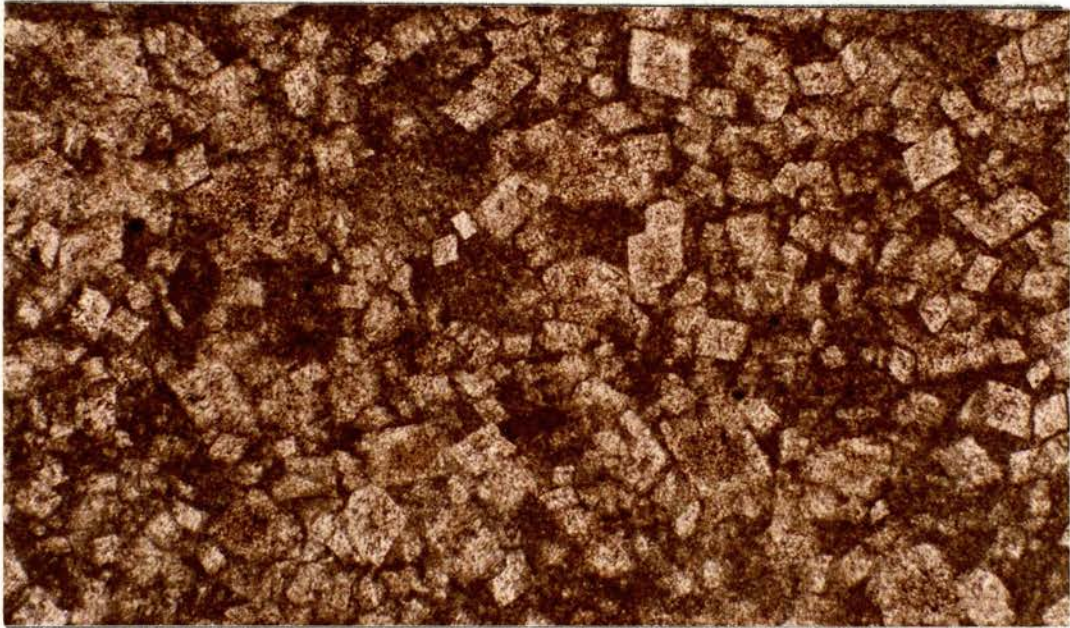


Figure 57. x40 Plane Polarized Light. Facies III
Cloudy Centers, Clear or White Rims
(20-100 microns)

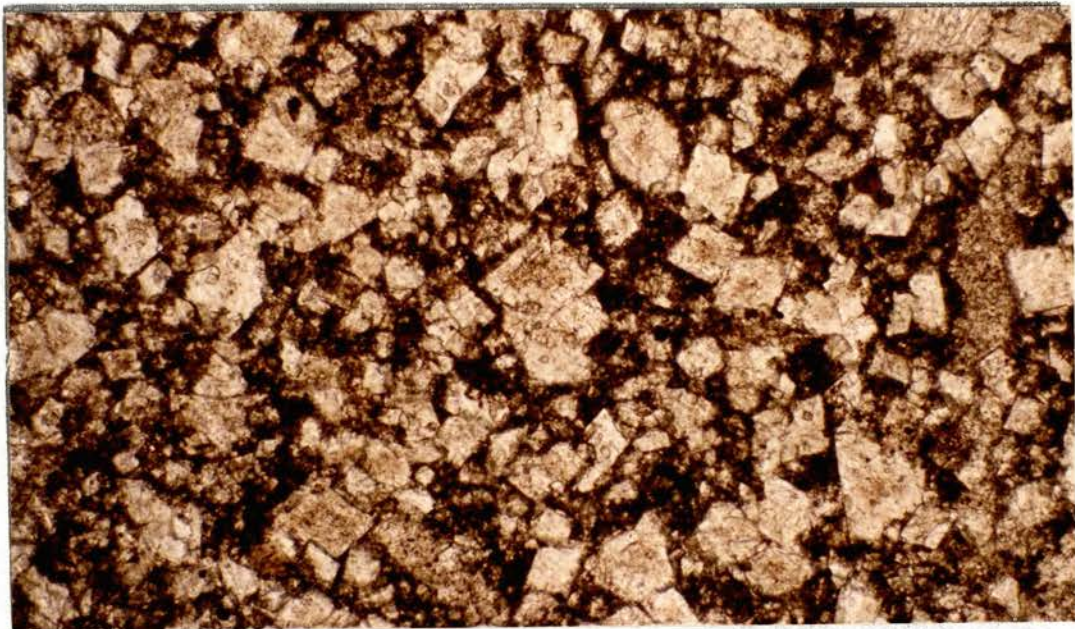


Figure 58. x100 Plane Polarized Light. (As above, dif-
ferent core.)

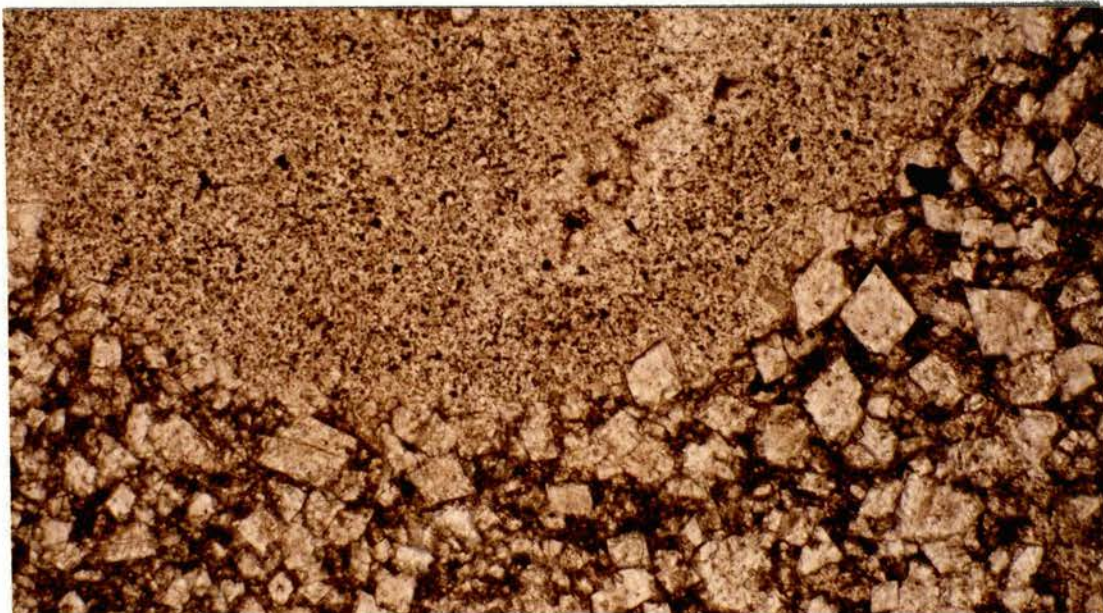


Figure 59. x100 Plane Polarized Light. Facies III Idiotopic Rhombs Impinging on an Unreplaced Crinoid Ossicle



Figure 60. x40 Plane Polarized Light. Typical Facies III Dolomitic Mudstone With Calcite Fossils Stained red and Idiotopic Halo Rhombs Floating in the Unreplaced Micrite Matrix

calcite matrix. Porosity is invariably absent from this facies.

The fabrics and textures described as progressive dolomitization by Amsden (1975) show a marked similarity to the fabrics and textures related in this section to depositional facies. The strong influence or possible control of dolomitization by the original sedimentary fabric suggests facies selective dolomitization may be a more appropriate description.

Porosity

The purpose of this section is to describe and document the various types of porosity present in the Henryhouse Formation observed during this investigation. An explanation for the distribution of these porosity types will also be pursued.

Porosity Types

The two general porosity types in carbonate rocks are fabric selective and not fabric selective (Choquette and Pray, 1970). Two fabric selective porosity types were observed in the Henryhouse: 1) moldic, and 2) intercrystalline. These two porosity types are responsible for all high porosity zones observed in sampled cores.

Moldic porosity is caused by dissolution of fossil grains, predominantly crinoid fragments. Evidence for moldic porosity is excellent. The characteristic outline of many molds clearly indicates previous presence of a fossil (Figures 61-64). Occasionally, partially dissolved remnants are found within molds, making alternative hypotheses for the origin of such mesopores unreasonable (Figure 65). Molds may be subsequently filled by late baroque dolomite (Figure 35) or calcite (Figure

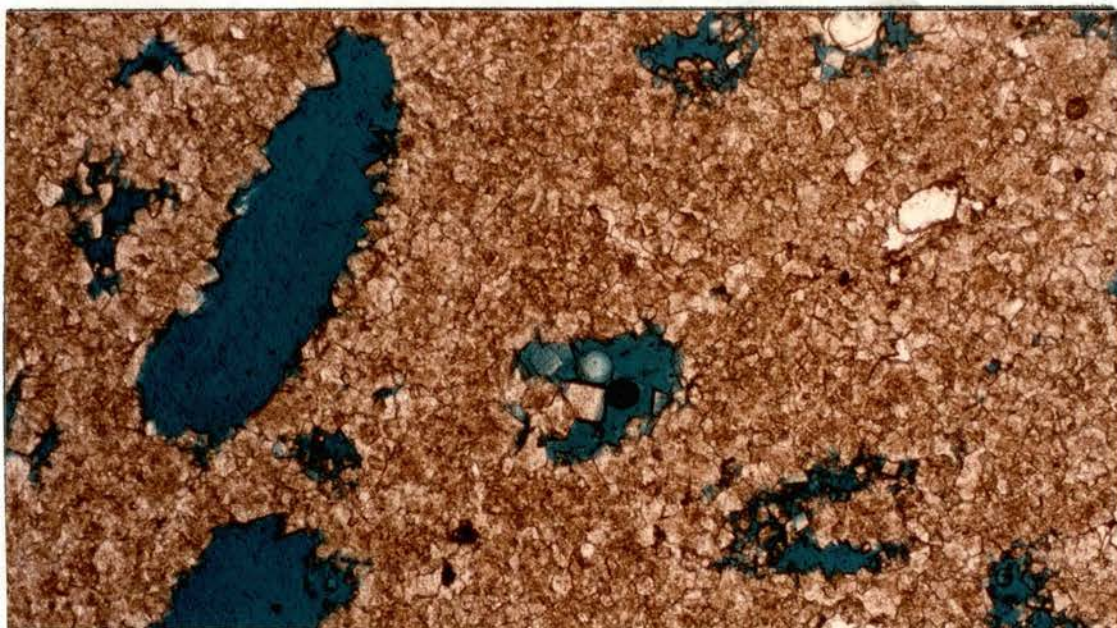


Figure 61. x40 Plane Polarized Light. Moldic Porosity
Developed in Facies II Dolowackestone

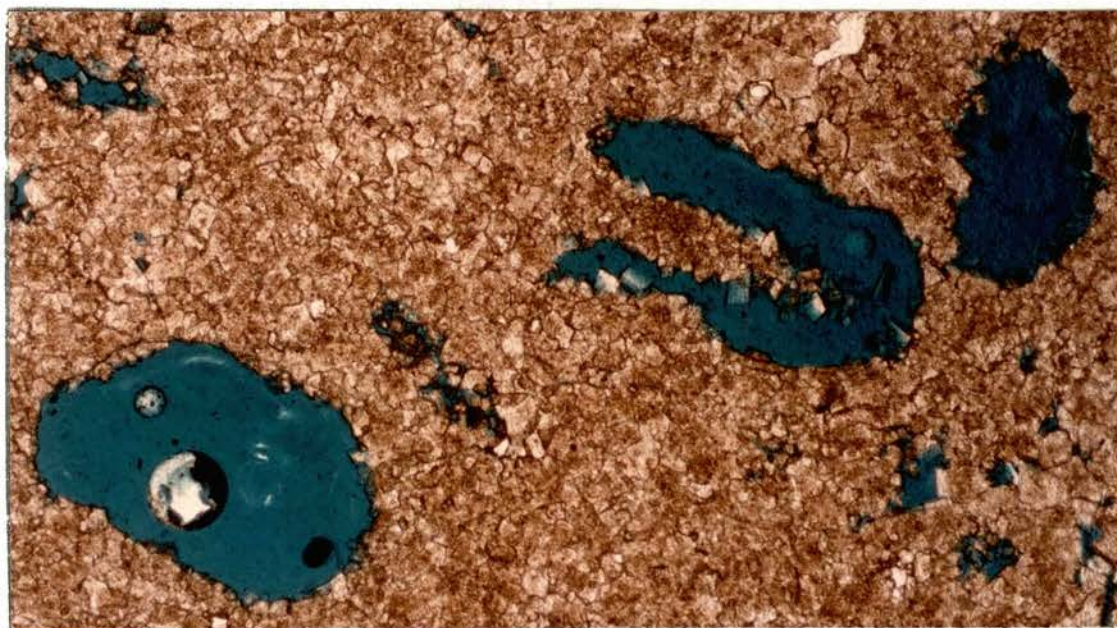


Figure 62. As above (note crinoid molds)

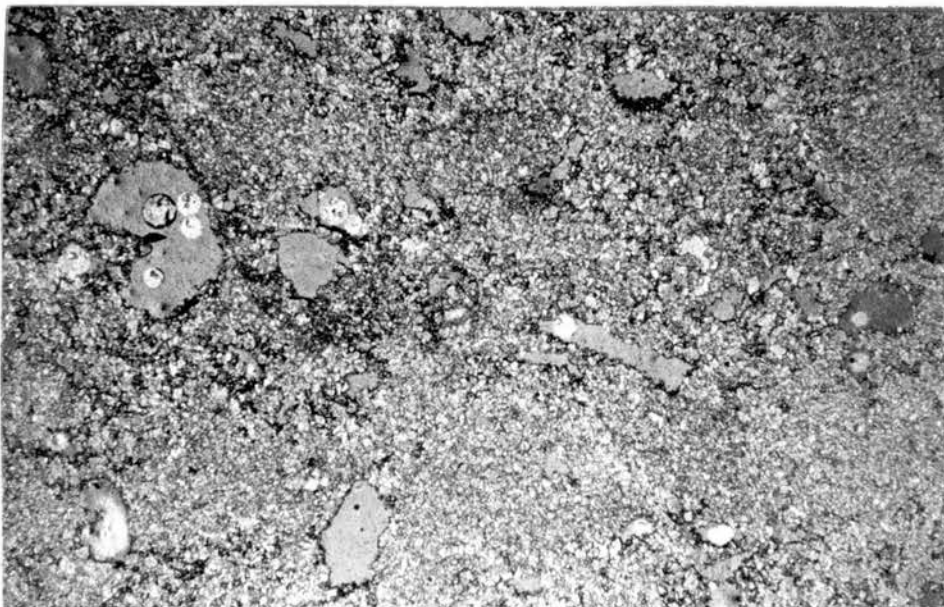


Figure 63. x20 . Plane Polarized Light. Moldic Porosity Developed in Facies II Dolowackestone. (Some pores lack a distinct fossil outline and are interpreted to be solution enlarged molds.)

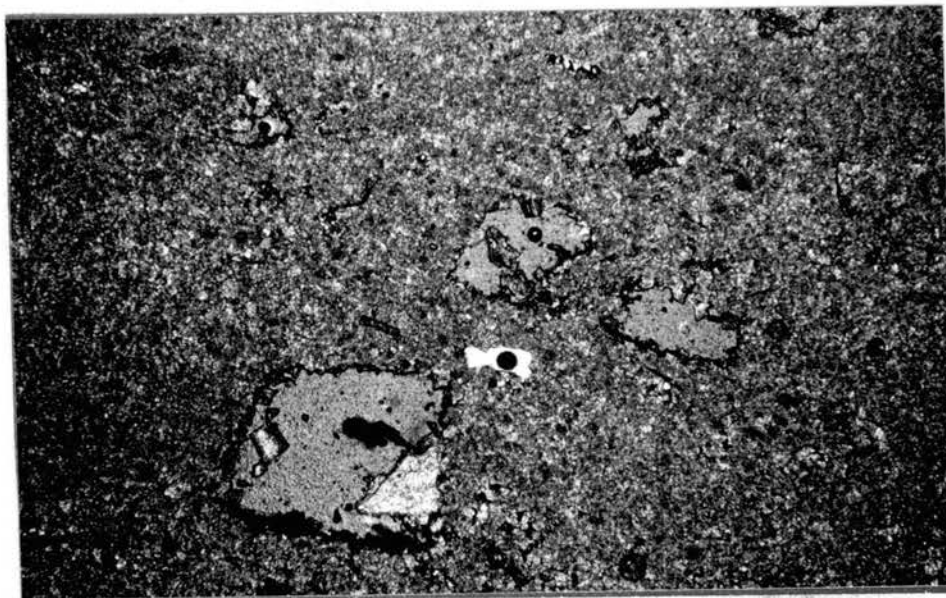


Figure 64. As Above

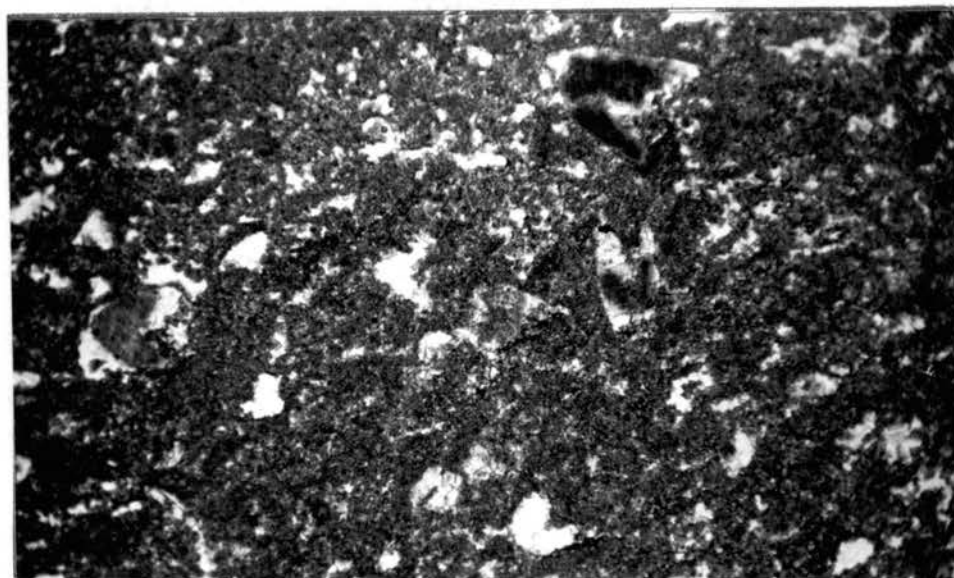


Figure 65. x20 Plane Polarized Light. Moldic Porosity
in Facies II Dolowackestone (some molds
contain partially dissolved fossils)

35) cements.

Intercrystalline pore space evolved as a consequence of dissolution of nonreplaced cryptocrystalline calcite matrix (Murray, 1960). Important solution enlargement of this porosity type is common (Figures 66-70). Intercrystalline porosity is prone to develop between larger rhombs in an idiotopic to hypidiotopic texture. Late calcite cement may occlude some intercrystalline pores (Figure 71).

The single non-fabric selective porosity is vuggy porosity. It is inferred that many vugular pores are molds later solution enlarged, destroying the distinct fossil outline. Coincidence of this porosity type with fossiliferous, moldic zones supports this interpretation. The largest vugs (up to 4 cm) are created by dissolution of incompletely replaced anhydrite nodules. In rare cases, partially dissolved anhydrite is present, surrounded by replacive euhedral quartz.

Mold and vug filling cements and pore lining rhombs commonly have been partially dissolved, creating minor amounts of tertiary porosity.

Porosity Controls

Previous investigations have related porosity to dolomitization (Amsden, Isom, Borak). In this thesis, the degree of dolomitization has been related to depositional facies. In Figure 72, the average porosity determined by thin section point counts and the average dolomite percent calculated from x-ray diffraction data are plotted as they vary with depositional facies. A positive relationship between dolomitization and porosity is clearly seen. Highest and lowest values of porosity correspond to highest and lowest values of dolomitization. Further consideration ^{, however,} reveals that this relationship is somewhat deceptive. When

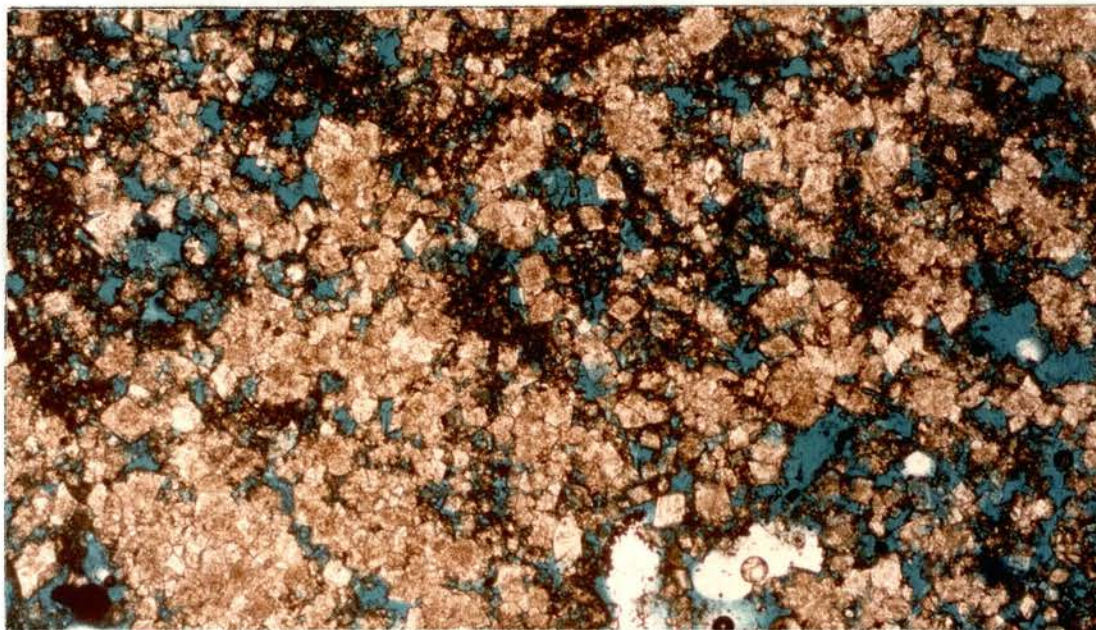


Figure 66. Plane Polarized Light. Extensive Intercrystalline Porosity in an Oil-stained Facies II Dolowackestone

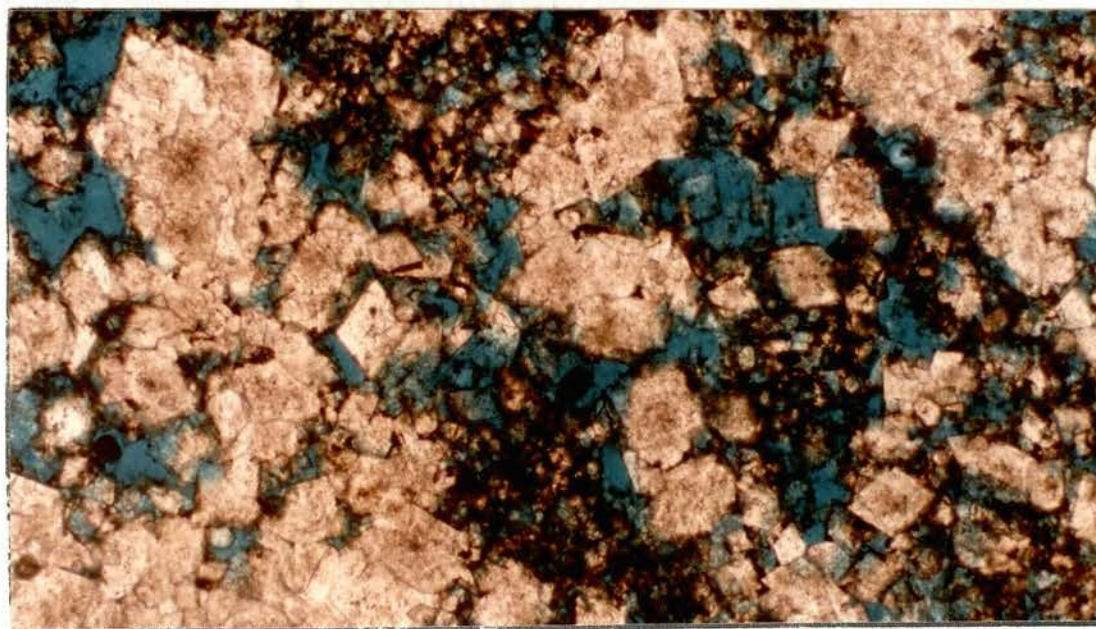


Figure 67. Plane Polarized Light. Extensive Intercrystalline Porosity in an Oil-stained Facies II Dolowackestone (closer view)

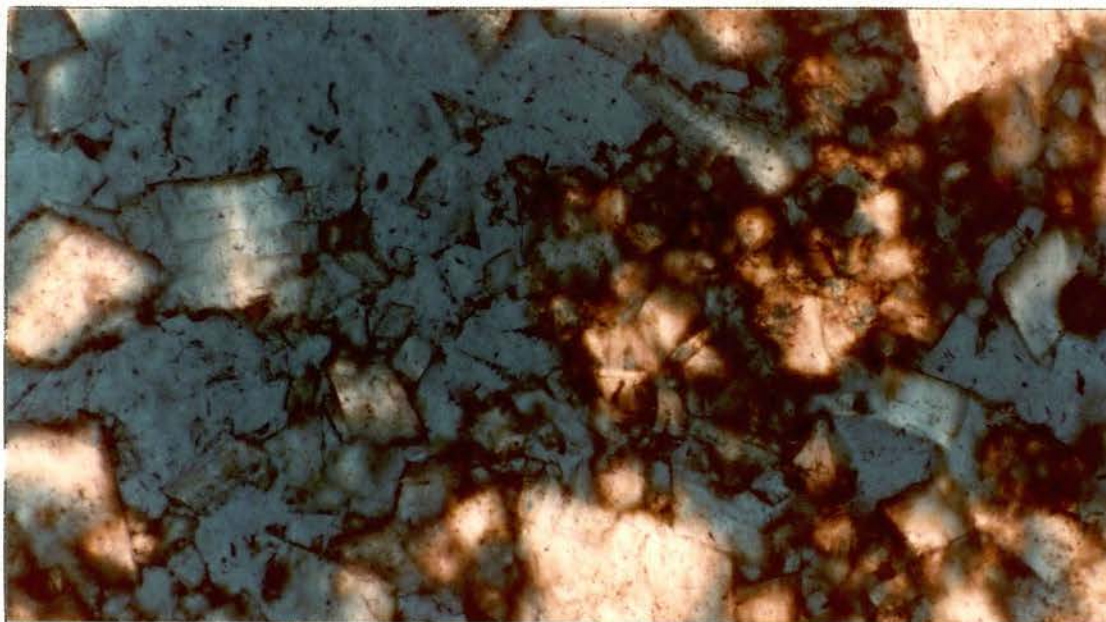


Figure 68. x200 Plane Polarized Light. Intercrystalline Porosity Enlarged at the Expense of Matrix Dolomite (Facies II)

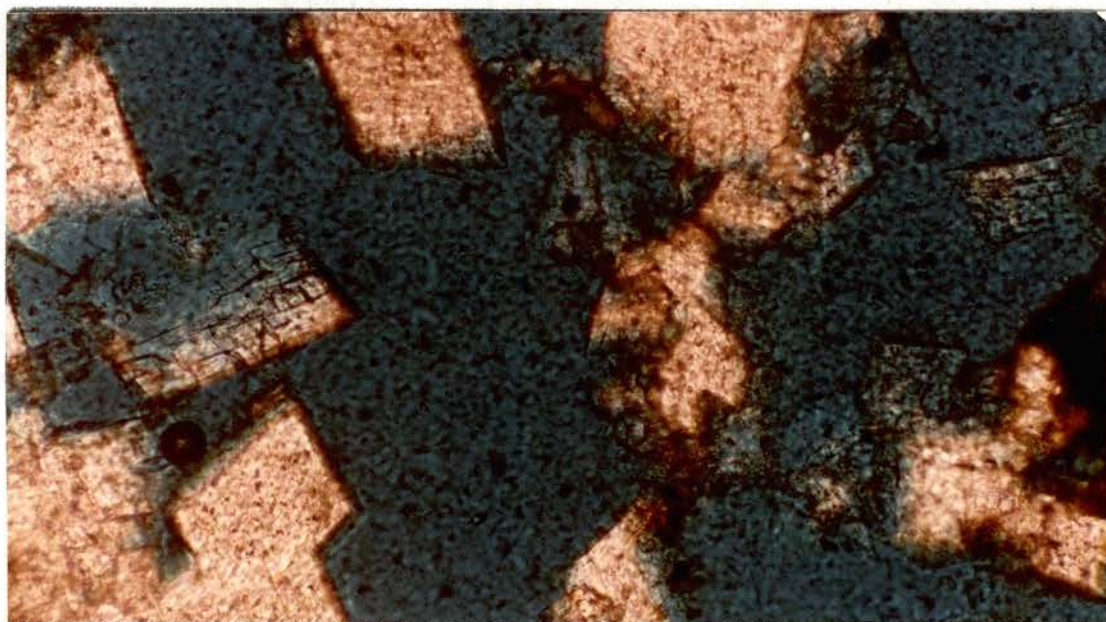


Figure 69. x400 Plane Polarized Light. Partially Dissolved Rhombs Bordering or Floating in Intercrystalline Pores. (Note oil stain.) (Facies II)

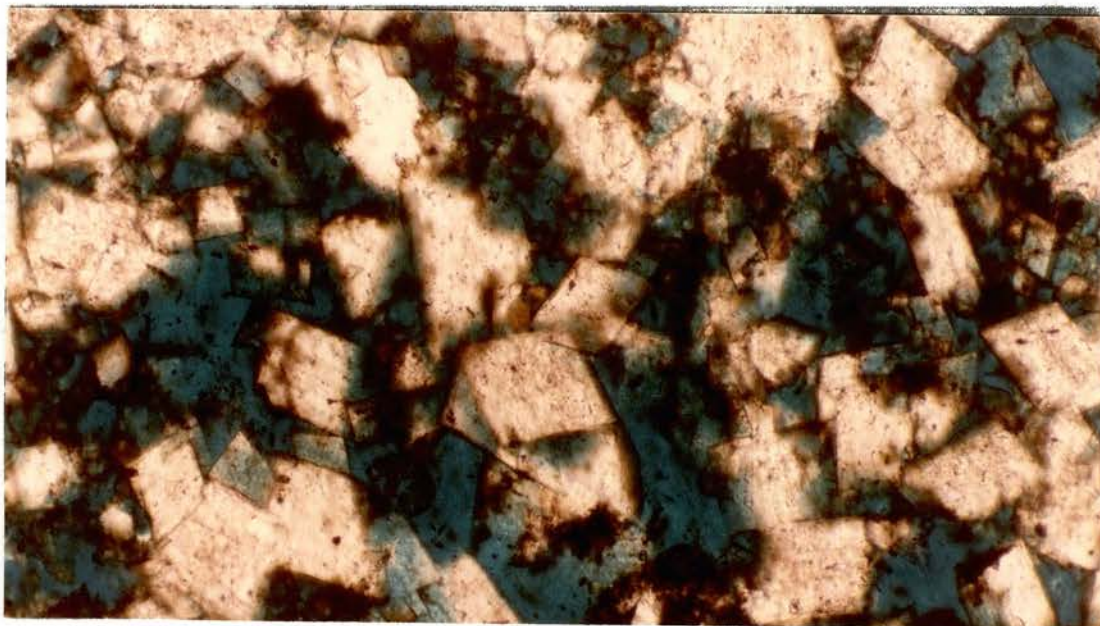


Figure 70. x200 Plane Polarized Light. Common Dissolved Rhombs Associated with Intercrystalline Pores. (Note oil stain.) (Facies II)

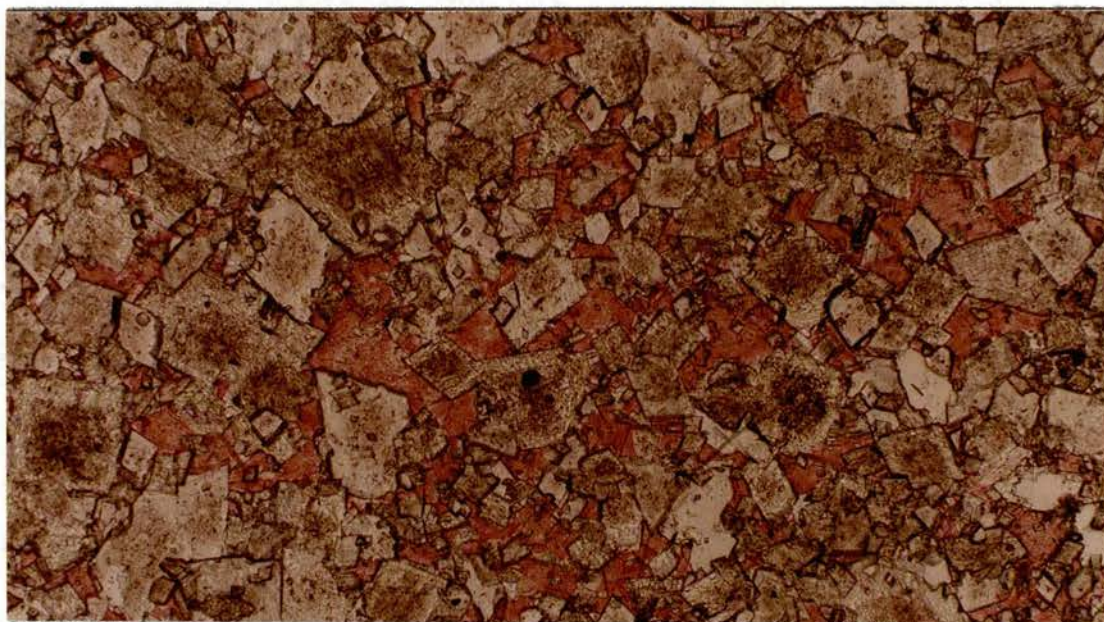


Figure 71. x400 Plane Polarized Light. Facies I Intercrystalline Porosity Partially Occluded by Late Calcite Cement (stained red). (Note well developed halo dolomite.)

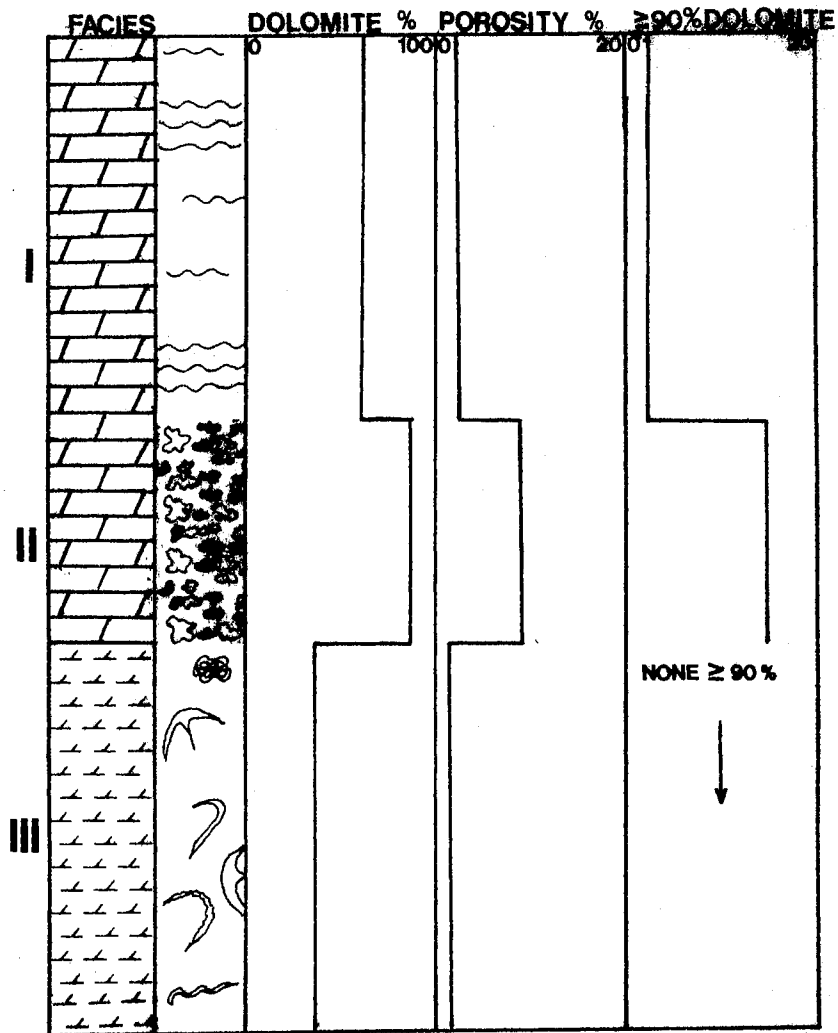


Figure 72. Relationships Between Depositional Facies, Porosity Percent, Dolomite Percent and Porosity of Zones With 90 Percent Dolomite. (Depositional facies have the strongest influence on porosity.)

porosity is plotted only for zones with high values of dolomite (≥ 90 percent), the dominating influence of depositional facies is revealed. That is, if both Facies I and Facies II are completely dolomitized, only Facies II will develop significant porosity. Facies ~~II~~^{III} was never observed to be either completely dolomitized or porous.

The properties of Facies II causing it to preferentially develop high porosity are the same ones that differentiate it from the other depositional facies--burrowing and common pelmatozoan debris. The effect of burrowing is to enhance permeability by redistributing the finer particles (Roehl, 1969). This effect increases the degree of dolomitization and is preserved by it, allowing subsequent dissolution of nondolomitized matrix and grains by percolating low pH solutions. The resulting patchy, irregular porosity distribution is very evident in hand specimen (see Facies II core photographs) and detectable in thin section.

In the absence of fossils, moldic porosity cannot develop. Both Facies II and Facies III are fossiliferous, yet only the highly dolomitized Facies II develops moldic porosity. High-magnesium echinoderm fragments may have increased the susceptibility of Facies II to dolomitization, allowing later dissolving fluids to reach them through the enhanced porosity-permeability. Pelmatozoan grains may not be a causal variable for preferential Facies II porosity development, but their subsequent dissolution serves to greatly increase it.

Diagenetic Events and Processes

The Henryhouse Formation has experienced a strong diagenetic overprint since deposition. The numerous diagenetic events have been

broadly grouped in Table III, based on whether they occurred before or after stylolitization. Timing relationships within these categories are indicated where possible.

Pre-compaction

The most pervasive and important pre-compaction diagenetic event is replacive dolomitization of cryptocrystalline calcite matrix. Sand-sized pelmatozoan fragments, especially in Facies II wackestones, have resisted dolomitization. Dissolution of nonreplaced fossils and matrix closely followed or accompanied dolomitization, creating intercrystalline and moldic porosity (Figures 66-72). Vuggy porosity is probably created by dissolution of unreplaced syntaxial overgrowths and their fossil cores along with simple solution enlargement of molds (Murray, 1960).

Initial dolomitization was early enough to preserve sedimentary structures and textures such as burrow mottling. Without dolomitization before significant burial, the enhanced permeability associated with burrows would probably be destroyed by recrystallization during burial, inhibiting later fluid migration (Moore and Druckman, 1981).

Henryhouse dolomite very commonly has cloudy centers with limpid rim cement. Such zonation is typical of platform dolomite (Land, 1980). These "halo" rhombs are found across facies and crystal textures. Formation of Henryhouse halo dolomite is interpreted to be the result of a second dolomitization phase that took place after development of moldic and vuggy porosity but before suturing of rhombs and stylolitization. Evidence supporting this timing interpretation is exaggerated limpid overgrowths on pore rimming rhombs (Figures 73-74), rare separate

TABLE III

ACCESSORY MINERALS AND PARAGENETIC SEQUENCE. SUTURED CONTACTS AND STYLOLIZATION
WERE USED AS COMPACTION INDICATORS

PRE-COMPACTION	POST-COMPACTION	ACCESSORY MINERALS
1. Sparry calcite 2. Microcrystalline chert 3. Chalcedonic chert 4. Megaquartz 5. Anhydrite nodules and laths	1. Pyrite 2. Sphalerite 3. Baroque dolomite 4. Calcite cement	
1. Fenestral pores 2. Equant calcite cement 3a Dolomitization of CaCO_3 mud matrix b Anhydrite nodules c Anhydrite laths 4. Dissolution of calcite grains and matrix 5a Neomorphism of 1st dolomite and development of limpid overgrowths; some entirely limpid rhombs form b Replacement of anhydrite by euhedral quartz	1. Pore filling and replacive polyhalite (?) 2. Pore filling and replacive calcite cement 3. Mold, vug, and fracture filling baroque dolomite Pyrite Sphalerite	



Figure 73. x100 Plane Polarized Light (original brown, cloudy rhomb with a large clean rim growing into a vug that has been recemented by late calcite cement)



Figure 74. x200 Plane Polarized Light, Large White or Limpid Rims can be Seen Developed Into Previous Pore Space

limpid or white rhombs growing in or into pores (Figures 75-76) and comparison features affecting both dirty core and overgrowth (Figures 77-79). A variety of pore fluid chemistry changes may affect zonation of dolomite, but an environment suffering from changes of salinity from hypersaline to dilute or fresh is particularly suitable (Folk and Siedleclca, 1974).

The more disseminated pre-compaction events include:

1. syndepositional formation of fenestral pores (Figure 80),
2. rapid occlusion of fenestral pores by a freshwater phreatic equant calcite cement (Figure 81),
3. growth of scattered anhydrite laths (Figures 82-83) and common anhydrite nodules,
4. growth of rare, replacive chert nodules (Figures 84-86),
5. replacement of anhydrite nodules by euhedral megaquartz.

Fenestral pores infilled by equant calcite cement were observed solely in the Apexco Green core, but may have been regionally present before pre-Woodford erosion. Fenestral fabric is believed to be largely related to interspaces within algal mats, as described by Ham (1956) and Philcox (1964). Isometric blocky calcite cement is most common in an active, saturated, freshwater phreatic zone (Longman, 1980), although it also forms in marine environments (Flugel, 1982). Early cementation is indicated by uncompacted algae and fenestrae.

Ghost structures in euhedral megaquartz ubiquitously have a fibrous felted texture typical of anhydrite (Figures 87-89). Bright anhydrite inclusions are also commonly observed in the replacive quartz (Figure 90). The precursor anhydrite is likely to have formed as a replacive mineral as well. Whether or not anhydrite was replacive, the spherical

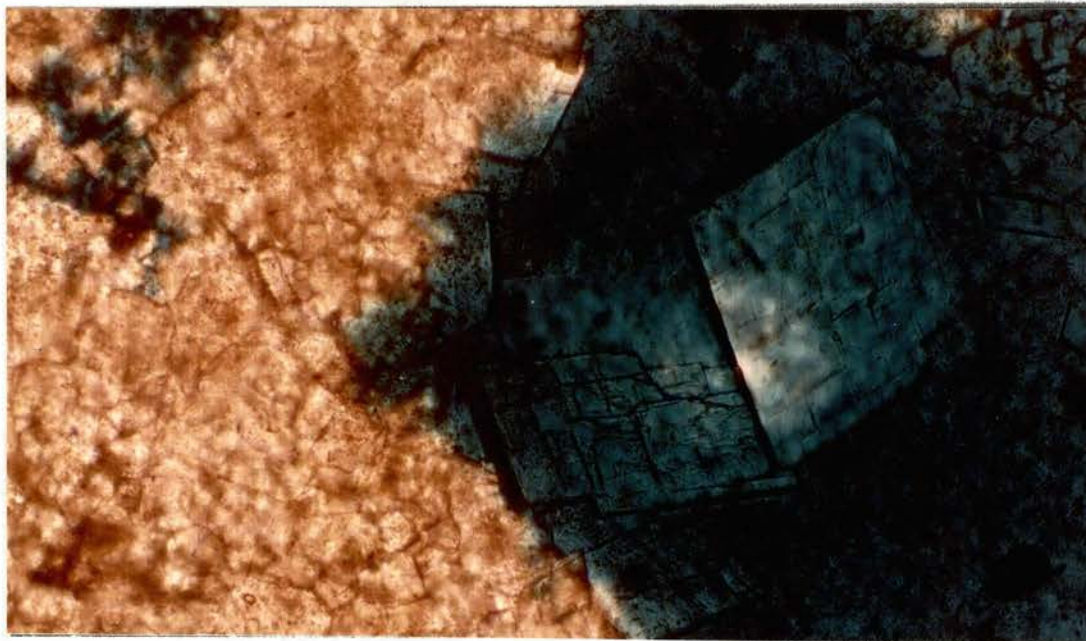


Figure 75. x400 Plane Polarized Light. Large, Limpid or White Rhombs Growing in or Into Pore Space. (Later dissolution is obvious.)



Figure 76. x40 Plane Polarized Light. Large, White Rhombs Infilling a Vug

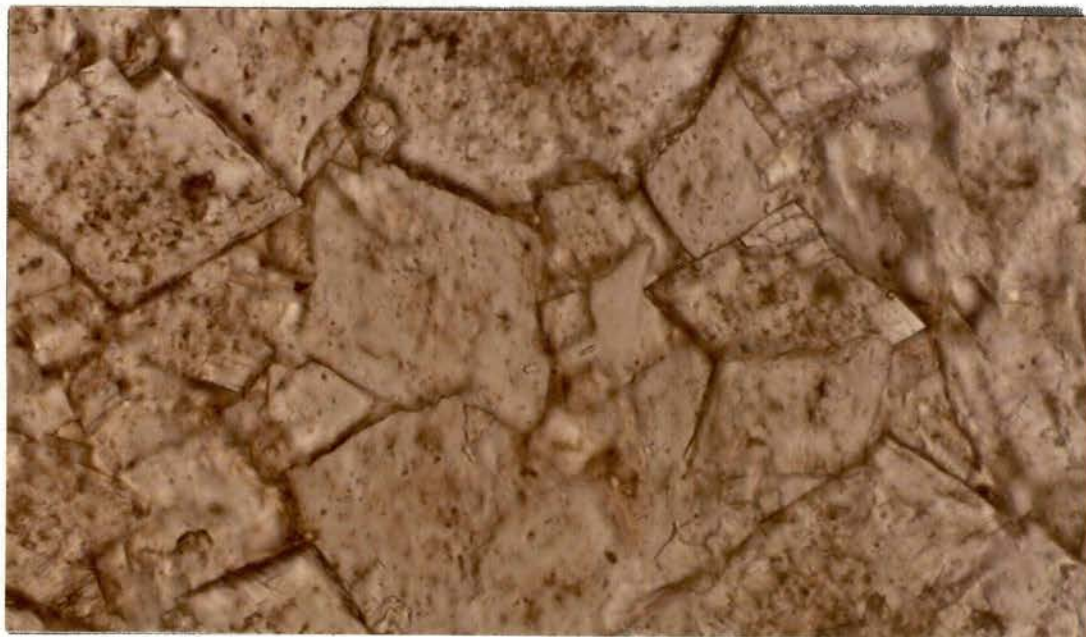


Figure 77. x400 Plane Polarized Light. Pre-compactional Idiotoxic Rhombs Now-distorted by Compaction Into Hypidiotoxic Rhombs. (Formation of the rhombs was pre-compactional.)

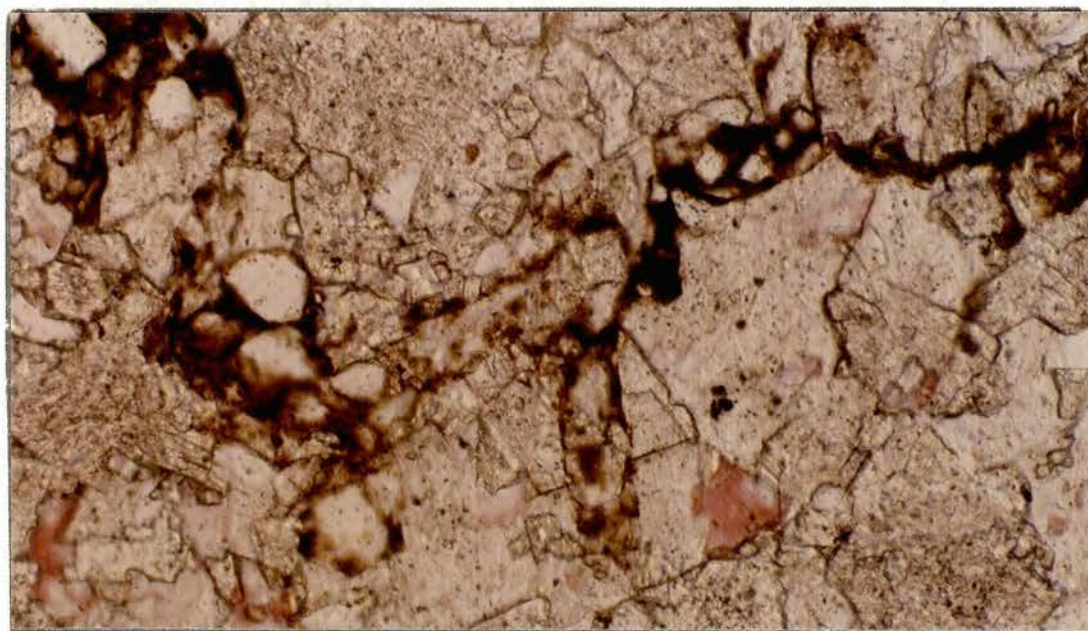


Figure 78. x200 Plane Polarized Light. Dolomite cut by Stylolite

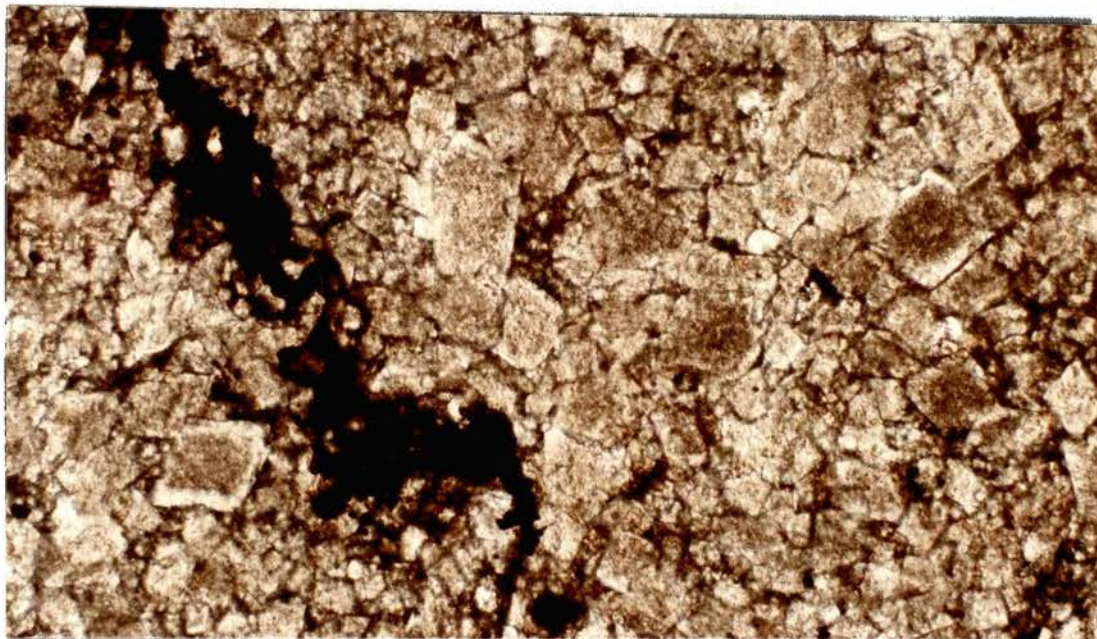


Figure 79. x100 Plane Polarized Light. Brown, Cloudy Dolomite and the Clean Rims Affected by Compaction Along a Stylolite

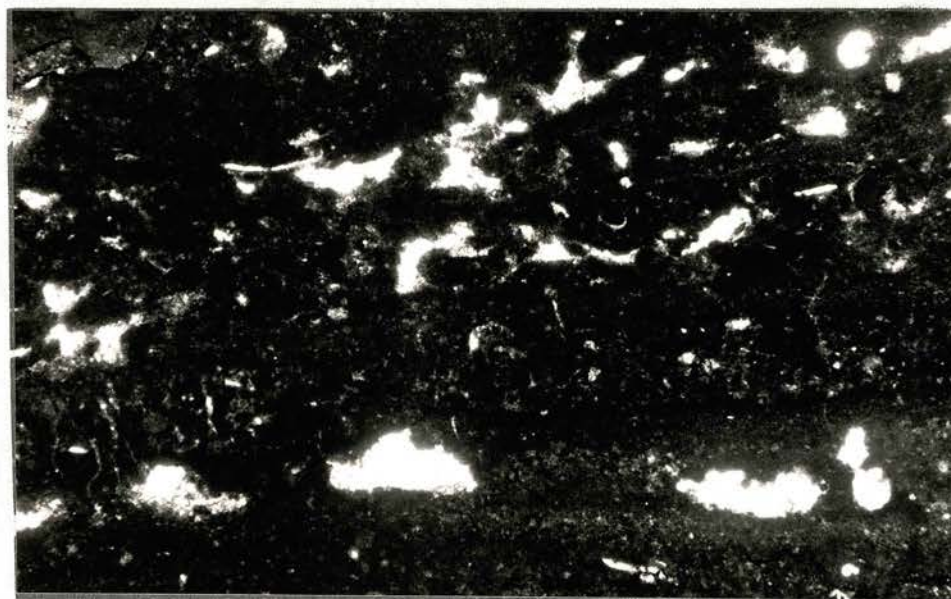


Figure 80. x40 Plane Polarized Light. Syndepositional Fenestral Pores in Facies I

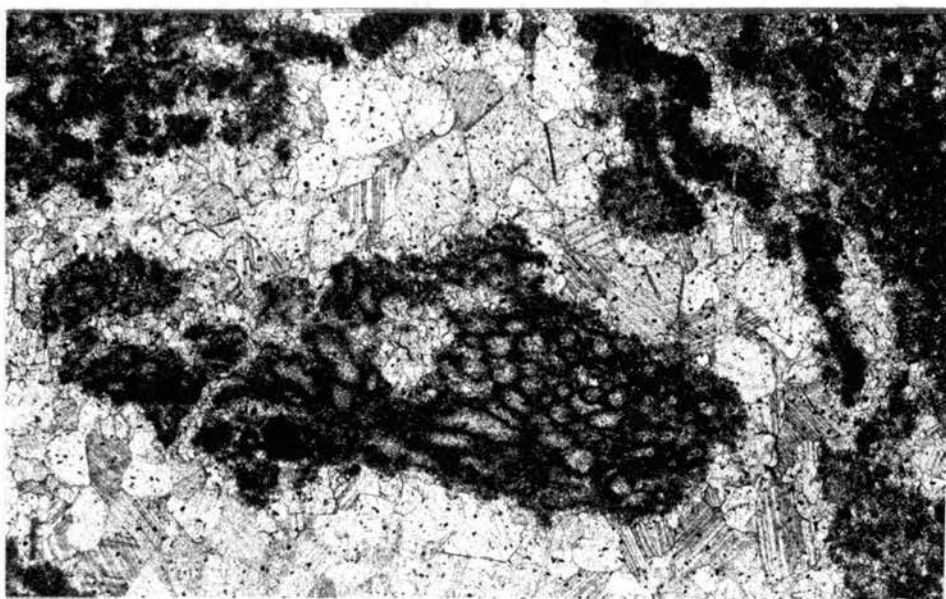


Figure 81. x200 Plane Polarized Light. Algae Surrounded
by Equant Calcite Cement in a Fenestral Pore

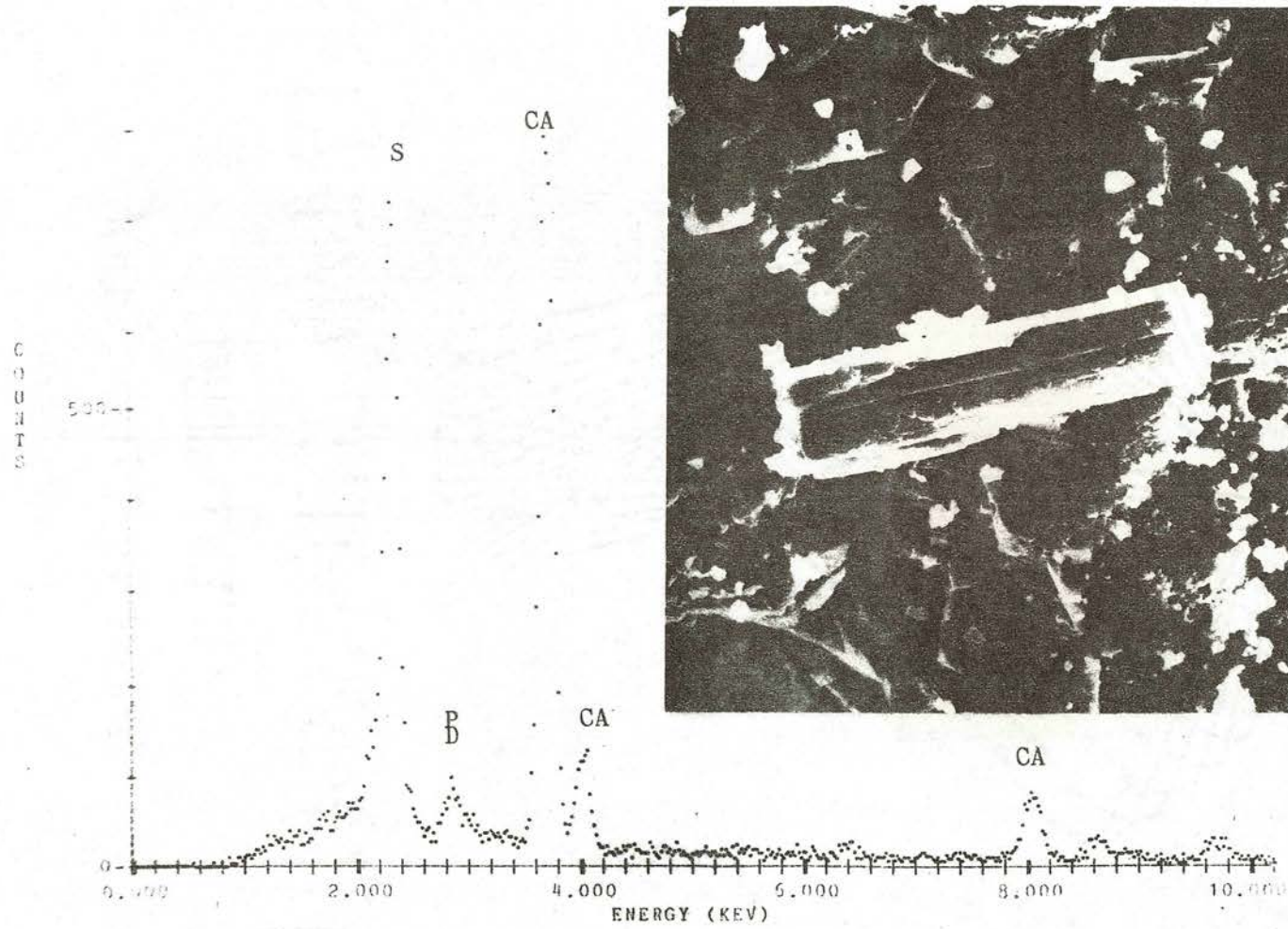


Figure 82. SEM Photograph of Small Anhydrite Lath with EDAX Element Peaks

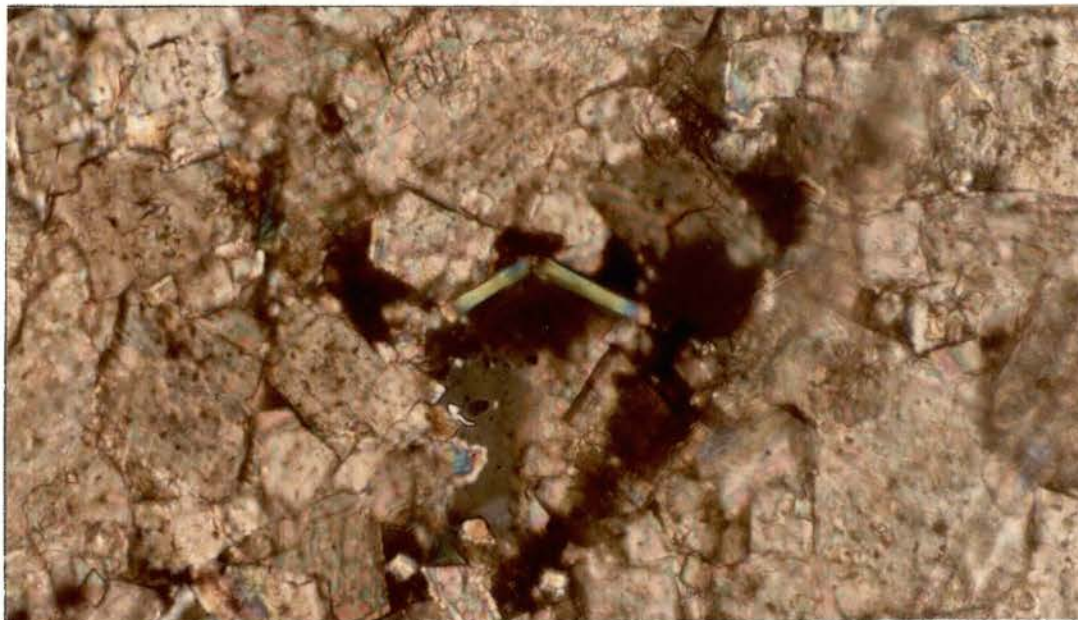


Figure 83. x 400 Crossed Nicols. Anhydrite Lath Bent by Compaction Across a Dolomite Rhomb. Anhydrite was Formed Before Compaction

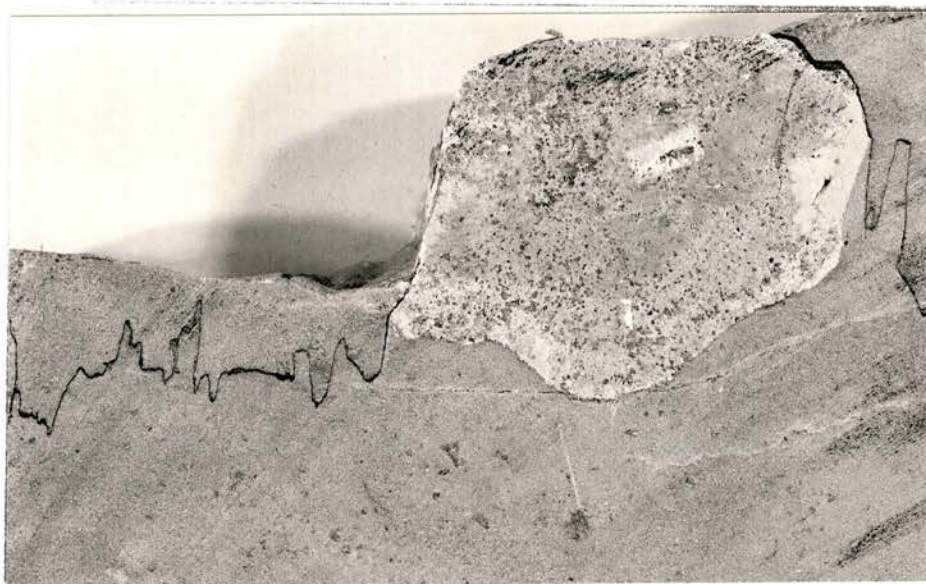


Figure 84. Core Photograph of Early Replacive Chert. (Note how stylolite wraps around nodule; therefore the nodule was pre-stylolitization. Nodule is 4 cm across.)

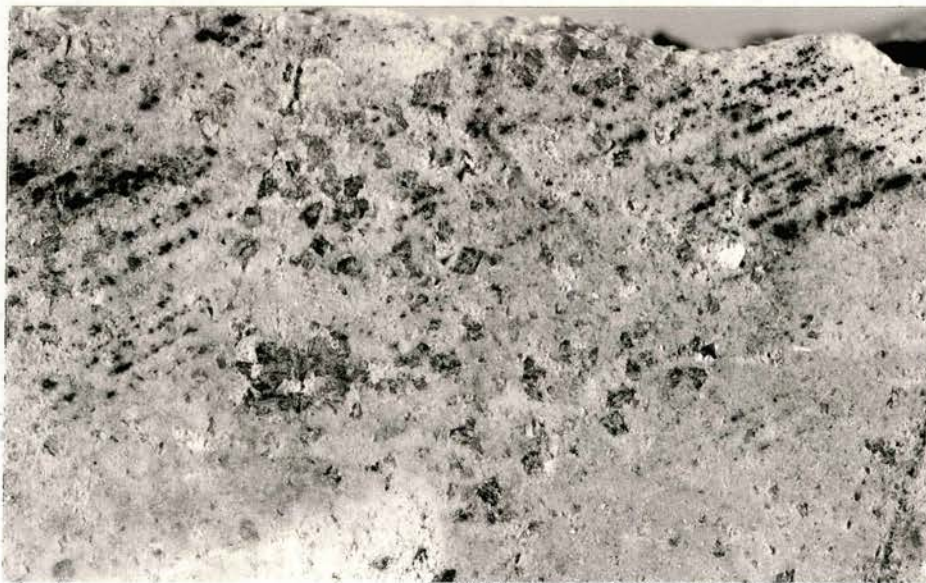


Figure 85. Closeup of Replacive Chert Nodule Showing Rhombs Floating in the Early Silica

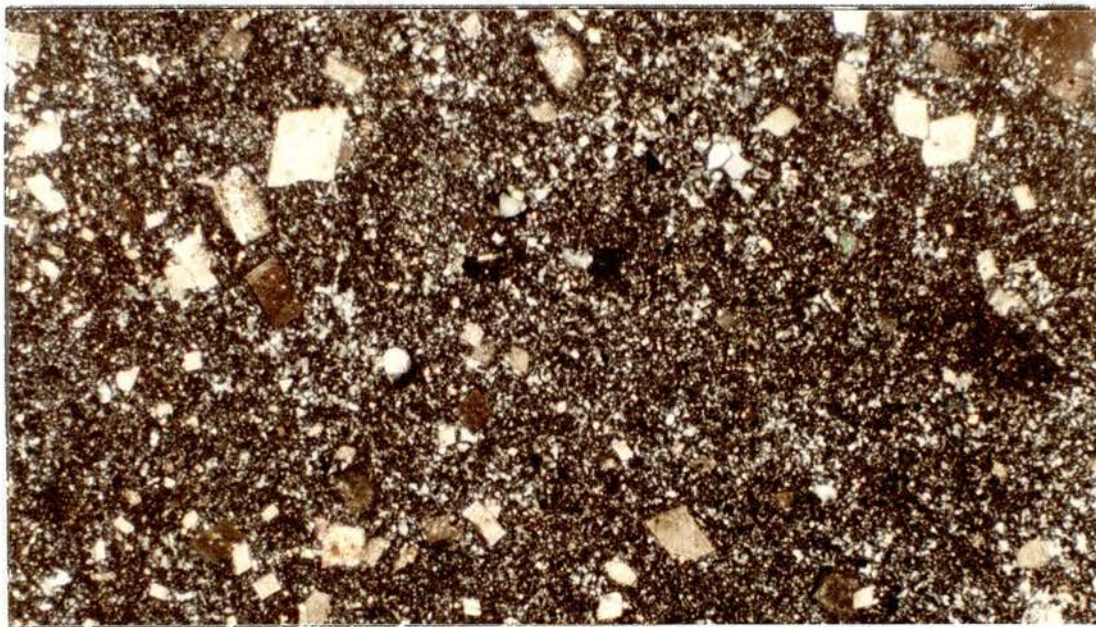


Figure 86. Photomicrograph of Replacive Chert Showing Early Well-formed Rhombs

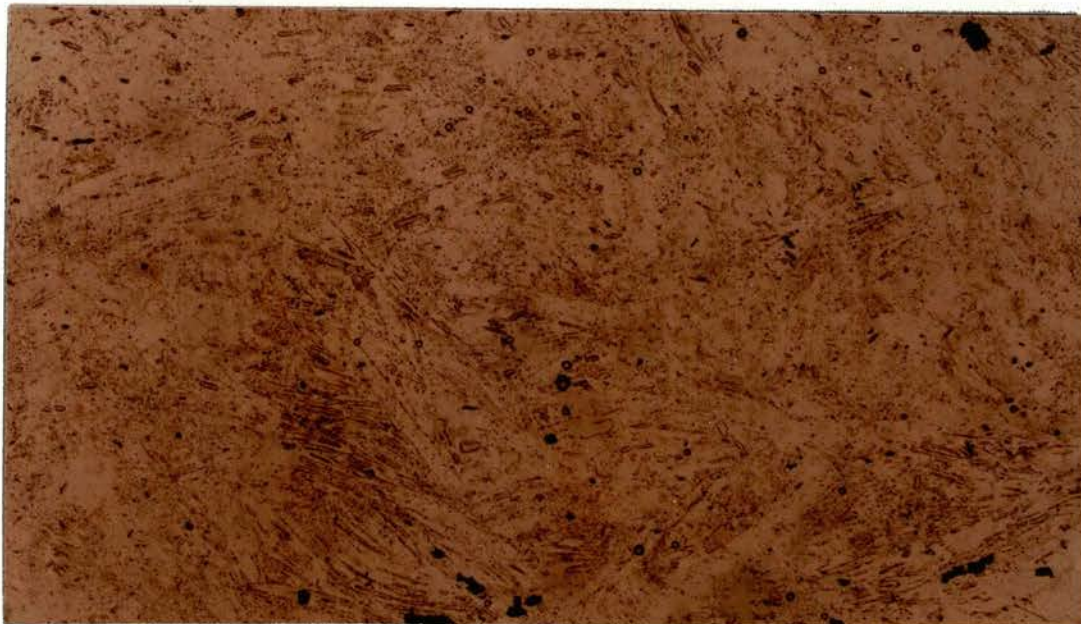


Figure 87. x40 Plane Polarized Light. Typical Fibrous Ghost Structure Observed in Replacive Euhedral Quartz, Indicating Former Anhydrite

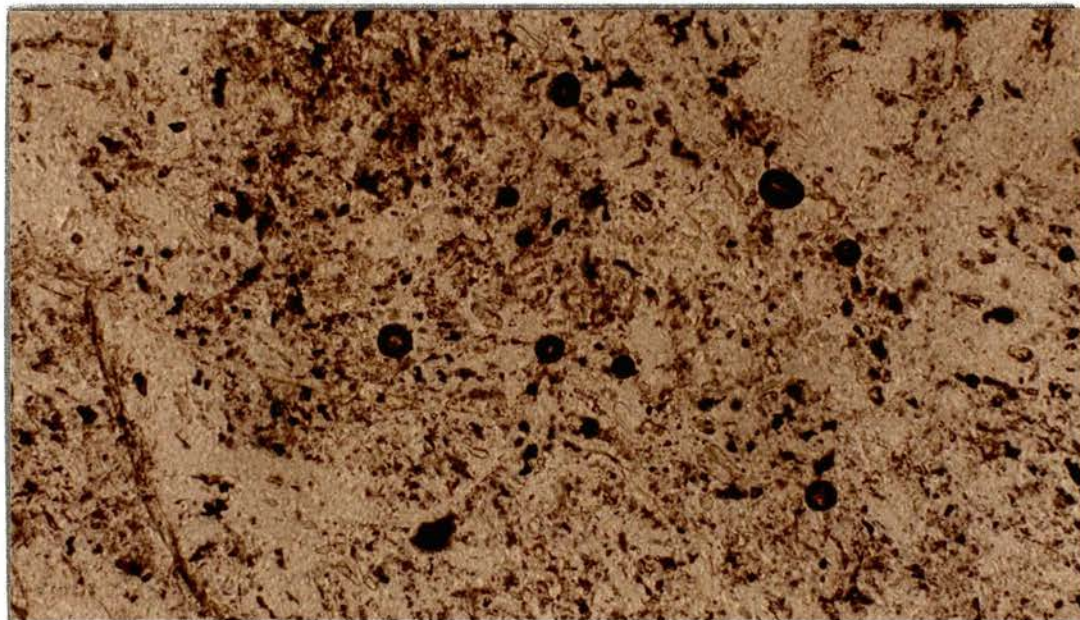


Figure 88. x100 Plane Polarized Light. Fibrous Texture and Organic Matter Observed in Quartz

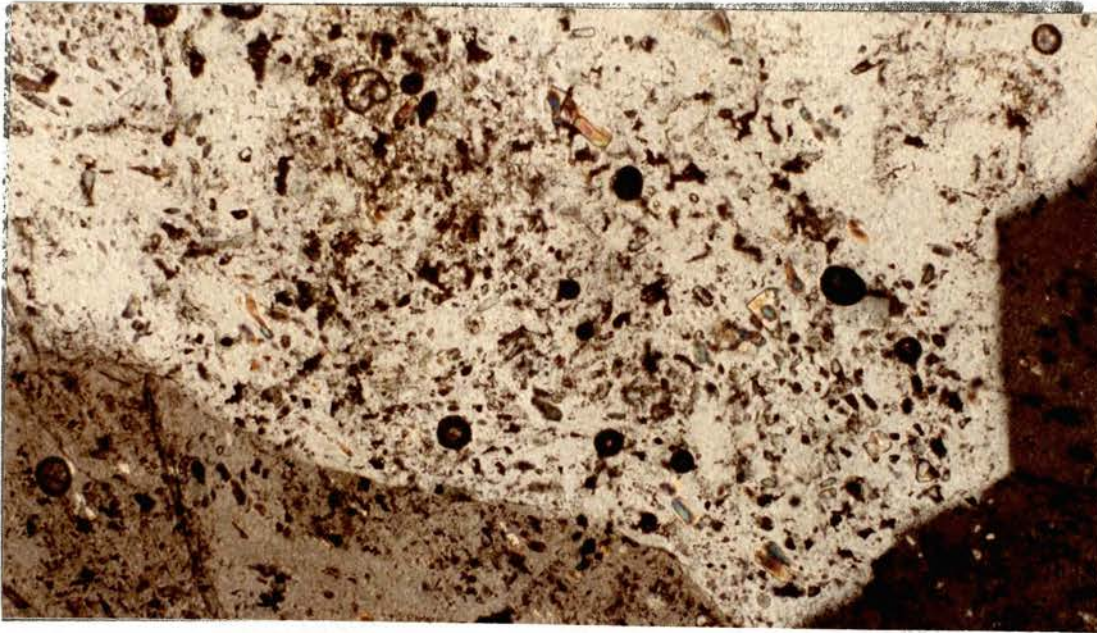


Figure 89. x100 Plane Polarized Light. Fibrous Texture and Organic Matter Observed in Quartz. (Crossed nichols.)



Figure 90. x200 Crossed Nichols. Bright Anhydrite Inclusion in Quartz

shape of the nodules (Figures 91-92) indicates growth through steady precipitation of anhydrite in sulphate-rich unconsolidated sediment (Tucker, 1976). Replacement of anhydrite by megaquartz was necessarily before stylolitization, evidenced by stylolites that wrap around the nodules.

Interruption of dolomitization by silicification has been reported by Dietrich and others (1963) and Dunham and Olson (1980). According to their results, silicification of calcium carbonate and dolomitization began at the same time. Dolomite is less soluble than calcium carbonate in most natural solutions, allowing nascent rhombs to be preserved while the surrounding calcium carbonate mud is dissolved with consequent silicification. Replacive silica in the Henryhouse is predominantly chert with rare chalcedony. Chert nodules containing small patches of micrite along with rhombs were observed, clearly indicating chertification concordant with earliest dolomitization.

Post-compaction

Late diagenetic accessory minerals are volumetrically unimportant, but may have considerable impact on porosity. Calcite, polyhalite (?) and rare anhydrite are present as intercrystalline, space filling, and replacive cements (Figures 93-97). Pyrite, baroque dolomite, and rare sphalerite occur in vugs and molds (Figures 98-102). Pyrite is found replacing anhydrite inclusions in euhedral megaquartz on rare occasions.

Late cements can all be seen growing onto or surrounding compaction deformed dolomite rhombs, establishing them as postcompactional. Cement replaces dolomite rhombs and is replaced by calcite cement. Very isolated small patches of anhydrite cement cannot be found in contact with other cements.

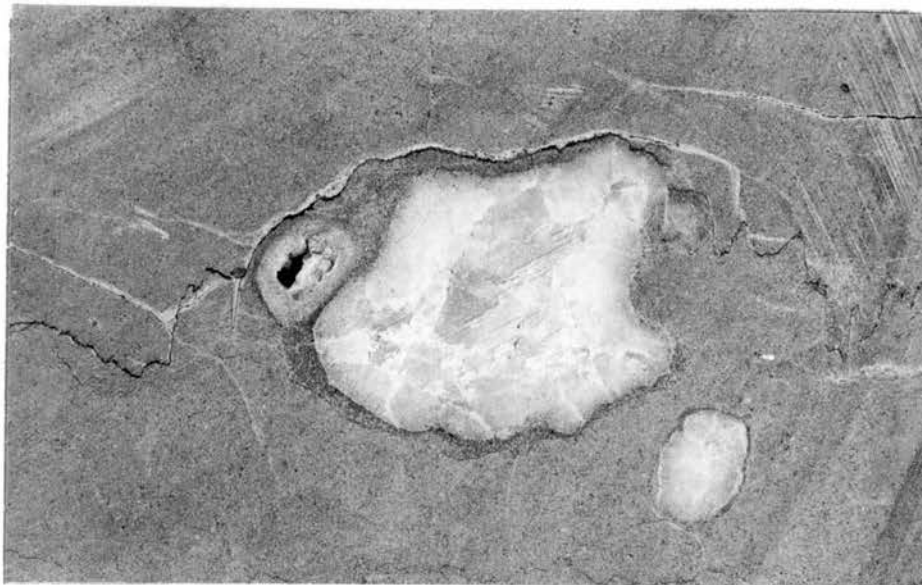


Figure 91. Core Photograph of Rounded Nodules of Replaced Anhydrite. Center Nodule is 4 cm Across. (Note the subsequent stylolitization.)

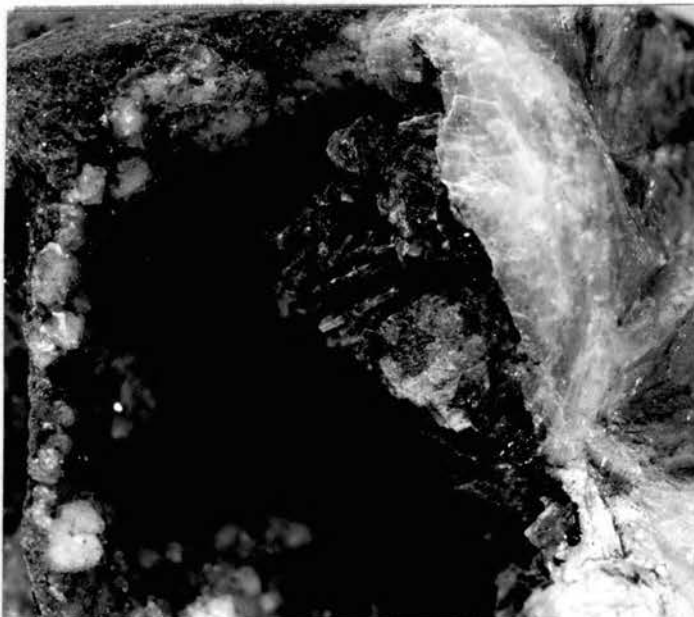


Figure 92. Core Photograph of Large (6 cm) Anhydrite Nodule that has been Rimmed by Replacive Euhedral Quartz, Partially Dissolved, and Oil-stained

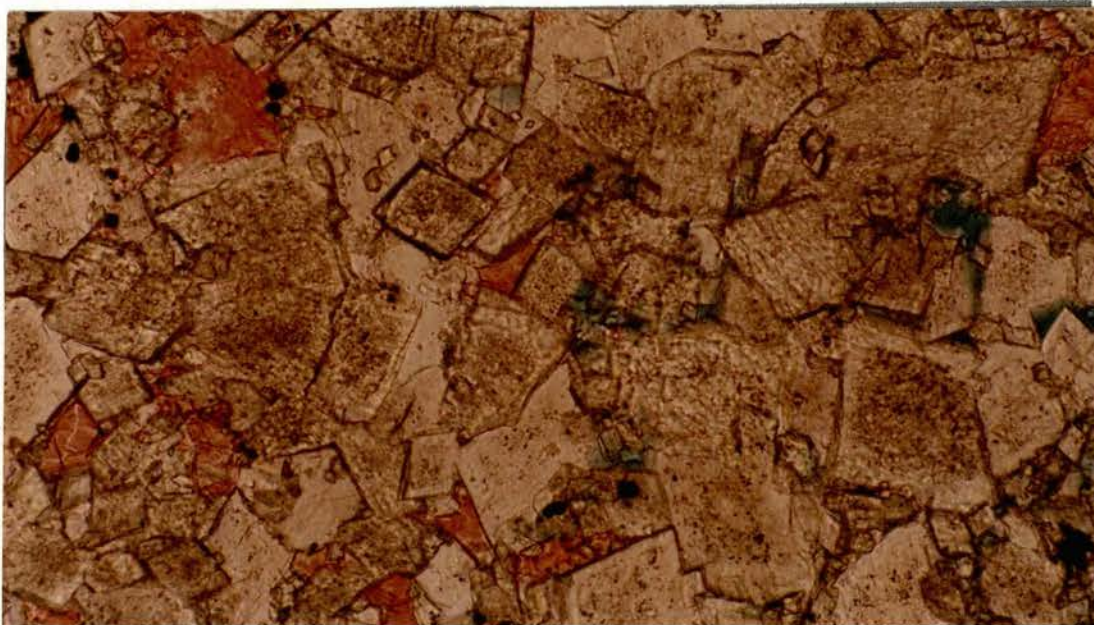


Figure 93. x100 Plane Polarized Light. Intercrystalline Calcite Cement Stained red. (Note halo type rhombs.)



Figure 94. x100 Crossed Nicols. Vug Filling Late Calcite Cement Stained red. (Note the overlapping of this cement onto euhedral quartz and dolomite rhombs, therefore post-dating them.)



Figure 95. x400 Crossed Nicols. Rare Intercrystalline Polyhalite (?) Cement

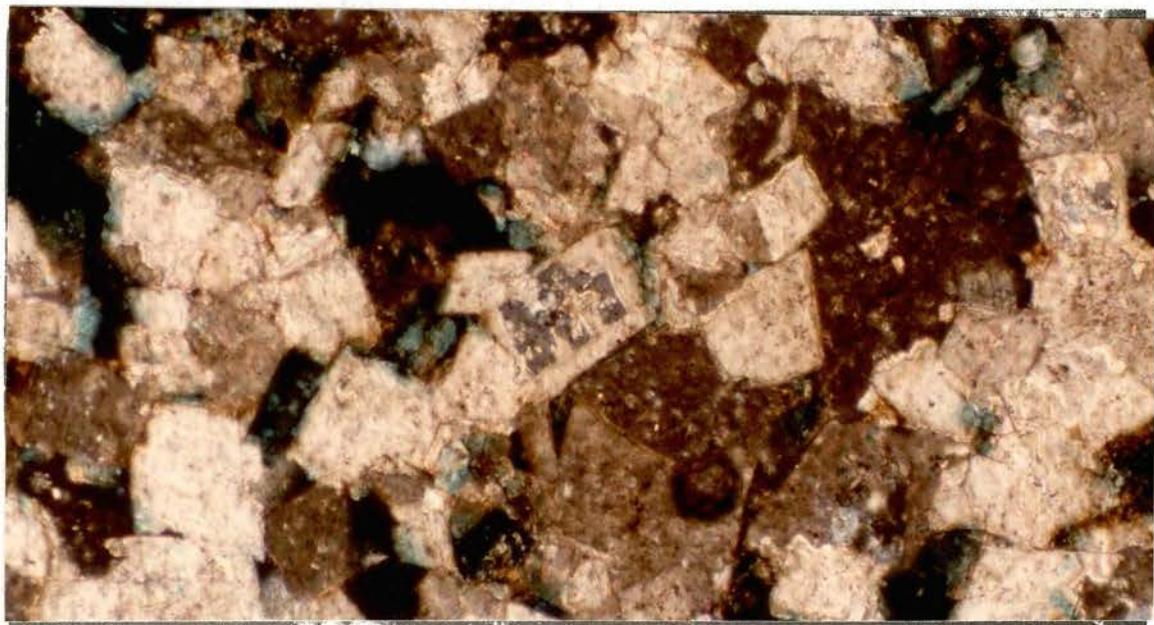


Figure 96. x200 Crossed Nicols Polyhalite (?) Cement Replacing Dolomite

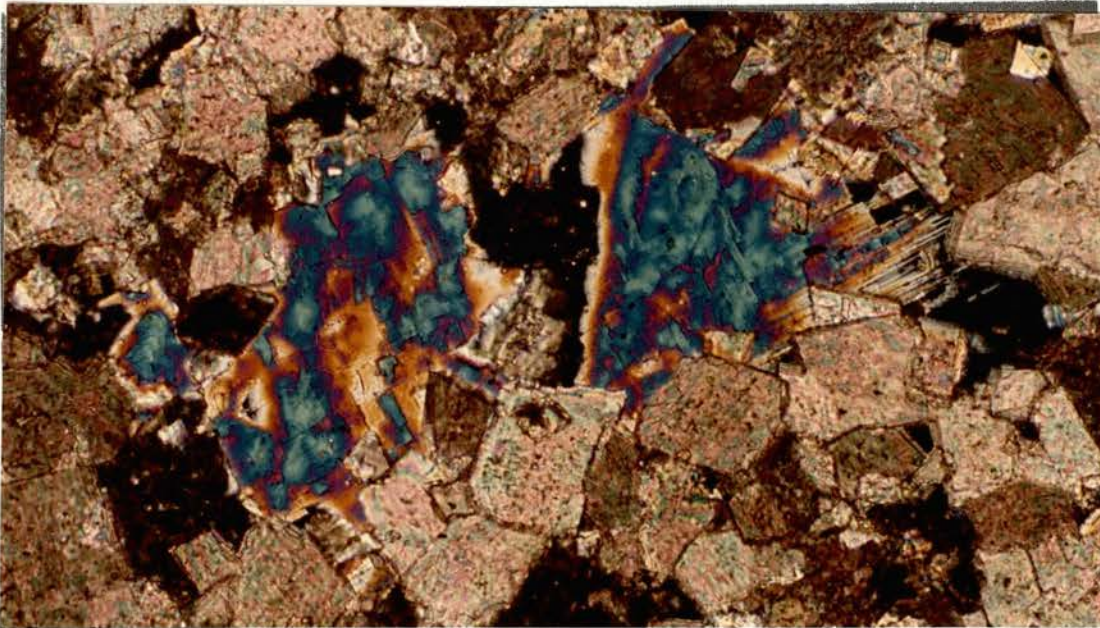


Figure 97. x400 Crossed Nicols. Rare Late Anhydrite Cement



Figure 98. x20 Crossed Nicols. Vug Filling Baroque Dolomite. (Note typical sweeping extinction.)

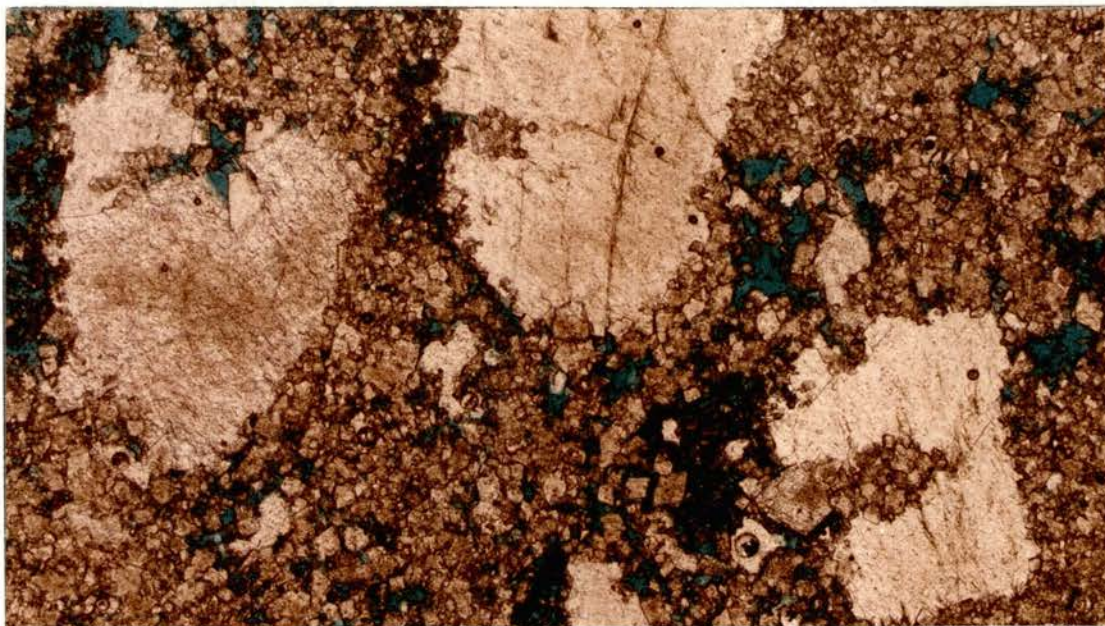


Figure 99. x40 Plane Polarized Light. Mold Filling
Baroque Dolomite

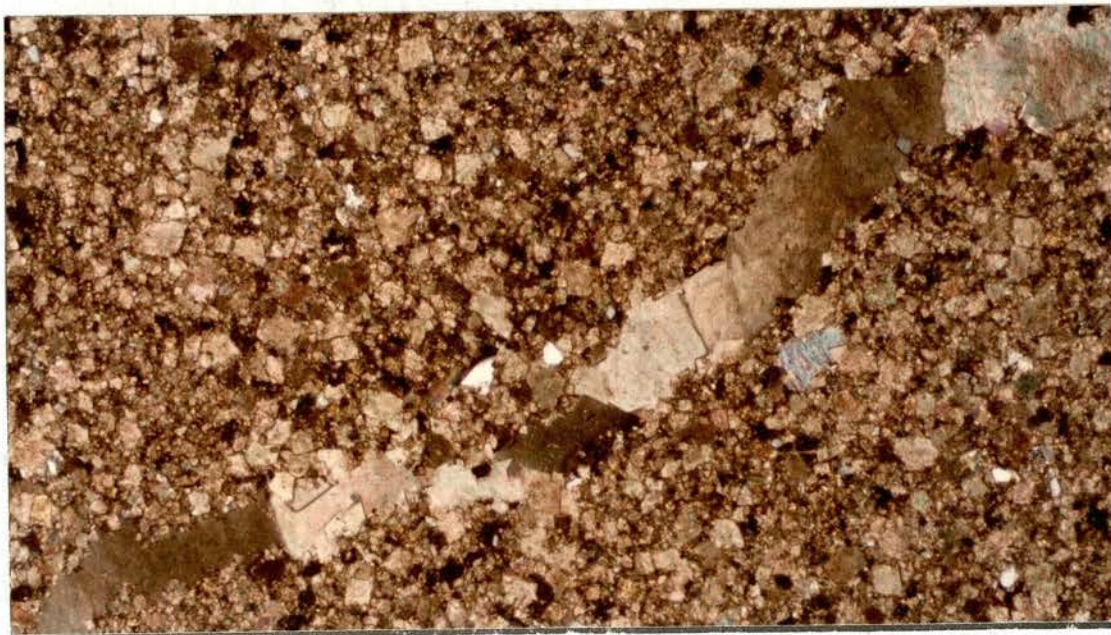


Figure 100. x40 Crossed Nicols. Fracture Filling
Baroque Dolomite

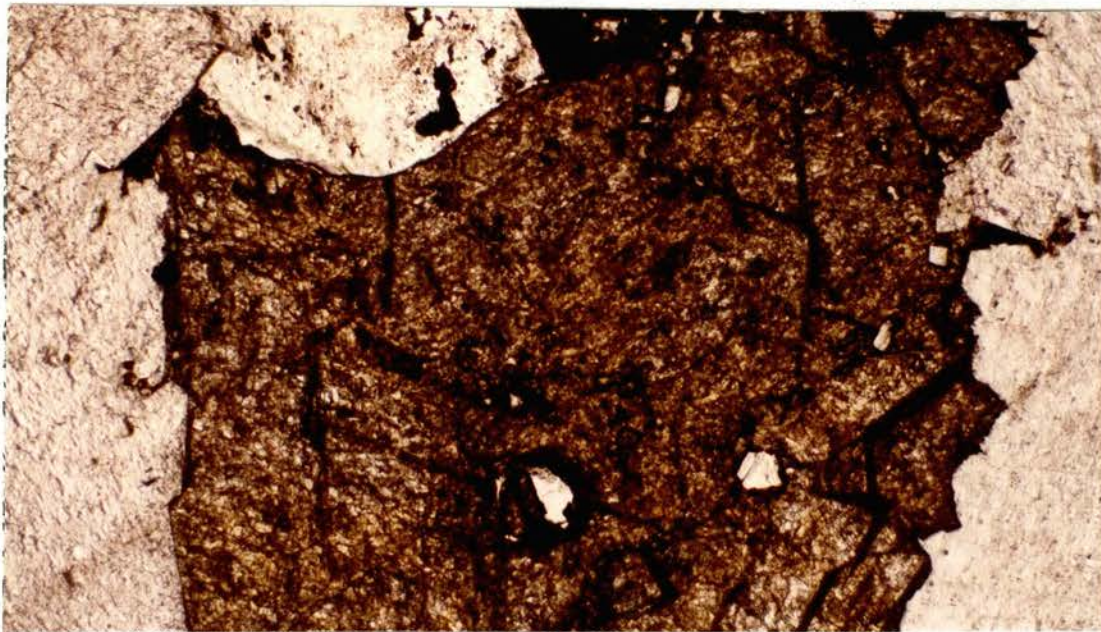


Figure 101. x100 Plane Polarized Light. Late Sphalerite Surrounded by Baroque Dolomite. (Note associated bitumen.)



Figure 102. x100 Plane Polarized Light. Anhydrite Inclusions in Quartz Replaced by Pyrite

CHAPTER V

DOLOMITIZATION

Introduction

Prevalent theory on dolomite formation favors a dissolution-precipitation mechanism with very little ancient dolomite explained by precipitation at or above the sediment-water interface (Zenger and Dunham, 1980). Most explanations offered for the origin of dolomite involve eogenetic hypersaline brine (Adams and Rhodes, 1960; Hsii and Siegenthaler, 1969; Deffeyes and others, 1965; Friedman and Saunders, 1967; Friedman, 1980; Beales and Hardy, 1980; and others), marine water-meteoric water mixing (Handshaw and others, 1971; Badiozamani, 1973; Land, 1973; Folk and Land, 1975; Dunham and Olson, 1980; and others), or both (Folk and Siedlecka, 1974; Sears and Lucia, 1980). Petrographic and geochemical evidence presented in this chapter support the latter explanation. Both hypersaline brine and marine-meteoric water mixing are proposed to have dolomitized Henryhouse limestone.

Paleogeography reconstructions of Briden and others (1979) and Irving (1979) place the Anadarko Basin within approximately 5 to 15° south latitude for most of Silurian time. Little is known about the paleoclimate, but it seems plausible to consider arid to semi-arid conditions during deposition of the Henryhouse. Low latitude, marginal marine areas in shallow epeiric seas may develop hypersalinity if high evaporation rates exceed precipitation. Elevated salinity on arid,

upper intertidal-lower supratidal, sabkha type deposits is favorable for evaporite mineral formation (Tucker, 1979). Some indication of evaporative minerals, then, is crucial for a dolomitization model involving hypersaline brines.

It should not be assumed that the initial dolomitization phase will escape later alteration. Examples of situations that may lead to modification of pre-existing dolomite and/or addition of a second species of dolomite are given by Folk and Siedlacka (1974). An appropriate situation for the Henryhouse sediments is a freshwater lense forced seaward under a hydrostatic head. Detection of secondary dolomite of a freshwater imprint on original dolomite may be accomplished with petrographic and isotopic analyses.

Petrographic Evidence

Indications of Hypersalinity

Dolomites formed under hypersaline conditions are commonly stripped of the evaporite minerals they were originally associated with (Dunham and Olson, 1980). However, subtle traces providing evidence for former presence of evaporites usually survive despite diagenetic overprint (Friedman, 1980; Dunham and Olson, 1980). Indications of former evaporites in the Henryhouse Formation include:

1. pseudomorphs of anhydrite,
2. disseminated anhydrite laths,
3. equant megaquartz,
4. stromatalitic algal structures,
5. paucity of fauna.

Siliceous pseudomorphs after anhydrite nodules have often been linked to vanished evaporites (Chowns and Elkins, 1974; Folk and Siedlecka, 1974; Tucker, 1976; Walker and others, 1977; Friedman, 1980). Early replacement of anhydrite nodules by silica, especially euhedral megaquartz, is common in Facies II. Hypersaline conditions are unequivocally indicated by the former presence of these sulphates (Folk and Siedlecka, 1974).

Intercrystalline euhedra of gypsum and anhydrite have been proposed as hypersaline indicators by Beales and Hardy (1980). According to their interpretation, ambient fluids at the time of formation and enclosure of Siedlecka anhydrite crystallites in a dolomite matrix are necessarily elevated in salinity.

Euhedral equant crystals of authigenic quartz ubiquitously polymorphose early displacive fibrous masses of anhydrite (see Figures 87-93). Similar authigenic quartz has commonly been reported in dolomites presumably formed in hypersaline conditions (Friedman, 1980). A direct relation between hypersalinity and euhedral quartz crystals has not been established (Folk and Siedlecka, 1974).

Sediment burrowers and organisms that graze on algal mats will not inhabit the harsh higher salinities of restricted areas. Preserved algal mats and non-burrowed sediment therefore indicate areas of increased salinity (Kendall and Skipwith, 1968; Friedman, 1980). Reduced diversity and occurrence of fossils is the predictable result of persistent hypersalinity.

Indications of Fresh Water Mixing

Petrographic evidence for mixing zone dolomite are less definitive

than those for hypersaline dolomite. Interpretation must be based on several possible indicators. Evidence for a mixing zone origin of some Henryhouse dolomite includes:

1. similarity to previously reported mixing zone dolomite,
2. the luminescent character,
3. the stable oxygen isotopic composition.

Euhedral limpid rhombs and cloudy rhombs with limpid rims have been proposed as mixing zone indicators by Folk and Siedlecka (1974) and were similarly interpreted by Sears and Lucia (1980). Changes other than dilution by freshwater may effect zonation of dolomite, but a brackish water mixing environment is an ideal place for this to be accomplished (Folk and Siedlecka, 1974).

Distinct bands or zones are revealed in Henryhouse dolomite with electron-induced luminescence. Variations of luminescent intensity are the result of different concentrations of activator (Mn^{2+}) and quencher (Fe^{2+}) ions within the rhombs. The zonation may rarely be complex (Figure 103) or simple (Figure 104). Usually, the rhombs have four zones, a core that is dark or very dull red, a thin bright second zone, a broad dull third zone, and a final thin bright zone that may be enlarged (Figures 105-108). This is interpreted to indicate a common water history and common origin (Choquette and Steinen, 1980).

Under near surface aerobic conditions, the oxidized Fe^{3+} and Mn^{3+} ions are too large to be incorporated into the dolomite crystal lattice. Dolomite formed at the surface or influenced by surface conditions (Phase I dolomite) therefore has a dull luminescence. More reducing conditions will permit the smaller Mn^{2+} ion to be introduced into the dolomite lattice, causing bright luminescence. The final brightly

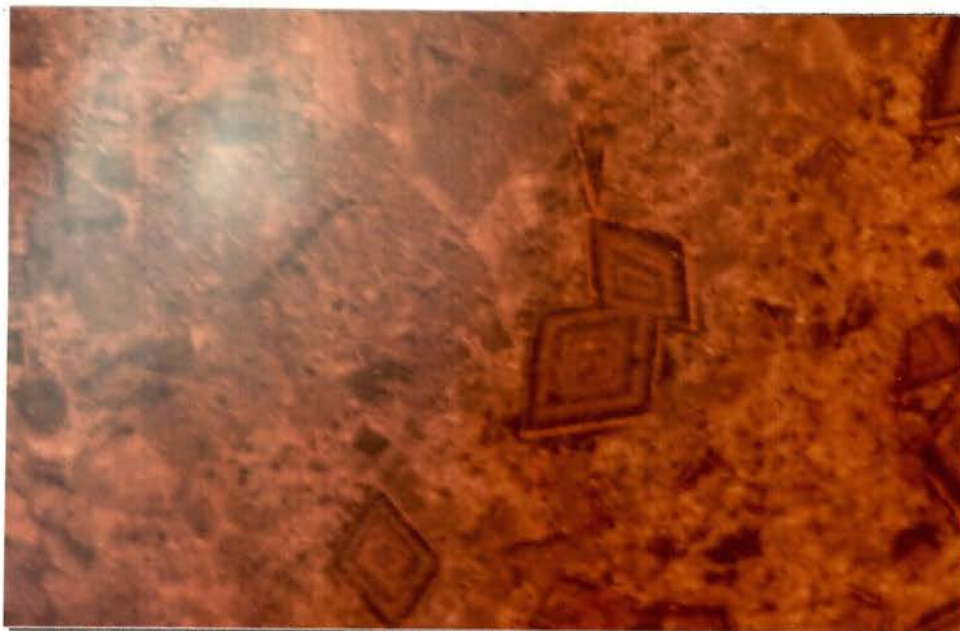


Figure 103. x40 Cathode Luminescence. (Eight or more zones of varying luminescence revealed in a large dolomite rhomb.)

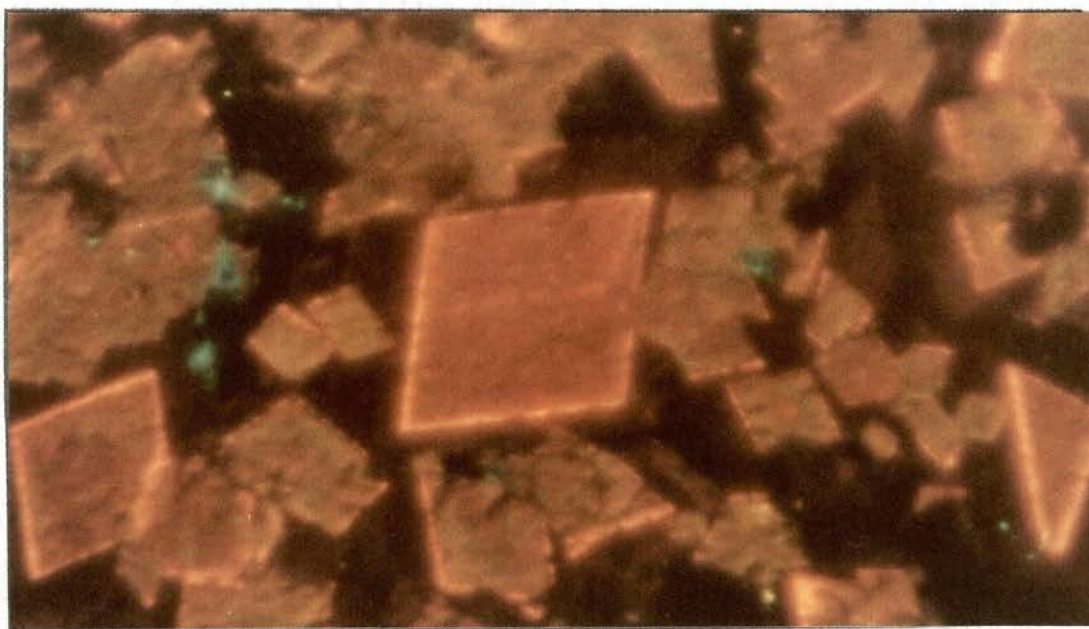


Figure 104. x200 Cathode Luminescence (non-complex zonation)

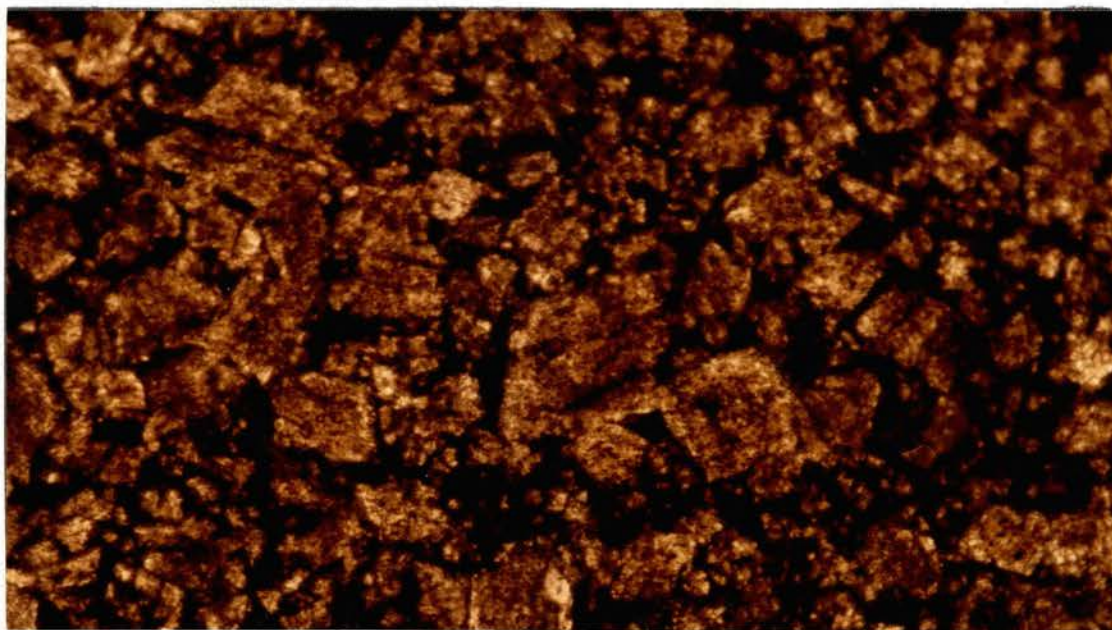


Figure 105. x100 Plane Polarized Light. (Note slightly visible cleaner rims.)

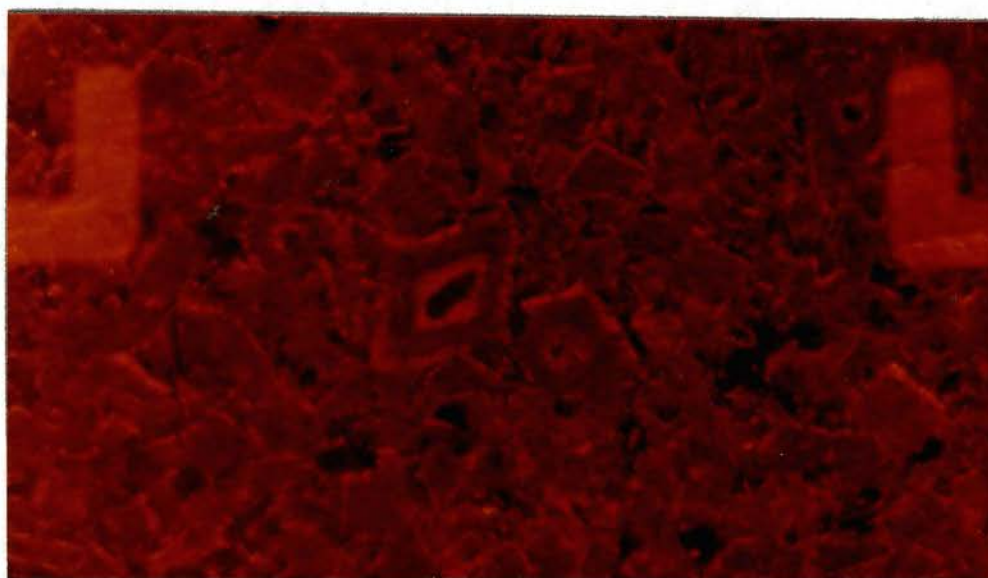


Figure 106. Cathode Luminescence of Above Thin Section Reveals Typical Four-part Zonation With Final Bright rim

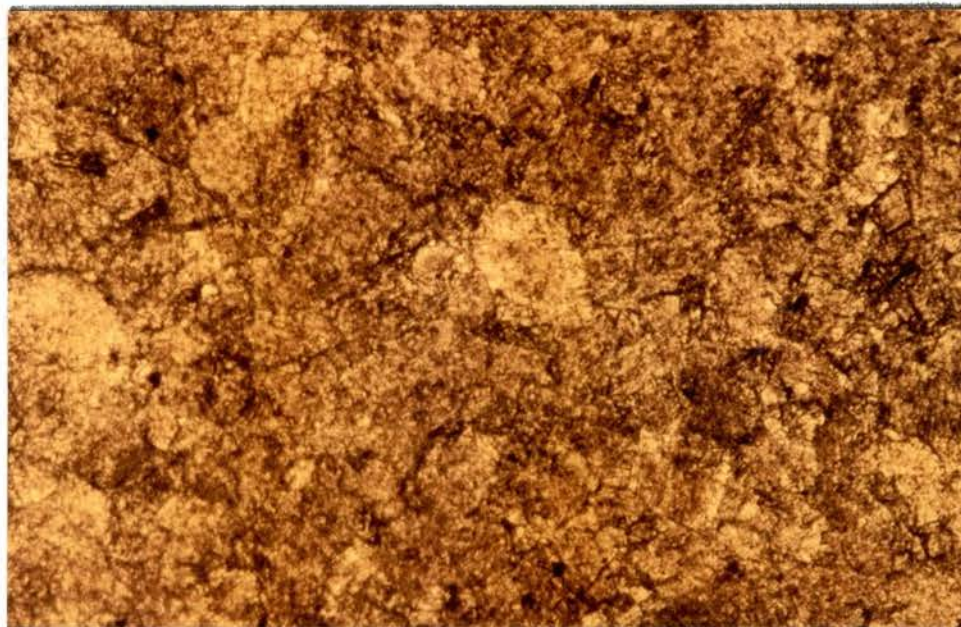


Figure 107. x 100 Plane Polarized Light. Large Limpid or White Overgrowth on Rhomb in the Center

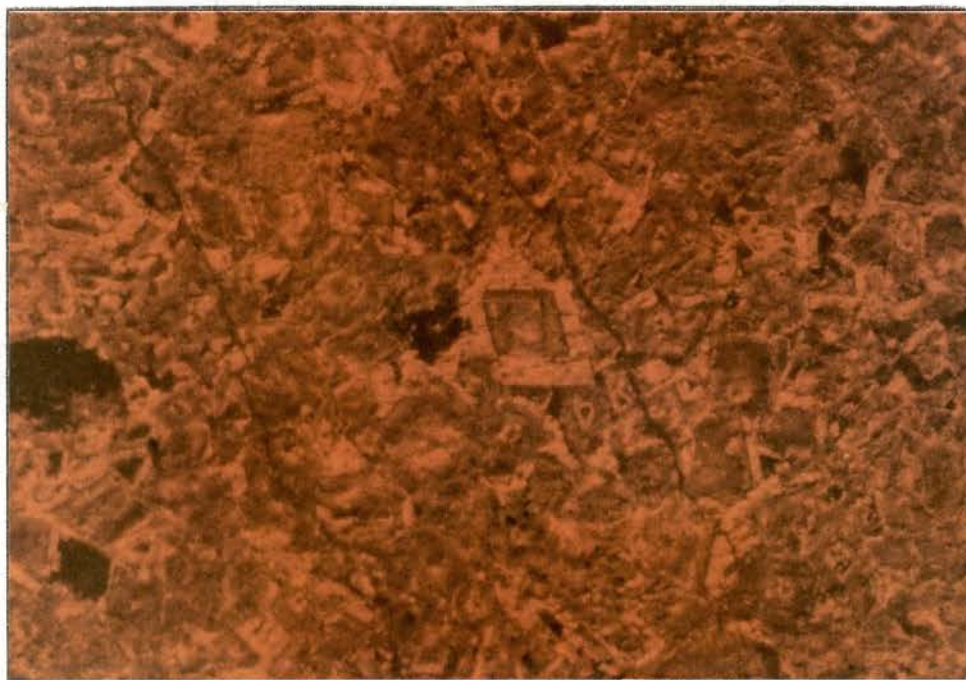


Figure 108. Cathode Luminescence of Above Thin Section Reveals Typical Four-part Zonation with Enlarged Outer rim. (Note how the overgrowth and final rim coincide.)

luminescent zone that coincides approximately with the clean overgrowths may be interpreted as mixed marine and freshwater dolomite formed at a slightly greater depth (Phase II dolomite). The addition of Fe^{2+} with increasingly reduced conditions would cause non-luminescence (Choquette and Steinen, 1980; Grover and Read, 1983).

Geochemical Evidence

Isotopes of oxygen and carbon are widely used as a tool for interpretation of the fluid responsible for dolomite formation. A thorough study of stable isotopes and their applications is available by Arthur and others (1983).

Carbon Isotopes

Modern $\delta^{13}\text{C}$ values for carbonates are generally between -2 and +4 parts per thousand on the PDB scale (Gross, 1964). Published carbon isotopic composition of ancient platform dolomite has a similar range (Land, 1980). The relatively constant values of $\delta^{13}\text{C}$ reflect its resistance to diagenetic alteration (Degens and Epstein, 1964; Land, 1980).

Isotopic data for the Henryhouse is presented in Table IV. Carbon isotope values for dolomite range between 0 and +3.38 (mean 1.4). The narrow range probably indicates a lack of significant alteration with close resemblance to the original marine carbon isotope values.

Figure 109 demonstrates how Henryhouse dolomite $\delta^{13}\text{C}$ values compare with those of a variety of common dolomite types. Although the range and mean do not fall outside the range for freshwater-marine water mixing, they most strongly indicate an early diagenetic reflux

TABLE IV
STABLE ISOTOPIC COMPOSITIONS OF HENRYHOUSE CARBONATE

Well	Depth	Description	Analysis*	
			C ¹³	O ¹⁸
Apexco Green	19615	dolomite host rock	+1.0	-4.0
Apexco Green	19660	dolomite host rock	+ .9	-3.6
Apexco Green	19740	limestone host rock	+2.5	-6.3
Apexco Green	19770	dolomite host rock	+3.8	-4.8
Tenneco J.A-1	8514	dolomite host rock	+ .5	-4.3
Tenneco J.A-1	8600	vug filling calcite	+ .9	-7.8
Tenneco J.A-1	8600	dolomite host rock	+1.1	-5.2
Tenneco J. 2-34	8474	dolomite host rock	+ .9	-4.1
Tenneco J. 2-34	8505	dolomite host rock	+1.2	-5.2
Tenneco J. 2-34	8565	dolomite host rock	+2.3	-4.5
Tenneco J. 2-34	8565	dolomite intraclasts	+2.2	-4.0
Tenneco J. 2-34	8565	calcite crystals	+2.0	-4.6
G.H.K. Hoffman	14268	dolomite host rock	0.0	-3.4
G.H.K. Hoffman	14346	dolomitic host rock	+1.2	-2.2
G.H.K. Hoffman	14346	limestone host rock	- .2	-4.9
L. S. Hanan	14349	dolomite host rock	+1.1	-9.9

*C¹³ - standard is PDB; O¹⁸ standard is PDB.

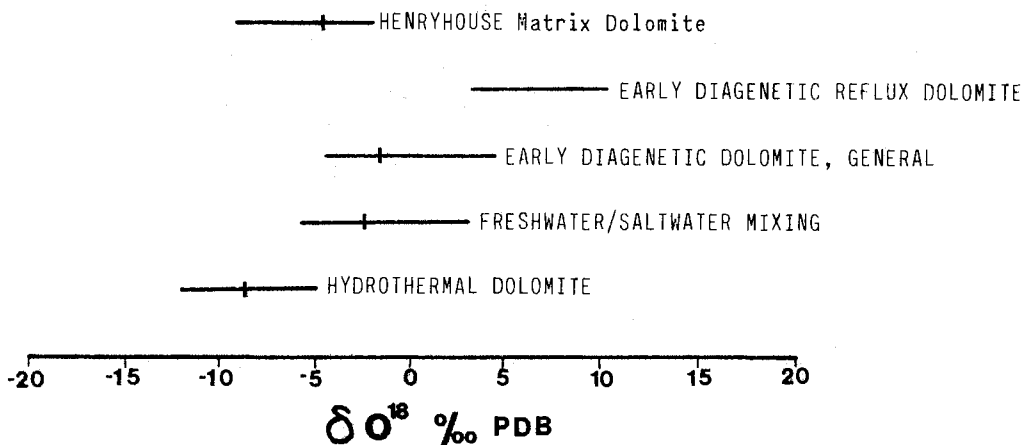
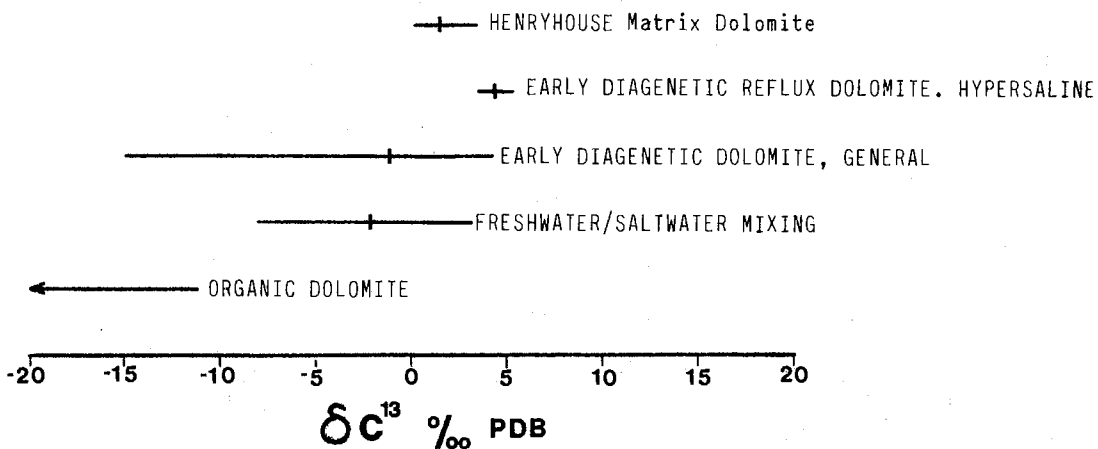


Figure 109. Bar Graphs for δC^{33} and δO^{18} Comparing Henryhouse Dolomites With Different Species of Dolomites. (Modified after Mattes and Mountjoy, 1980, p. 211.)

dolomite origin.

Oxygen Isotopes

According to Land (1980) "the $\delta^{18}\text{O}$ of dolomite is dependent at least as much upon the δ^{18} of the water and the temperature at which it formed as upon the $\delta^{18}\text{O}$ of its precursor" (p. 90). Ubiquitous oxygen isotopic depletion (low or negative values) of ancient dolomites is therefore the result of precipitation (or recrystallization) from $\delta^{18}\text{O}$ depleted fluids or higher temperatures, or both (Land, 1980). Pre-holocene platform dolomite has a general range of +2 - +5. Dolomite with values less than about -2 parts per thousand must bear the imprint of meteoric water and/or elevated temperatures (Land, 1983).

Oxygen isotope values for Henryhouse dolomite have a range from -2.2 to -9.9 (mean -4.6). When plotted with the range and mean of other common dolomite types, the isotopic imprint strongly favors freshwater marine water mixing over hypersaline conditions (Figure 109).

Dolomitization Model

Petrographic isotopic character of Henryhouse dolomite (summarized in Table IV) indicate two phases of dolomitization:

1. penecontemporaneous hypersaline dolomitization, and
2. eogenetic mixed water dolomitization.

Phase I - Hypersaline Dolomitization

A facies has been recognized within the Henryhouse Formation that suggests an arid to semi-arid supratidal depositional environment (see Chapter III). Evaporation of marine water from this restricted inner

TABLE V
SUMMARIZATION OF EVIDENCE FOR HYPERSALINE AND
MIXED WATER DOLOMITIZATION

Phase I - Hypersaline

Paleogeography	- Sabkha-type Environment
Algal Structures	
Fenestral Fabric	
Sparse Fauna	

Anhydrite Laths	- Cause Increased $\frac{\text{Mg}^{2+}}{\text{Ca}^{2+}}$ Ratio
Replaced Anhydrite Nodules	

Carbon isotope composition - suggests early Hypersaline

Dolomite decreases with depth - dolomitizing fluids from above

Cloudy brown centers - characteristic of hypersalinity

Phase II - Mixed Water

Prograding shoreline - advancing freshwater lense

Oxygen isotope composition - suggests early mixing

Clean overgrowths - characteristic of fresher water

Cathodoluminescence - suggests a late anaerobic, phreatic influence

shelf area (Facies I) permitted formation of gypsum and/or anhydrite later pseudomorphed by euhedral megaquartz. A result of precipitation of CaSO_4 is a rise in the $\text{Mg}^{++}/\text{Ca}^{2+}$ ratio which is of major significance for formation of dolomite (Bathurst, 1975) by the reaction:



Dense, hypersaline brines with an elevated $\text{Mg}^{2+}/\text{Ca}^{2+}$ ratio are believed to have then flowed downward and seaward at a lower level, as suggested by Adams and Rhodes (1960); Deffeyes and others (1965); Sears and Lucia (1980); and Muir and others (1980). Figure 110 is an illustration depicting the overall regressive pattern of Henryhouse carbonates and the proposed movement of dolomitizing brines.

Both relative impermeability and diminished head explain incomplete dolomitization of Facies III even when placed stratigraphically below Facies I and II during progradation.

Phase II - Mixed Water Dolomitization

As Henryhouse sediments prograded seaward, gradual burial of seaward facies by landward facies would take place. Eventually, a zone of migrating meteoric water would pass through these sediments as the shoreline advanced across the wide shelf. At the interface between fresh groundwater and ocean-derived brines, a brackish zone of mixing would develop (Figure 111). Such waters could be saturated with respect to dolomite (Handshaw and others, 1971) and precipitate it by enlarging already existing crystals (Land, 1973). Distribution of this second dolomite is generally uniform across facies.

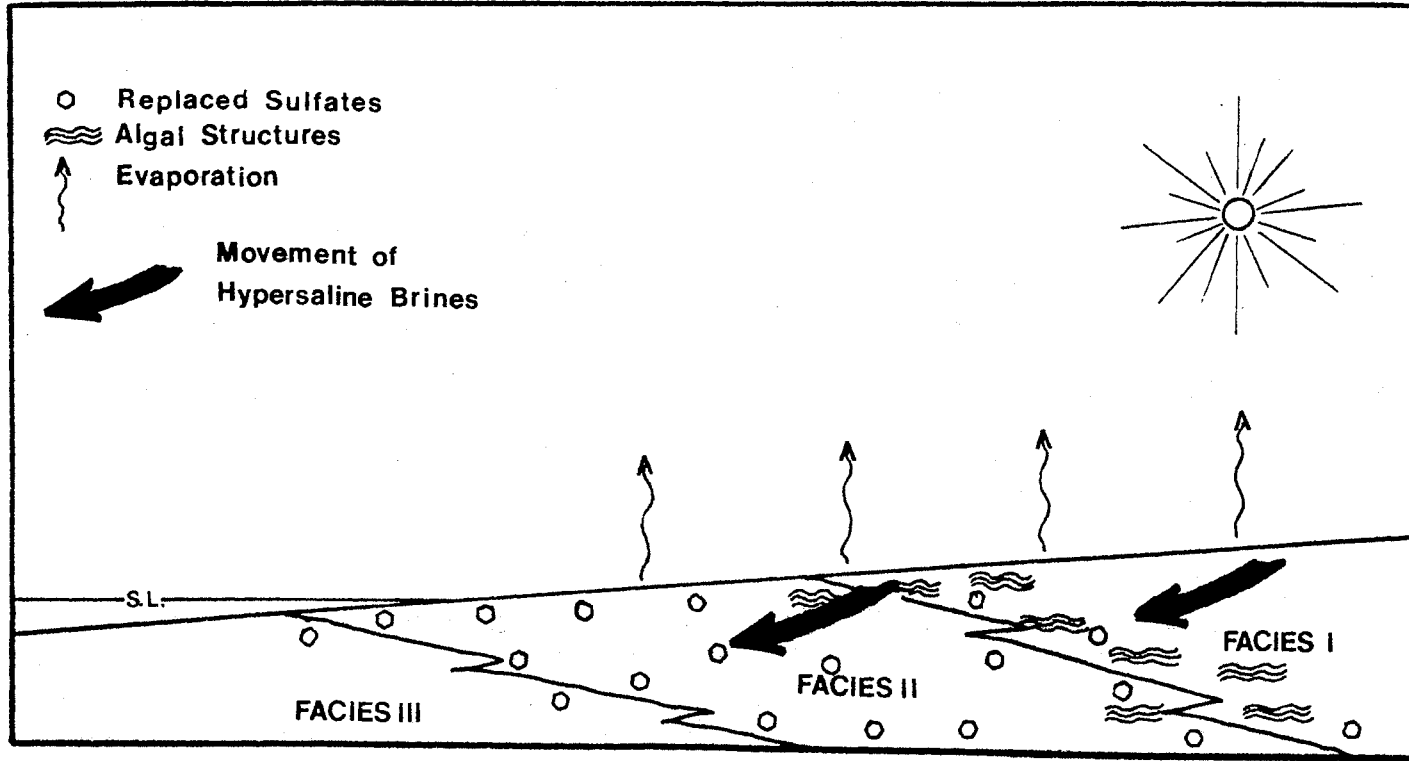


Figure 110. Illustration Depicting Phase I Dolomitization of Regressive-Progradational Henryhouse Carbonates by Hypersaline Brines

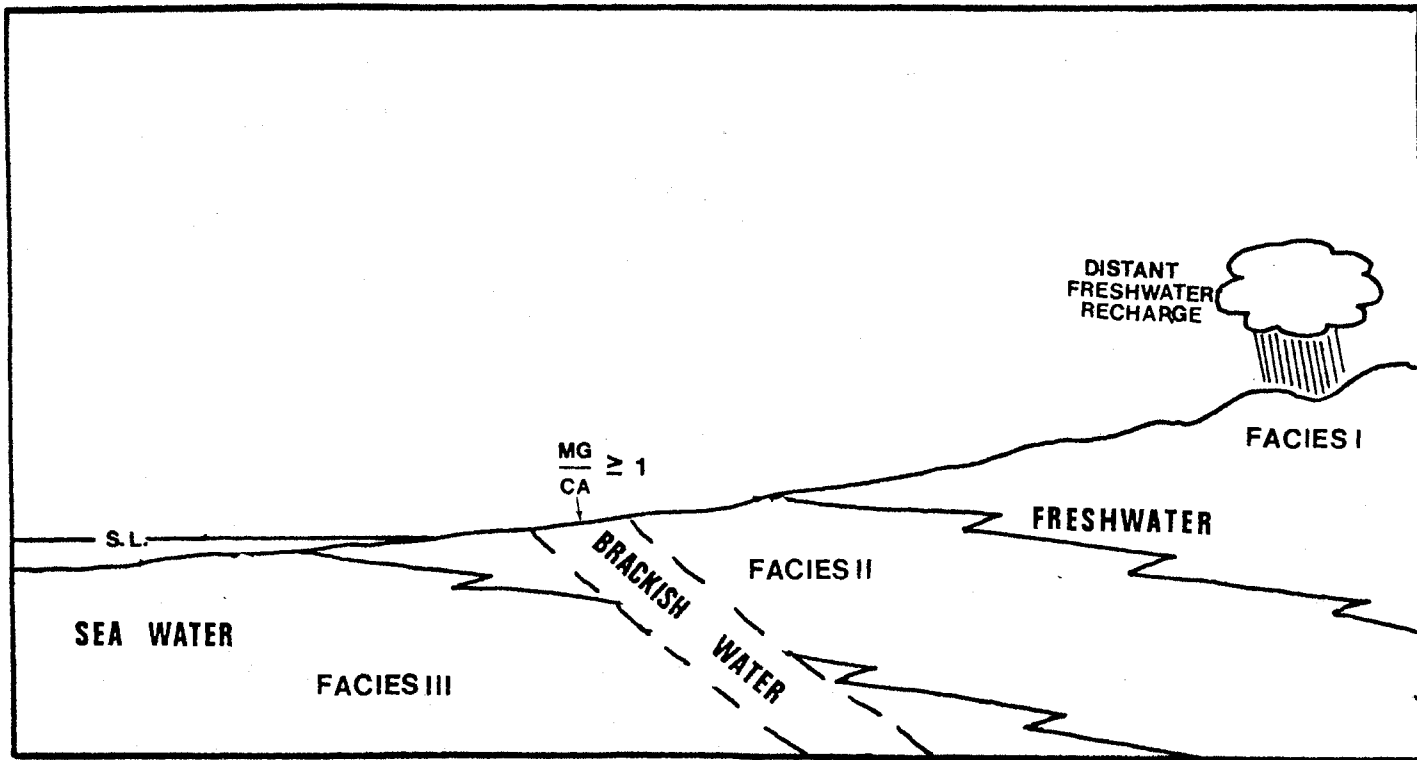


Figure 111. Illustration Depicting Phase II Dolomitization by Sea Water/Freshwater Mixing

CHAPTER VI

CONCLUSIONS

The following conclusions have been made from this study:

1. Sedimentary structures can be recognized in the Henryhouse Formation and used to construct a depositional model with three broad depositional facies: upper intertidal to supratidal/tidal flat (Facies I), shallow subtidal to upper intertidal (Facies II), and open shelf subtidal (Facies III).
2. These depositional facies were deposited in a predominantly regressive manner.
3. Three main species of dolomite were noted: 1) brownish, cloudy, hypidiotopic dolomite formed shortly after deposition at the expense of the micrite matrix due to magnesium enriched hypersaline brines; 2) white or limpid idiotopic dolomite formed after the hypersaline dolomite but before significant compaction due to freshwater/marine water mixing; 3) postcompactional mold, vug, and fracture filling dolomite with undulous extinction (baroque dolomite).
4. Penecontemporaneous hypersaline brownish, cloudy, hypidiotopic dolomite is volumetrically the most important.
5. Dolomitization was most complete in the shallow subtidal to upper intertidal facies (Facies II) due to proximity to the source of dolomitizing fluids and burrow enhanced permeability increasing movement and saturation by the fluids.

6. Three types of porosity were developed: moldic porosity, vuggy porosity, and intercrystalline porosity. Moldic and vuggy porosity are secondary, intercrystalline is both primary porosity preserved by dolomitization and late secondary dissolution porosity. Moldic porosity is volumetrically the most important.

7. Porosity is related directly to the depositional environment. Porosity was best developed in the shallow subtidal to upper intertidal facies (Facies IIa and b). The features characteristic of facies IIa and b that caused it to preferentially develop porosity are burrowing and abundant pelmatozoan fossils. Burrowing enhanced the porosity and permeability of the sediment, allowing dolomitizing fluids to more effectively operate, which preserved the enhanced porosity and permeability. Subsequent dissolving fluids were then able to attack the non-dolomitized fossils, creating moldic porosity. The upper intertidal to supratidal facies (Facies I) is often considerably dolomitized yet without burrowing and fossils, no significant porosity developed. Subtidal Henryhouse carbonate (Facies III) was never highly dolomitized due to both relative impermeability (never highly burrowed) and increased distance from the source of dolomitizing fluids. Facies III fossils were never dissolved.

8. During Phase II dolomitization and continued exposure, porosity was undoubtedly enhanced. However, the unconformity surface was not required for porosity development.

REFERENCES CITED

- Adams, J. E. and Rhodes, M. L. 1960. Dolomitization by Seepage Refluxion: Amer. Assoc. Petrol. Geol. Bull. Vol. 44, pp. 1912-1920.
- Adler, F. J. 1971. Future Petroleum Provinces of the Mid-Continent. Future Petroleum Provinces of the United States, Their Geology and Potentials: Amer. Assoc. Petrol. Geol. Memoir No. 15, pp. 985-1120.
- Amsden, T. W. 1957. Stratigraphy of the Hunton Group: Okla. Geol. Survey Circular 44, 49 pp.
- Amsden, T. W. 1960. Hunton Stratigraphy: Okla. Geol. Survey Bull. 84, 298 pp.
- Amsden, T. W. and Rowland, T. L. 1971. Silurian and Lower Devonian (Hunton) Oil and Gas-producing Formations: Amer. Assoc. Petrol. Geol. Bull., Vol. 55, pp. 104-109.
- Amsden, T. W. 1975. Hunton Group (Late Ordovician, Silurian, and Early Devonian) in the Anadarko Basin of Oklahoma: Okla. Geol. Survey Bull. 121, 214 pp.
- Arthur, M. A., Anderson, T. F., Kaplan, T. R., Veiser, J., and Land, L. S. 1983. Stable Isotopes in Sedimentary Geology, Soc. Econ. Paleon and Min. Shortcourse No. 10, 432 pp.
- Badiozamani, K. 1971. The Dorag Dolomitization Model - A;ocation to the Middle Ordovician of Wisconsin: Jour. Sed. Pet. Vol. 43, pp. 965-984.
- Bathurst, R. G. C. 1975. Developments in Sedimentology: Carbonate Sediments and Their Diagenesis. Amsterdam: Elsevier Scientific Publishing Company, 658 pp.
- Beales, F. W. and Hardy, J. W. 1980. Criteria for the Recognition of Diverse Dolomite Types With an Emphasis on Studies of Host Rocks for Mississippi Valley-type Ore Deposits. In Concepts and Models of Dolomitization: Soc. Econ. Paleon. and Min. Spec. Publication No. 28, pp. 197-215.

- Borak, B. 1978. Progressive and Deep Burial Diagenesis in the Hunton (Late Ordovician to Early Devonian) and Simpson (Early to Middle Ordovician) Groups of the Deep Anadarko Basin of Southwestern Oklahoma: Unpublished Master's Thesis, Rensselaer Polytechnic Institute, Troy, New York.
- Briden, J. C., Drewry, G. E., and Smith, A. G. 1974. Phanerozoic Equal Area Maps: Jour. Geol. Vol. 82, pp. 555-574.
- Choquette, P. W. and Pray, L. C. 1970. Geologic Nomenclature and Classification of Porosity in Sedimentary Carbonates: Amer. Assoc. Petrol. Geol. Bull. Vol. 54, pp. 207-250.
- Choquette, P. W. and Steinen, R. P. 1980. Mississippian Non-supratidal Dolomite, Ste. Genevieve Limestone, Illinois Basin: Evidence for Mixed-Water Dolomitization. In Concepts and Models of Dolomitization: Soc. of Econ. Paleon. and Min. Spec. Publication No. 28, pp. 163-196.
- Chowns, T. M. and Elkins, J. E. 1974. Origin of Quartz Geods and Cauliflower Cherts Through Silicification of Anhydrite Nodules: Jour. Sed. Pet. Vol. 44, pp. 885-903.
- Deffeyes, K. S., Lucia, F. J., and Weyl, P. R. 1965. Dolomitization of Recent and Plio-Pleistocene Sediments by Marine Evaporative Waters on Bonaire, Netherlands Antilles. In Dolomitization and Limestone Diagenesis: Soc. Econ. Paleon. and Min. Spec. Publication 13, pp. 71-87.
- Dietrich, R. V., Hobbs, C. R. B., Jr., and Lowry, W. D. 1963. Dolomitization Interrupted by Silicification: Jour. Sed. Pet. Vol. 33, pp. 646-663.
- Dunham, J. B. and Olson, E. R. 1980. Shallow Subsurface Dolomitization of Subtidally Deposited Carbonate Sediments in the Hanson Creek Formation (Ordovician-Silurian) of Central Nevada. In Concepts and Models of Dolomitization: Soc. Econ. Paleon. and Min. Spec. Publication No. 28, pp. 139-163.
- Dunham, J. B., Crawford, G. A., and Panasiuk, W. 1983. Sedimentology of the Slave Point Formation (Devonian) at Slave Field, Lubicon Lake, Alberta. In Carbonate Buildups: Soc. Econ. Paleon. and Min. Core Workshop No. 4, pp. 73-112.
- Enos, P. 1983. Shelf Environment. In Carbonate Depositional Environments: Amer. Assoc. Petrol. Geol. Memoir 33, pp. 268-295.
- Esteban, M., and Klappa, C. F. 1983. Subaerial Exposure. In Carbonate Depositional Environments: Amer. Assoc. Petrol. Geol. Memoir 33, p. 2.
- Feinstein, S. 1981. Subsidence and Thermal History of Southern Oklahoma Aulacogen: Implications for Petroleum Exploration: Amer. Assoc. Petrol. Geol., V. 65, No. 12, pp. 2521-2533.

- Flügel, E. 1982. *Microfacies Analysis of Limestones*. Berlin: Springer-Verlag, 633 pp.
- Folk, R. L. 1959. Practical Petrographical Classification of Limestones: *Amer. Assoc. Petrol Geol. Bull.* Vol. 43, No. 1, pp. 1-38.
- Folk, R. L. 1965. Some Aspects of Recrystallization in Ancient Limestones. In *Dolomitization and Limestone Diagenesis*. A Symposium: *Soc. Econ. Paleon. and Min. Spec. Pub.* 13, pp. 14-48.
- Folk, R. L. and Siedlecka, A. 1974. The "Schizohaline" Environment: Its Sedimentary and Diagenetic Fabrics as Exemplified by Late Paleozoic Rocks of Bear Island, Svalboard: *Sedimentary Oecology* Vol. 11, pp. 1-15.
- Folk, R. L. and Land, L. S. 1975. Mg/Ca Ratio and Salinity: Two Controls Over Crystallization of Dolomite: *Amer. Assoc. Petrol. Geol. Bull.* 59, Vol. 59, pp. 60-68.
- Friedman, G. M. 1965. Terminology of Crystallization Textures and Fabrics in Sedimentary Rocks: *Jour. Sed. Pet.* Vol. 35, pp. 643-655.
- Friedman, G. M. and Saunders, J. E. 1967. Origin and Occurrence of Dolostones. In *Carbonate Rocks, Part A: Origin, Occurrence and Classification*. New York: Elsevier Publishing Company, pp. 267-348.
- Friedman, G. M. 1980. Dolomite is an Evaporite Mineral: Evidence From the Rock Record and From Sea-Marginal Ponds of the Red Sea. In *Concepts and Models of Dolomitization: Soc. of Econ. Paleon. and Min. Spec. Publication No. 28*, pp. 69-80.
- Ginsberg, R. N. 1975. Tidal Deposits. New York: Springer-Verlag, 427 pp.
- Gross, M. G. 1964. Variations in the O^{18}/O^{16} and C^{13}/C^{12} Ratios of Diagenetically Altered Limestones in the Bermuda Islands: *Jour. Geol.* Vol. 72, pp. 170-194.
- Grover, G. Jr. and Read, J. F. 1983. Sedimentology and Diagenesis of Middle Ordovician Carbonate Buildups, Virginia. In *Carbonate Buildups: Soc. of Econ. Paleon. and Min. Core Workshop No. 4*, pp. 2-25.
- Ham, W. E. 1952. Algal Origin of the "Birdseye" Limestone in the McLish Formation: *Okla. Acad. Sci., Proc.* 33, pp. 200-203.
- Ham, W. E., Dennison, R. E., and Merritt, C. A. 1964. Basement Rocks and Structural Evolution of Southern Oklahoma: *Okla. Geol. Survey Bull.* Vol. 95, pp. 142-167.

- Handshaw, B. B., Back, W., and Deike, R. G. 1971. A Geochemical Hypothesis for Dolomitization by Ground Water: *Econ. Geol.* Vol. 66, pp. 710-724.
- Harvey, R. L. 1968. Westcambell-Key to Unlock the Hunton, P + 1: *Oil Gas Jour.* Vol. 66, pp. 124-132. Surface Only Scratched in Hunton Search, Pt. 2: *Oil Gas Jour.* Vol. 66, pp. 142-143.
- Hsü, K. S. and Siegenthaler, C. 1969. Preliminary Experiments on Hydrodynamic Movement Induced by Evaporation and Their Bearing on the Dolomite Problem: *Sedimentology* Vol. 12, pp. 11-25.
- Irving, E. 1979. Paleopoles and Paleolatitudes of North America and Speculations About Displaced Terrains: *Canad. Jour. of Earth Sci.* Vol. 16, pp. 669-694.
- Irwin, M. L. 1965. General Theory of Epeiric Clear Water Sedimentation: *Amer. Assoc. of Petrol. Geol. Bull.* Vol. 49, pp. 445-459.
- Isom, J. W. 1973. Subsurface Stratigraphic Analysis, Late Ordovician to Early Mississippian, Oakdale-Campbell Trend, Woods, Major, and Woodward Counties, Oklahoma: *Shale Shaker* Vol. 24, pp. 32-42, 52- (pts. 1 and 2).
- Kendall, C. A. St. C. and Skipwith, P. A. 1968. Recent Algal Mats of a Persian Gulf Lagoon: *Jour. Sed. Pet.* Vol. 38, pp. 1040-1058.
- Land, L. S. 1973. Contemporaneous Dolomitization of Pleistocene Limestone, North Jamaica: *Sedimentology* Vol. 20, pp. 411-424.
- Land, L. S. 1980. The Isotopic and Trace Element Geochemistry of Dolomite: The State of the Art. In Concepts and Models of Dolomitization: *Soc. of Econ. Paleon. and Min. Spec. Publication No. 28*, pp. 87-111.
- Land, L. S. 1983. The Application of Stable Isotopes to Studies of the Origin of Dolomite and to Problems of Diagenesis of Clastic Sediments. In Stable Isotopes in Sedimentary Geology: *Soc. of Econ. Paleon. and Min. Short Course No. 10*, pp. 41; 4-22.
- Longman, M. W. 1980. Carbonate Diagenetic Textures From Nearshore Diagenetic Environments: *Amer. Assoc. Petrol. Geol. Bull.* Vol. 64 No. 4, pp. 461-487.
- Mattes, B. W. and Mountjoy, E. W. 1980. Burial Dolomitization of the Upper Devonian Miette Buildup, Jasper National Park, Alberta. In Concepts and Models of Dolomitization: *Soc. Econ. Paleon. and Min. Spec. Publication No. 28*, pp. 259-297.
- Moore, C. H. and Druckman, Y. 1981. Burial Diagenesis and Porosity by Evolution, Upper Jurassic Smackover, Arkansas and Louisiana: *Amer. Assoc. Petrol. Geol. Bull.* Vol. 65, No. 4, pp. 597-627.

- Murray, R. C. 1960. Origin of Porosity in Carbonate Rocks: Jour. Sed. Pet. Vol. 30, pp. 59-84.
- Philcox, M. E. 1963. Banded Calcite Mudstone in the Lower Carboniferous "Reef" Knolls of the Dublin Basin, Ireland: Jour. Sed. Pet. Vol. 33, No. 4, pp. 904-913.
- Reeds, C. A. 1911. The Hunton Formation of Oklahoma: Amer. Jour. Sci. Vol. 182, pp. 256-268.
- Reeds, C. A. 1927. The Arbuckle Mountains, Oklahoma: Okla. Geol. Survey Circular 14.
- Roehl, P. O. 1967. Stony Mountain (Ordovician) and Interlake (Silurian) Facies Analogs of Recent Low-energy Marine and Subaerial Carbonates, Bahamas: Amer. Assoc. Petrol. Geol. Bull. Vol. 51, pp. 1979-2032.
- Sears, S. O. and Lucia, F. J. 1980. Dolomitization of Northern Michigan Niagara Reefs by Brine Refluxion and Freshwater/Sea Water Mixing. In Concepts and Models for Dolomitization: Soc. of Econ. Paleon. and Min. Spec. Publication No. 28, pp. 215-237.
- Shannon, P. J. Jr. 1962. Hunton Group (Silurian-Devonian) and Related Strata in Oklahoma: Amer. Assoc. Petrol. Geol. Bull. Vol. 46, pp. 1-29.
- Taylor, J. M. 1950. Pore Space Reduction in Sandstone: Amer. Assoc. Petrol. Geol. Bull. Vol. 34, pp. 701-716.
- Tucker, M. 1976. Replaced Evaporites From the Late Precambrian of Finnmark, Arctic Norway: Sed. Geol. Vol. 16, pp. 193-204.
- Walker, R. N., Muir, M. D., Diver, W. L., Williams, N. and Wilkins, N. 1977. Evidence of Major Sulfate Evaporite Deposits in the Proterozoic, McArthur Group, Northern Territory, Australia: Nature, vol. 265, pp. 526-529.
- Zenger, D. H. and Dunham, J. B. 1980. Concepts and Models of Dolomitization. In Concepts and Models of Dolomitization: Soc. of Econ. Paleon. and Min. Spec. Publication No. 28, pp. 1-11.

APPENDIX

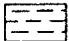

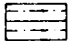

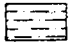



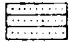
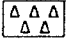

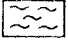
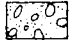
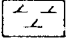
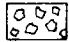
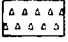
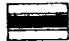
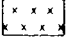
CORE DESCRIPTIONS

HUNTON GROUP



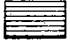
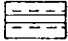
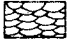
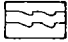


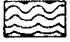

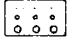
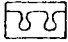

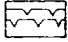


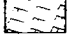
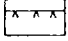
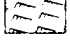
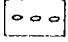
PETROLOG

Well _____
 Location _____ Sec. T. N., R. W.
 Co., OKLAHOMA




Lithology

 CLAY/ CLAYSTONE	 LIMESTONE
 SILTY CLAYSTONE/ MUDSTONE	 DOLOMITE
 SILT/SILTSTONE	 GYPSUM/ ANHYDRITE
 SAND/SANDSTONE	 HALITE
 INTERBEDDED SANDSTONE/ MUDSTONE	 CHERT
 MUDDY SANDSTONE	 MARL
 CONGLOMERATE	 DOLOMITIC ROCKS
 BRECCIA	 CHERTY ROCKS
 COAL/LIGNITE	 GYPSIFEROUS/ ANHYDRITIC ROCKS



Sedimentary Structures

 HORIZONTAL BEDDING	 ALGAL LAMINATION
 HORIZONTAL LAMINAE	 LINEATION
 TROUGH CROSSBEDS	 CURRENT SOLE MARKS
 TABULAR CROSSBEDS	 LOW-ANGLE INCLINED STRATIFICATION
 DISTURBED BEDDING	 BURROWS
 GRADED BEDDING	 LOADCASTS
 NODULAR OR KNOBBY/HUMMOCKY BEDDING	 MUDCRACKS
 MASSIVE BEDDING	 BURROW-MOTTLED
 RIPPLE CROSS-LAMINAE	 ROOTLETS
 FLASER LAMINAE	 CONCRETIONS


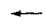



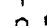
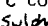
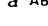

Fracture

 OPEN
 CLOSED
 FILLED

Stylolites

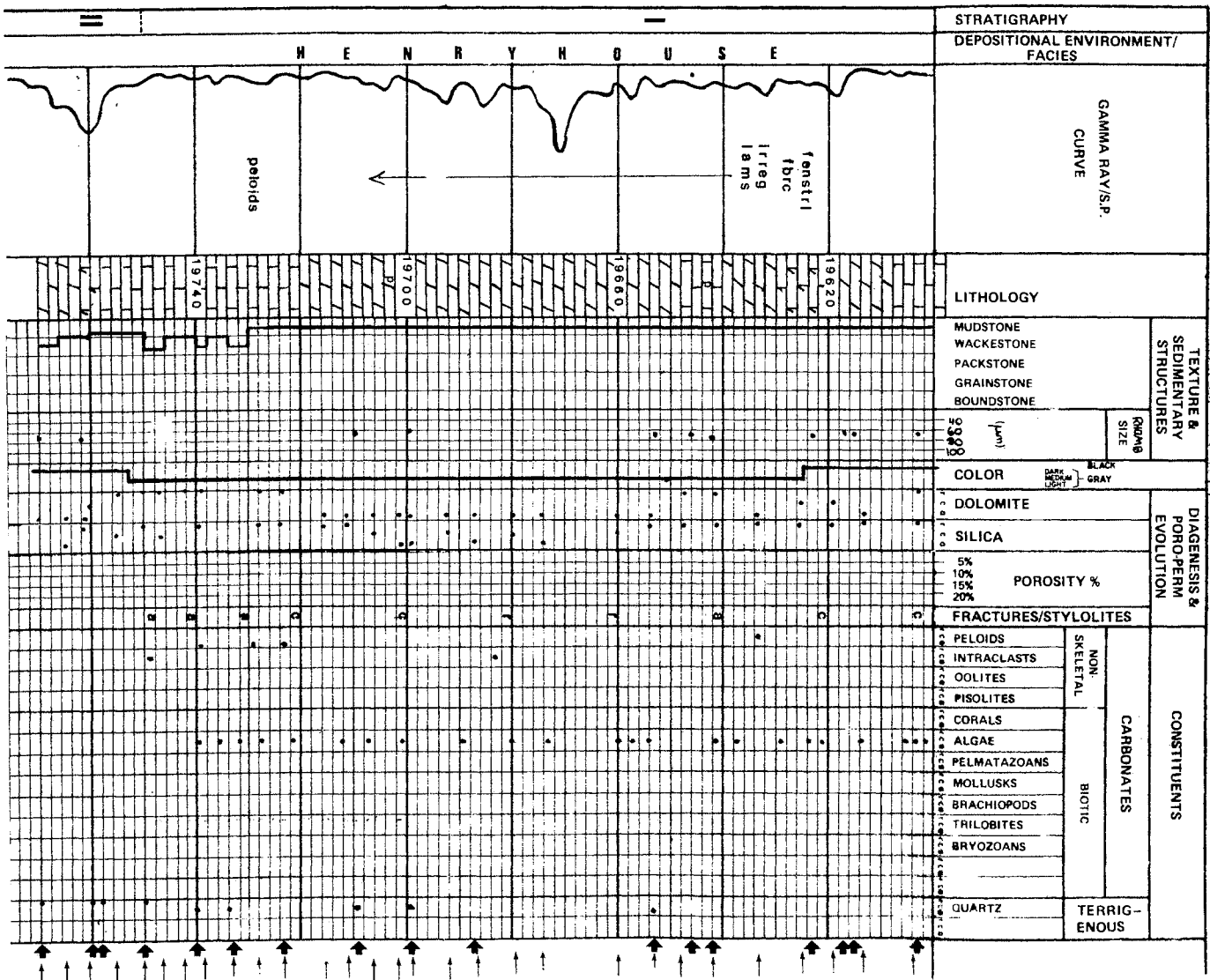
 COARSE
 FINE

Miscellaneous

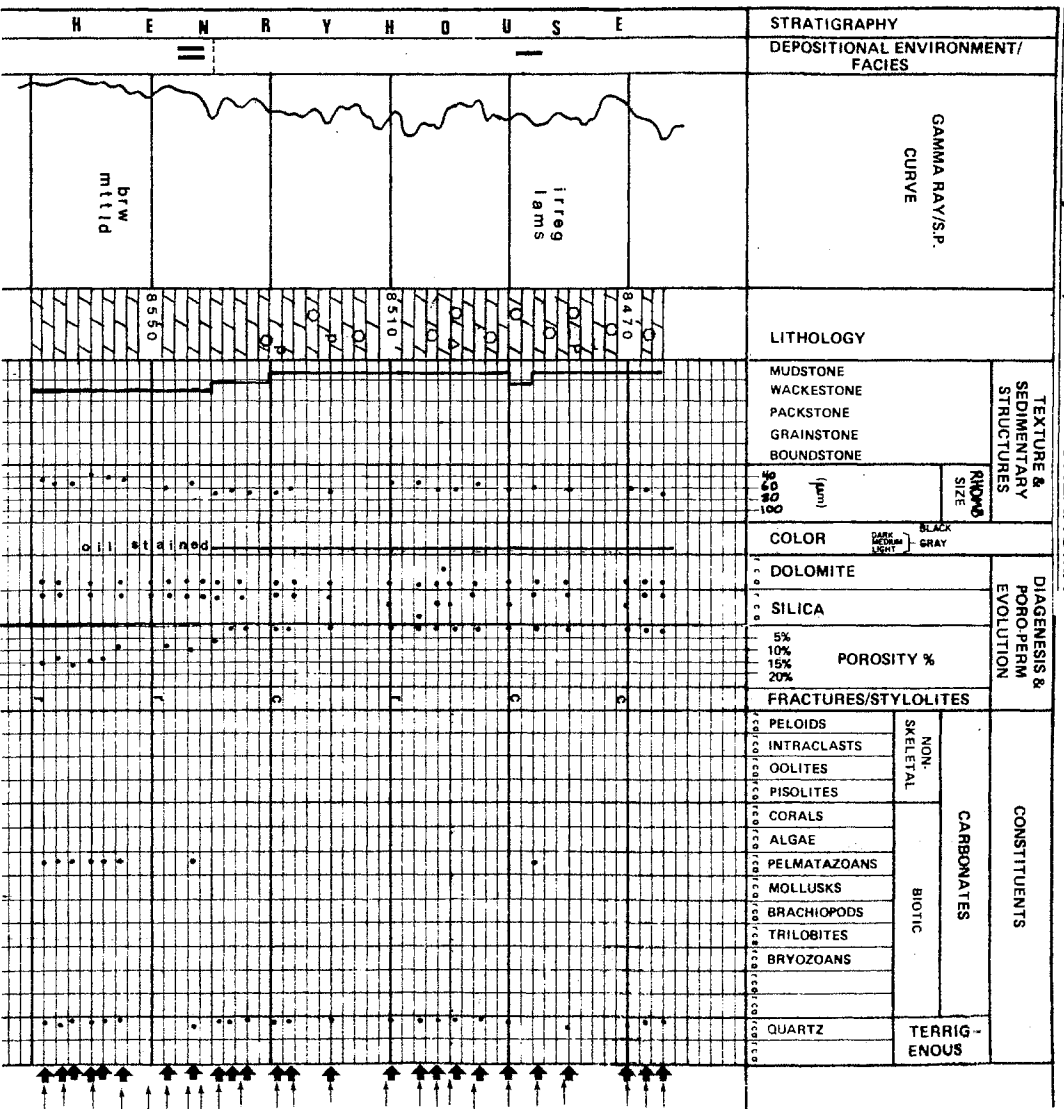
 THIN SECTION		
 X-RAY DIFFRACTION SAMPLE		
 GLAUCONITE		
 PYRITE		
 CARBONACEOUS DETRITUS		
 RARE	 COMMON	 ABUNDANT
 Replaced Sulphates		

KEY: This key applies to the following core descriptions

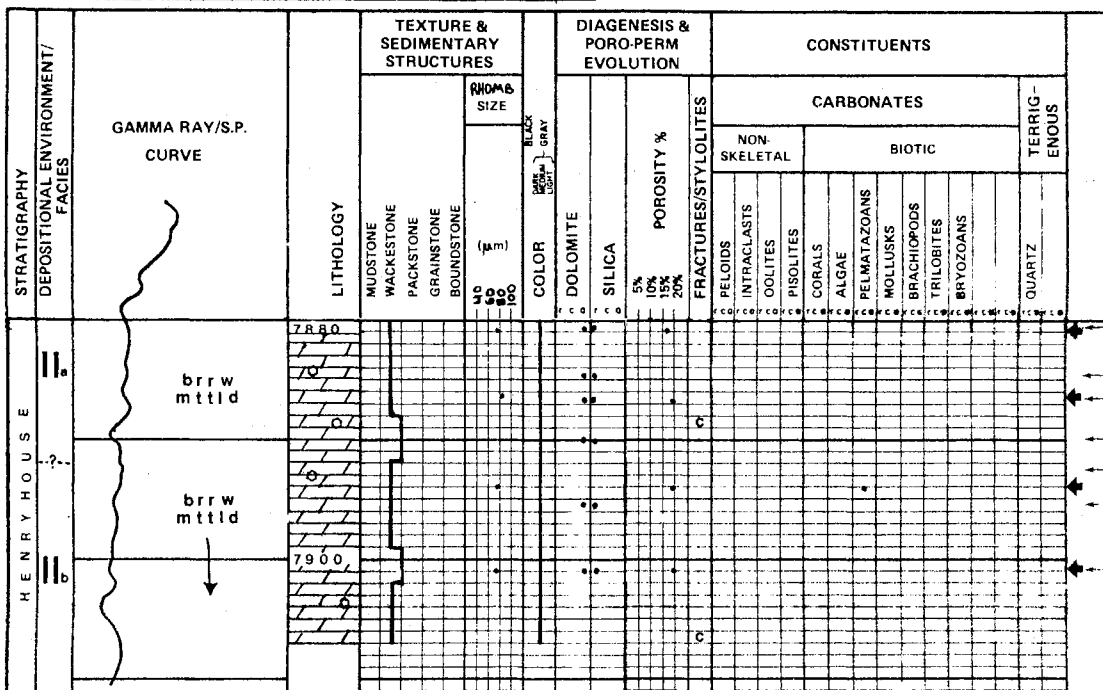
Well Apexco Green
 Location Beckham Co., OKLAHOMA
 Sec. 31 T. 10 N., R. 26 W.



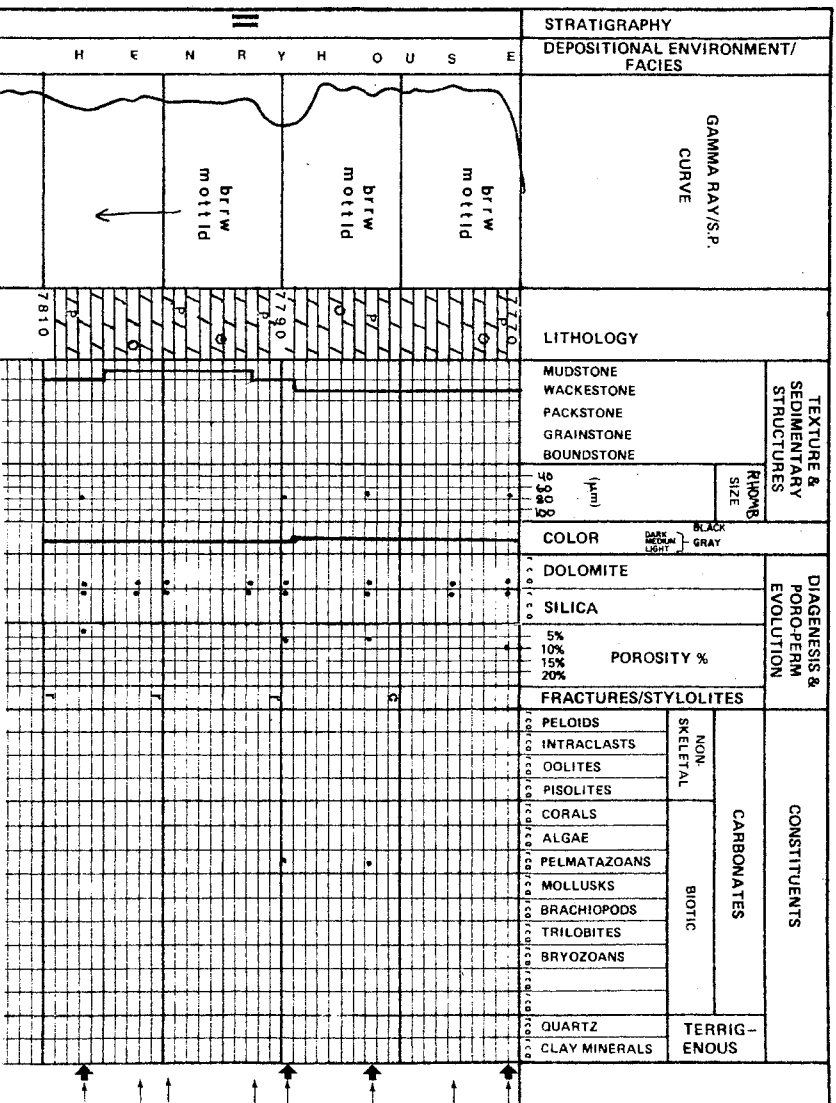
Well Tenneco J. Jordan No. 2-34
 Location Sec. 34 T. 22 N. R. 14 W.
Major Co., OKLAHOMA



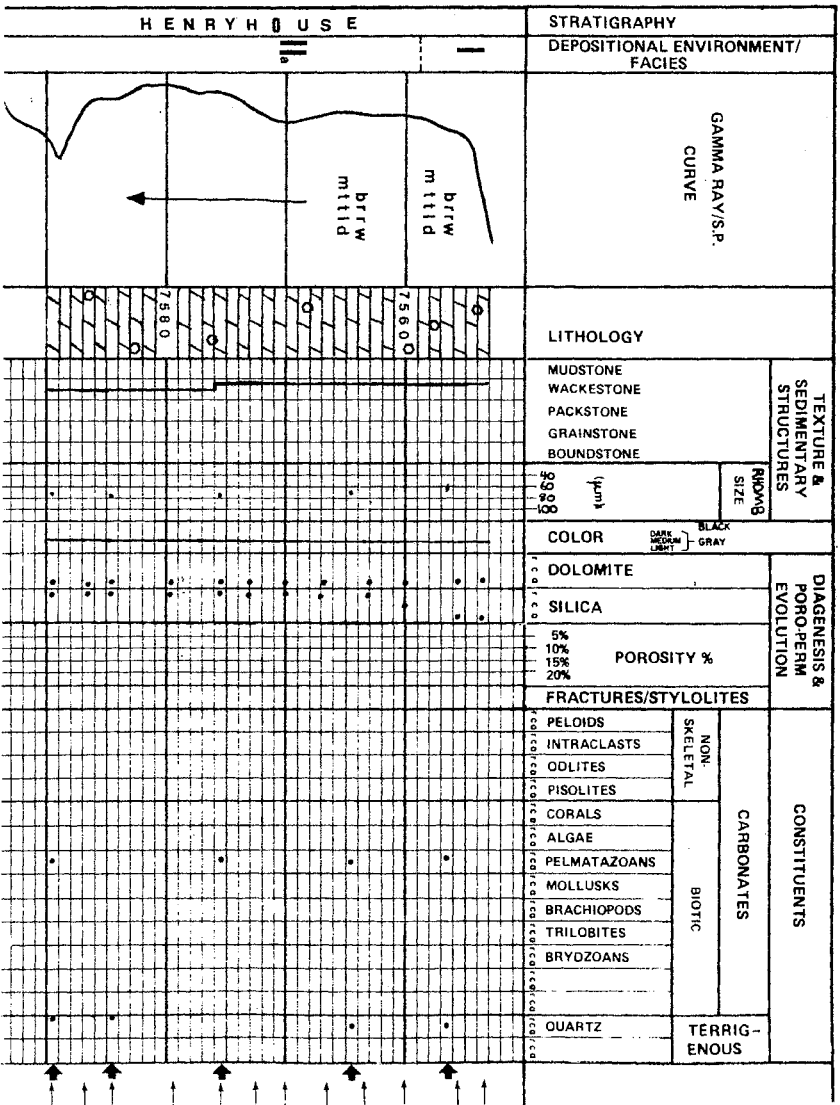
Well Kirkpatrick Nichel Unit No. 1
 Location Sec. 34 T. 22 N., R. 12 W.
 Major Co., OKLAHOMA



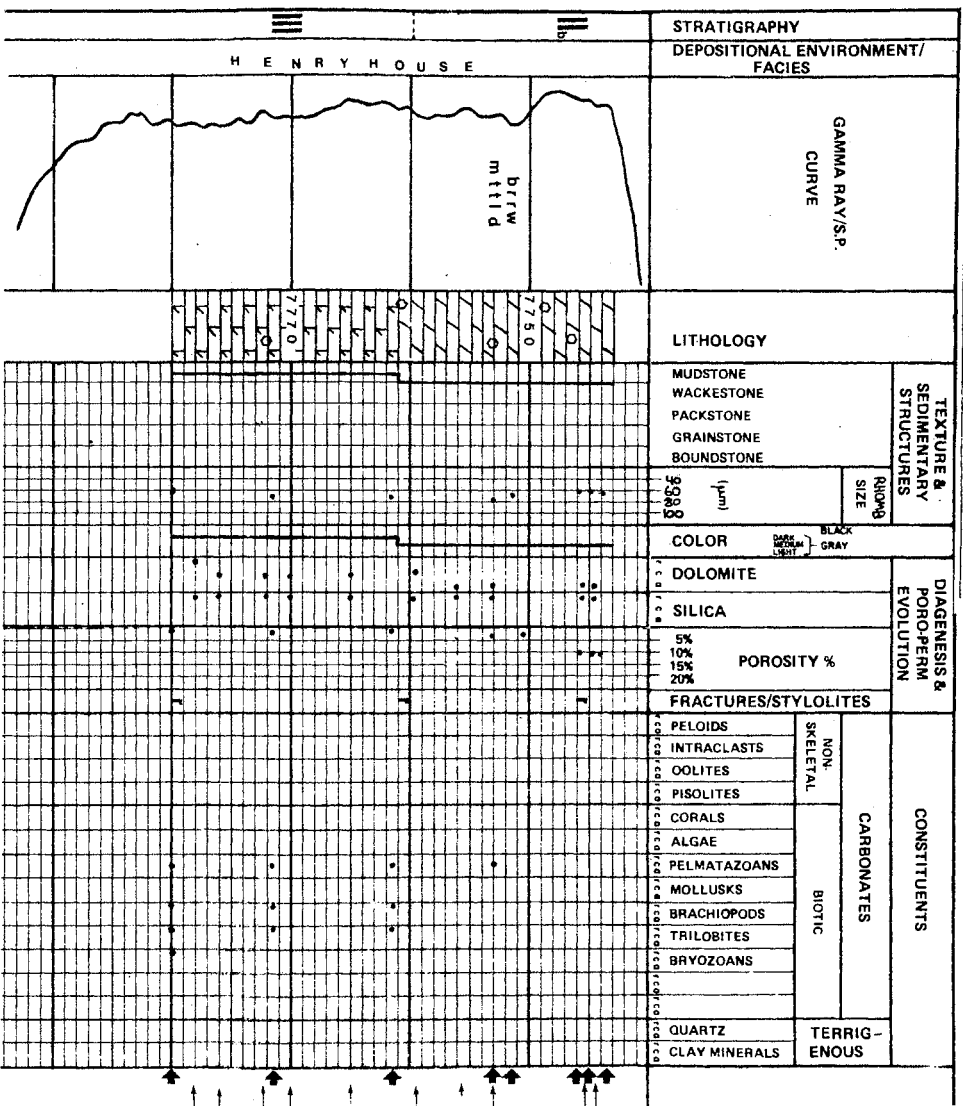
Well Kirkpatrick, Natol, & NCRA Wicherl No. 1
 Location SE NW Sec. 26 T. 22 N, R. 12 W,
 Major Co., OKLAHOMA



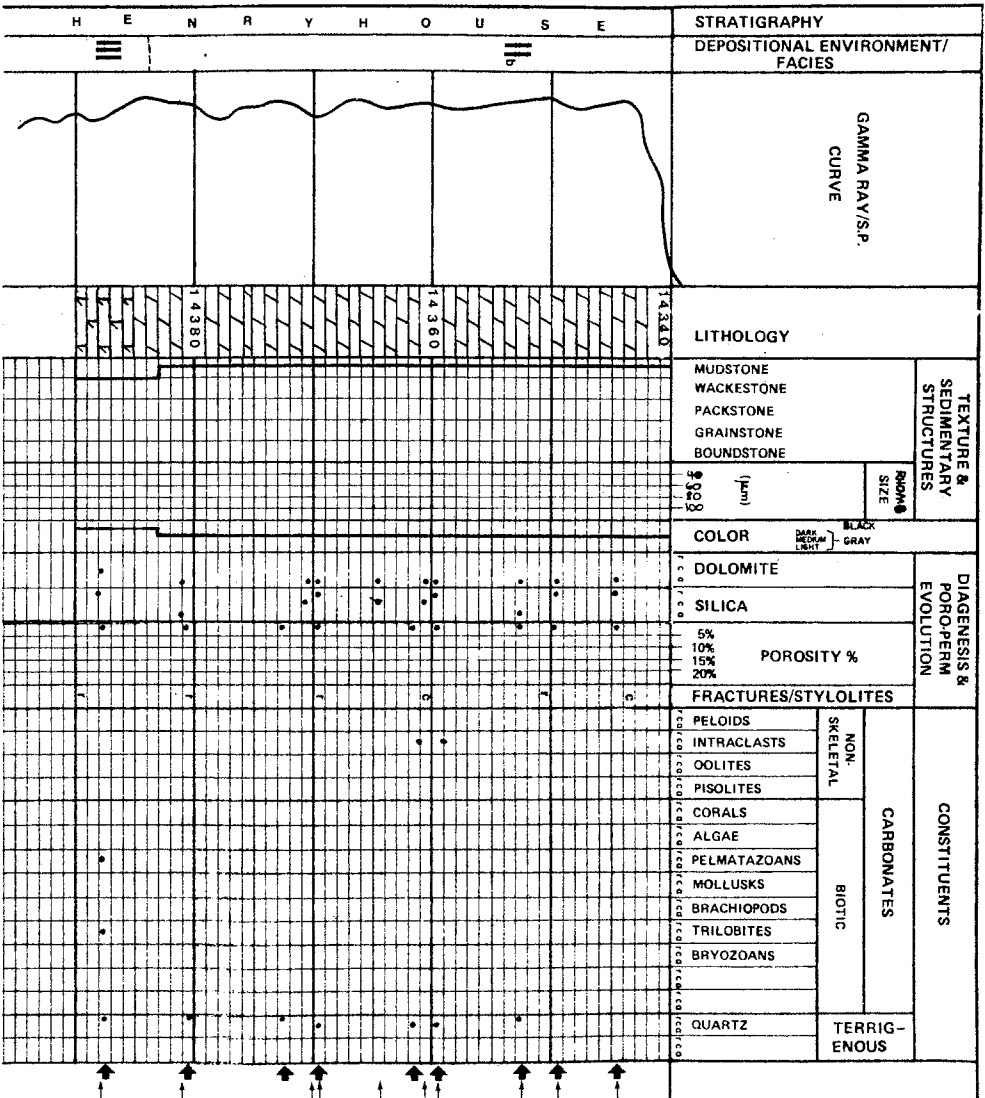
Well Cleary Rose No. 1-12
 Location Sec. 12 T. 22 N., R. 12 W.
 Major Co., OKLAHOMA



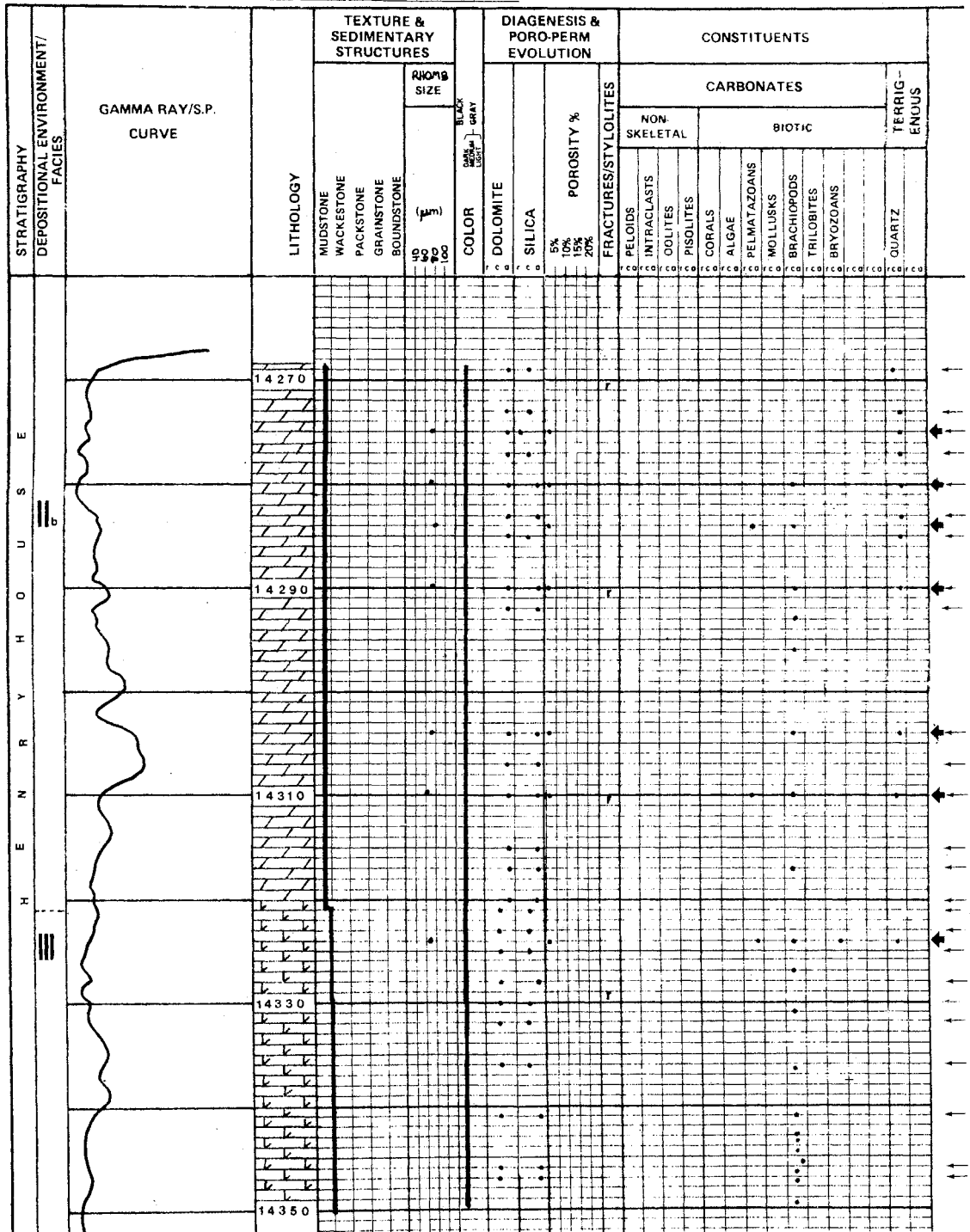
Well NFC Dietz No. 6-30
 Location Sec. 30 T. 23 N, R. 13 W.
 Major Co., OKLAHOMA



Well Lone Star Hanan Unit No. 1
 Location NE Sec. 6 T. 19 N., R. 24 W.
Ellis Co., OKLAHOMA



Well G H K Hoffman No. 1
 Location Sec. 1 T. 14 N., R. 16 W.
 Custer Co., OKLAHOMA



VITA 2

Geoffrey Bonser Beardall, Jr.

Candidate for the Degree of

Master of Science

Thesis: DEPOSITIONAL ENVIRONMENT, DIAGENESIS AND DOLOMITIZATION OF
THE HENRYHOUSE FORMATION, IN THE WESTERN ANADARKO BASIN AND
NORTHERN SHELF, OKLAHOMA

Major Field: Geology

Biographical:

Personal Data: Born in Winchester, Virginia, the son of Geoffrey
and Margaret Beardall.

Education: Received Bachelor of Science degree in Geology in
December, 1979, from Mary Washington College, Fredericksburg,
Virginia; completed requirements for the Master of Science
degree at Oklahoma State University in December, 1983.